Title

Near-Source Modeling of Transportation Emissions in Built Environments Surrounding Major Arterials

Authors

Boarnet, Marlon G.
Edwards, Rufus
Princevac, Marko
et al.

Publication Date

2009-09-01

University of California Transportation Center
UCTC Research Paper No. 886

Near-Source Modeling of Transportation Emissions in Built Environments Surrounding Major Arterials

Marlon G. Boarnet, University of California, Irvine,
Rufus Edwards, University of California, Irvine,
Marko Princevac, University of California, Riverside,
Jun Wu, University of California, Irvine,
Hansheng Pan, University of California, Riverside,
Christian Bartolome, University of California, Riverside,
Gavin Ferguson, University of California, Irvine,
Anahita Fazl, University of California, Irvine, and
Raul Lejano, University of California, Irvine

Summer 2009

Near-Source Modeling of Transportation Emissions in Built Environments Surrounding Major Arterials

Final Report to the University of California Transportation Center

Marlon G. Boarnet[1], Rufus Edwards[2], Marko Princevac[3], Jun Wu[2], Hansheng Pan[3], Christian Bartolome[3], Gavin Ferguson[1], Anahita Fazl[4], and Raul Lejano[5]

[1] Department of Planning, Policy, and Design and Institute of Transportation Studies, University of California, Irvine

[2] Department of Epidemiology, University of California, Irvine

[3] Department of Mechanical Engineering, Bourns College of Engineering, University of California, Riverside

[4] Institute of Transportation Studies, University of California, Irvine

[5] Department of Planning, Policy, and Design, University of California, Irvine

August, 2009

Acknowledgements: This research was funded by a grant from the University of California Transportation Center.

Near-Source Modeling of Transportation Emissions in Built Environments Surrounding Major Arterials

1. Introduction

Project included three major parts: 1) field measurements of particulate matter in five urban areas, 2) laboratory modeling of flow and dispersion within model urban areas, and 3) numerical modeling. Project website and database are located at http://emissions.engr.ucr.edu/.

2. Field Measurements

Field measurements were conducted from June 19th to August 1st, 2008, at five urban locations in the greater Los Angeles region (Table 2.1). Instrumented domains were approximately 500 m x 500 m and included one or more major arterials. Site maps with instrumentation and description are given in Appendix A. Pictures of typical building geometry in the five selected urban areas are shown in Figure 2.1. Each location was equipped with one sonic anemometer (CSAT3, Campbell Sci.), measuring mean wind speed, turbulence and virtual temperature; six DustTraks (TSI Inc.), measuring $PM_{2.5}$ concentration; and three digital cameras (JVC), recording traffic flow. Measurements were taken on three days in each area, and on each day three rush-hour periods were covered: morning, from 7 am to 9 am; lunch-time, from 11 am to 1 pm; and evening, from 4 pm to 6 pm. For this project the database of the dimensions of buildings at five sites was supplied to us by the Los Alamos National Laboratory (Dr. Michael Brown).

Table 2.1 Urban area descriptions

Type No.	Urban Type	Description	Selected Location
Type 1	Low-density settlement	One or two stories	Anaheim
Type 2	Low-rise settlement	Three to four stories	Pasadena
Type 3	Mid-rise settlement	Ten to twenty stories	Downtown Long Beach
Type 4	High-rise settlement	More than twenty stories	Downtown Los Angeles
Type 5	Strip mall	With surface parking	Huntington Beach

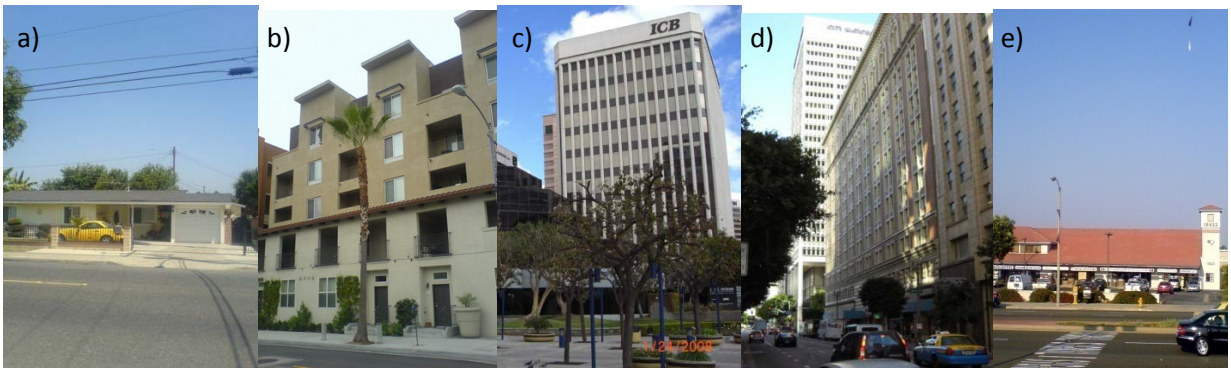

Figure 2.1 Building types: a) Low-density settlement; b) Low-rise settlement; c) Mid-rise settlement; d) High-rise settlement; and e) Strip mall.

Wherever possible, to avoid the influence of surface elements on meteorological measurements, the sonic anemometer was mounted on the upper level of a parking structure. However, not all five locations had such an elevated place suitable for the sonic anemometer. In such cases a relatively open area such as a park or parking lot was selected instead. A sequence of quality assurance procedures were conducted prior to measurement. Procedures included zero calibration and synchronization of DustTraks. In addition, in order to minimize errors due to individual differences among the DustTraks, all six DustTraks were sampled for 10 minutes at the same place, and the data was used to correct $PM_{2.5}$ concentration calibration. Some photographs of the deployed instrumentation are given in Figure 2.2.

Figure 2.2 a) Sonic anemometer deployed on the parking structure in Long Beach; b) DustTrak on the street in Long Beach; c) DustTrak deployed together with video camera for traffic recording in Los Angeles.

2.1 Downtown Los Angeles case

As an example of micrometeorological data analysis we here present the Los Angeles data set. The average building height in the selected domain is 52±43 m, the plan area fraction, λ_P, is 0.36±0.15, and the frontal area fraction, λ_F, is 0.47±0.54 (see Appendix D for urban morphometry definitions). Urban displacement height, z_d, is calculated to be 27.3 m, and the roughness length, z_0, is 0.14 m (see Appendix D for urban morphometry definitions).

Wind roses for all three days of measurements are presented in Figure 2.3. Detailed measurements of wind speed, air temperature, turbulent flux, sensible heat flux and $PM_{2.5}$ concentrations at all six sites are given in the Appendix E. The mean wind speeds for each day are 0.51±0.22, 0.52±0.27 and 0.58±0.23 m/s. The mean temperatures are 31.2±3.6, 29.3±2.4 and 26.8±2.5ºC. Turbulent fluxes of momentum and sensible heat exhibit a significant increase after 10 am and an even larger increase in the afternoon, which results in more efficient mixing within the urban boundary layer and growth of the boundary layer height. This boundary layer development and efficient mixing is mainly responsible for decreasing concentrations observed at all six sites from morning to late afternoon. There is a strong correlation of turbulent momentum and sensible heat flux with $PM_{2.5}$ concentration. During the morning, we found that the concentration of $PM_{2.5}$ stayed at the same level when turbulent flux and sensible heat flux

increased gradually (06/19/2008 and 06/23/2008); however, the concentration of $PM_{2.5}$ increased when turbulent flux and sensible heat flux were low (06/30/2008).

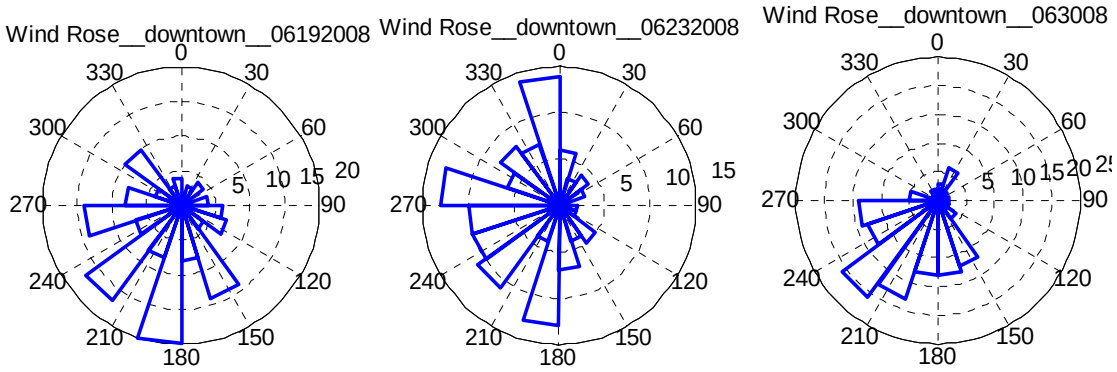

Figure 2.3 Wind Roses for three days of measurements in downtown Los Angeles.

3. Laboratory Modeling

Laboratory experiments are needed to provide detailed flow and dispersion data under controlled conditions from street level sources. Green dye release for visualization of dispersion from two line sources (representing two arterials) in a laboratory model of Long Beach is given in Figure 3.1. Quantitative concentration and flow measurements were performed using Planar Laser Induced Fluorescence (PLIF) and Particle Image Velocimetry (PIV), respectively. Detailed description of the laboratory facility together with the scaling procedure is given in Appendix B.

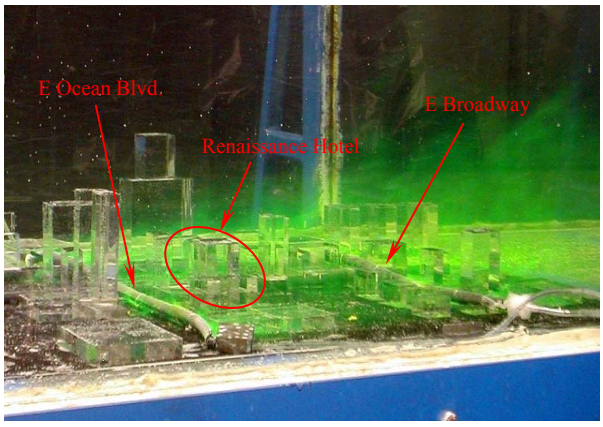

Figure 3.1 Visualization of dispersion through the laboratory model of Long Beach.

4. Numerical Modeling

The Quick Urban and Industrial Complex model was deployed in this study. Detailed model description is given in Appendix C.

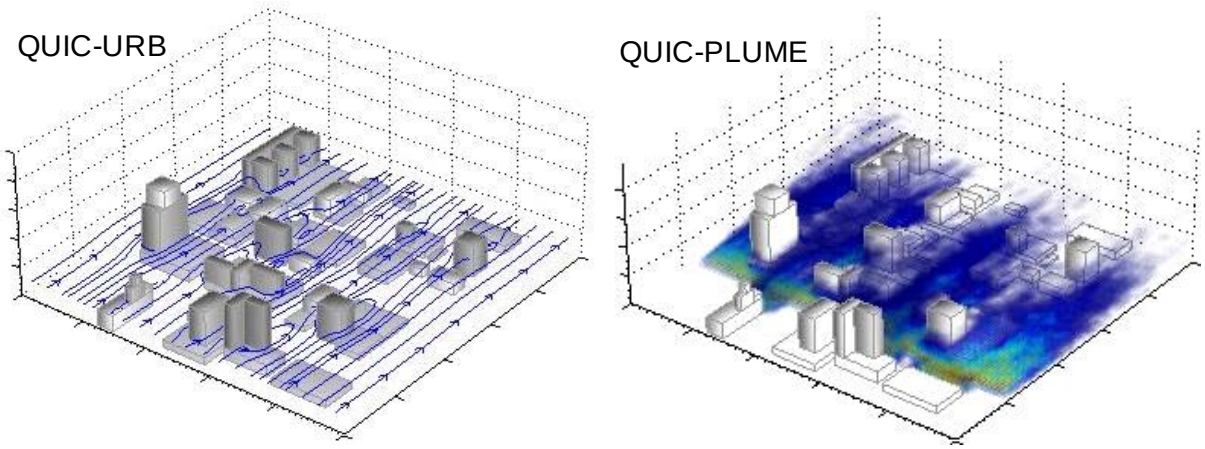

Figure 4.1 Streamlines produced by QUIC (left) and dispersion from a line source (right) at East Ocean Boulevard.

Case study of 07/16/2008 measurements in Huntington Beach is given next.

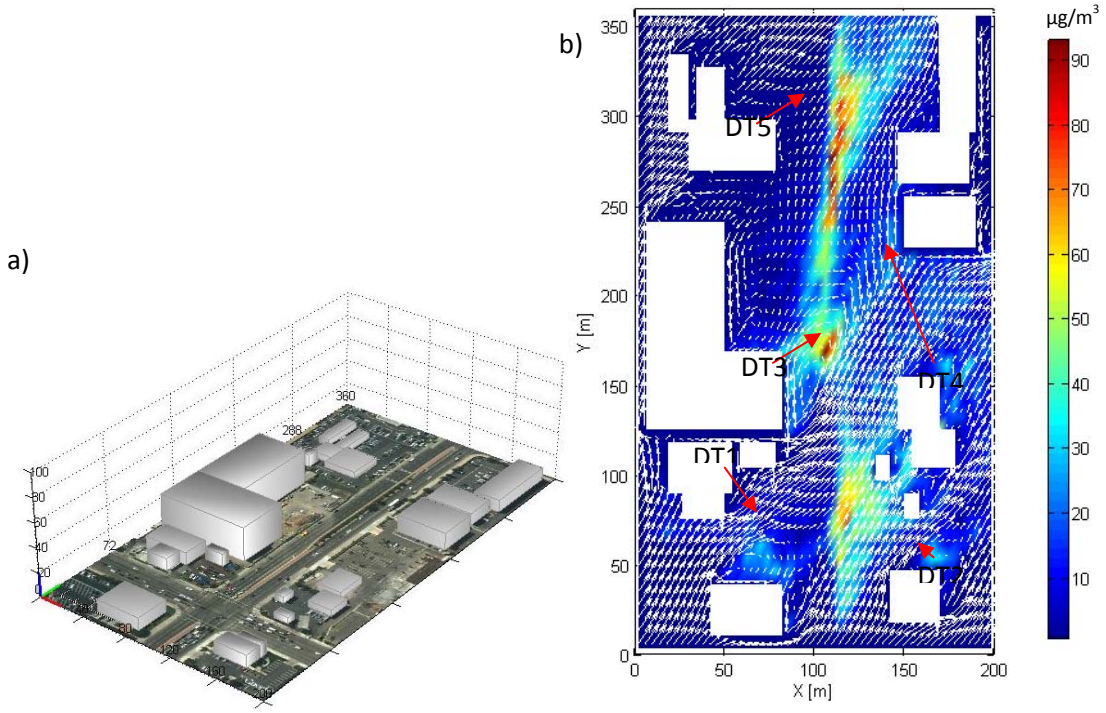

Figure 4.2 a) QUIC setup for a strip mall in Huntington Beach; b) QUIC modeling results of concentration and velocity fields at z=2.5 m for 07/16/2008.

QUIC domain size (Figure 4.2a) for the selected case is 200m×360m×100m. Grid size is 2m×3.6m×1m. Meteorological parameter setup is based on actual field measurements. Mean wind velocity is 1.1 m and wind direction is 216°. Emission factor is adopted from Caltrans database as 0.1073 g/veh/mile for light-duty vehicle and 1.1244 g/veh/mile for heavy-duty vehicle. Mass flow rate of source is calculated based on the actual traffic flow measurement and adopted emission factor. Results are shown in Table 4.1.

Table 4.1 Traffic flow measurement and source emission rate calculation

Day	Street Name	Street Length [mile]	Hourly Traffic [vehicle/hour]		Mass Flow Rate [mg/s]
			Light-duty	Heavy-duty	
07/16/2008	Garfield Ave.	0.12	912	113	7.5
07/18/2008			915	152	9.0
07/21/2008			895	117	7.6
07/16/2008	Beach Blvd.	0.22	2501	305	37.4
07/18/2008			2575	379	42.9
07/21/2008			2410	335	38.8

From Figure 4.2b, the modeled concentration at site DT3 is higher than at other sites which is in excellent agreement with field measurements and it is contributed to the strong trapping of PM in the building wake. No large buildings are present in vicinity to produce channeling effects that may flush these high concentrations.

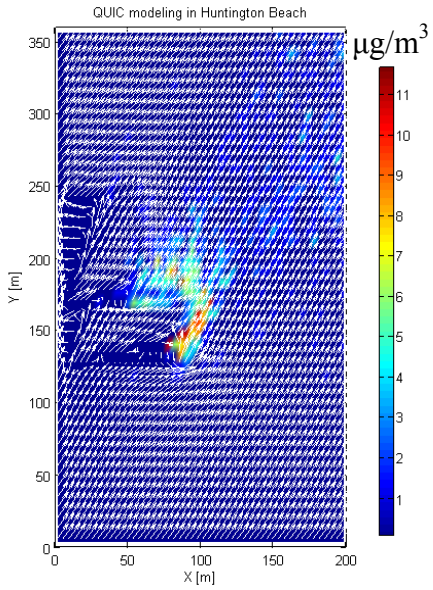

Figure 4.3 QUIC modeling results of concentration and velocity fields at z=28.5 m (roof level) for 07/16/2008.

To calculate the vertical transport of emissions, we also investigated concentration fields at a higher level, z=28.5 m (roof level), in Figure 4.3. The mean concentrations at ground level (z=2.5 m) and roof level (z=28.5 m) are 8.55 and 0.36 μg/m^3, respectively. The ratio of them is 4.2%, representing the transport efficiency of emissions from within urban canopy to above urban canopy.

5. Results

Field experiments delineated the influence of local meteorological variables and geometry within the urban canopy on particulate concentration. Wind perpendicular to the street canyon prevents flushing and causes high concentrations within the urban canopy. In addition to wind

direction, turbulent fluxes of momentum and sensible heat flux affect concentrations in enhancing the vertical mixing and boundary layer depth. Detailed flow and dispersion characteristics measured in a model urban area created in a water channel facility equipped with PIV/PLIF system were compared with numerical results produced by the QUIC model. The QUIC model produced relatively weaker updrafts which resulted in slight over-prediction of near ground particle concentration.

Analysis of particulate concentration data and comparison with the national air quality standard for each site is given next.

5.1 Stationary DustTrak Data

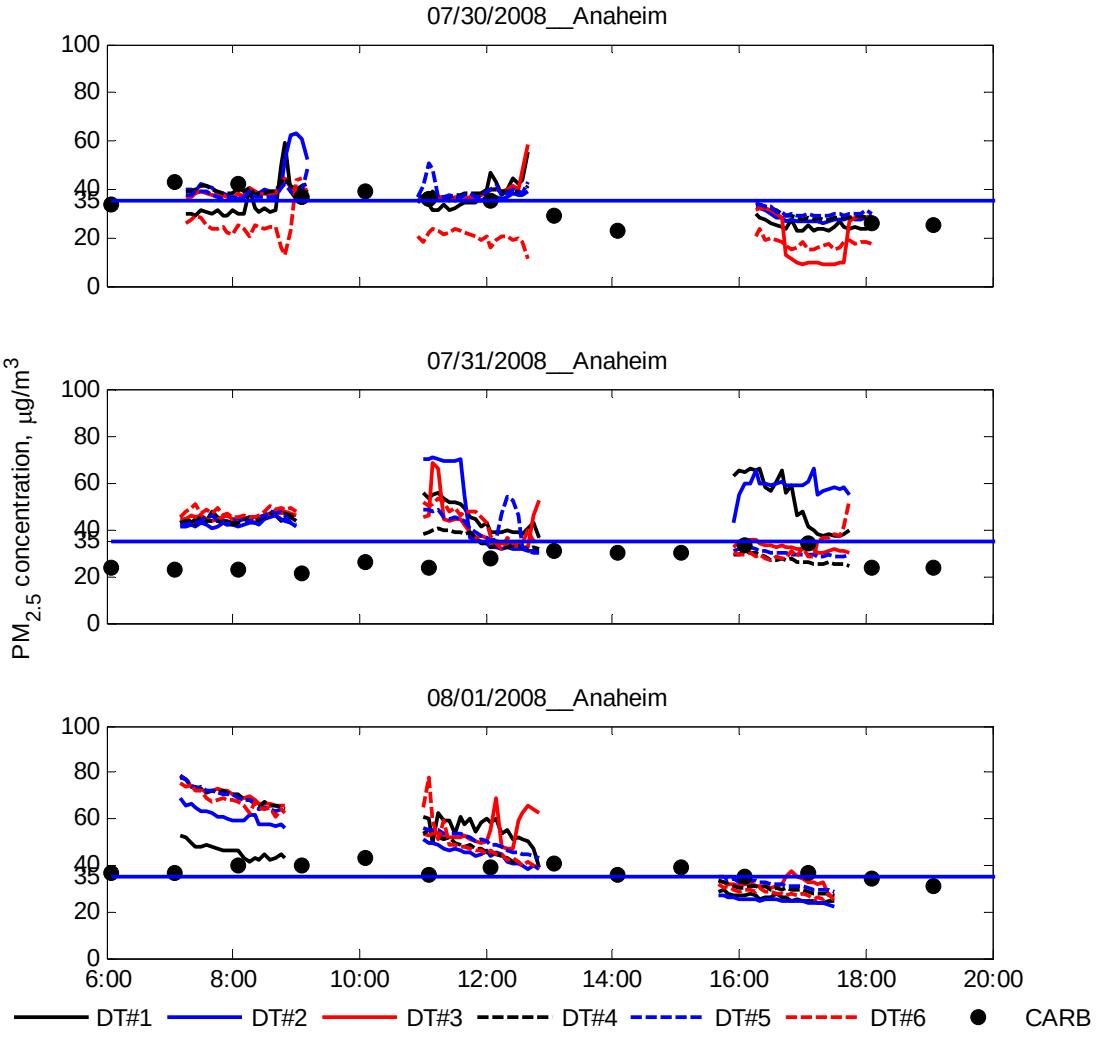

Figure 5.1 Three days of particulate measurements in Anaheim. The straight blue line represents national ambient Air Quality standards for $PM_{2.5}$ for 24-hour concentration (35 $\mu g/m^3$). DT stands for a DustTrak at the corresponding location. For the location map please refer to Appendix A. CARB is routinely taken data. See text for details.

In Figure 5.1 CARB stands for data taken by California Air Resource Board monitoring station, which is located at Pampas Lane in Anaheim. In the morning hours of Day 2, measured concentrations were uniform across all sites due to low wind conditions, while during midday, when wind speed increased, concentration differences among sites became significant. In the afternoon of the same day, DustTraks DT1 and DT2 (located in the same arterial) measured much higher concentrations than the others. The concentration increased due to the traffic flow at the rush hour with an absence of wind and heating.

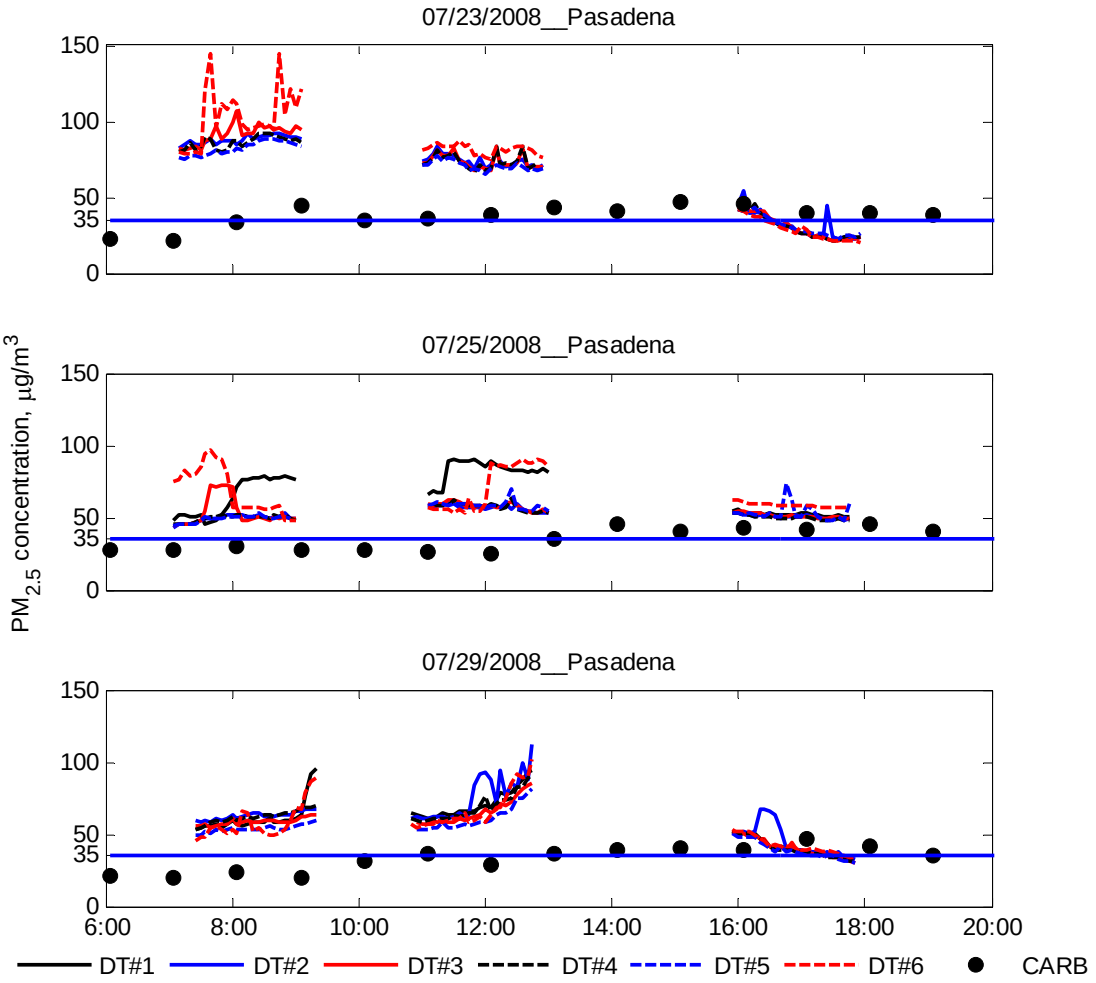

Figure 5.2 Three days of particulate measurements in Pasadena. The straight blue line represents national ambient Air Quality standards for $PM_{2.5}$ for 24-hour concentration (35 $\mu g/m^3$). DT stands for a DustTrak at the corresponding location. For the location map please refer to Appendix A. CARB is routinely taken data. See text for details.

In Figure 5.2, CARB stands for data taken from California Air Resource Board monitoring station, which is located at North Main Street in Los Angeles (the closest station to Pasadena). We measured extremely high concentrations during the morning hours on Day 1 in Pasadena. In particular, DT6 always presented much higher concentrations than other sites. Since DT6 was

on the roof of a parking garage, having less impact from arterials, there might be other sources, such as emission sources from nearby highways or stationary sources in this area, which need to be investigated further.

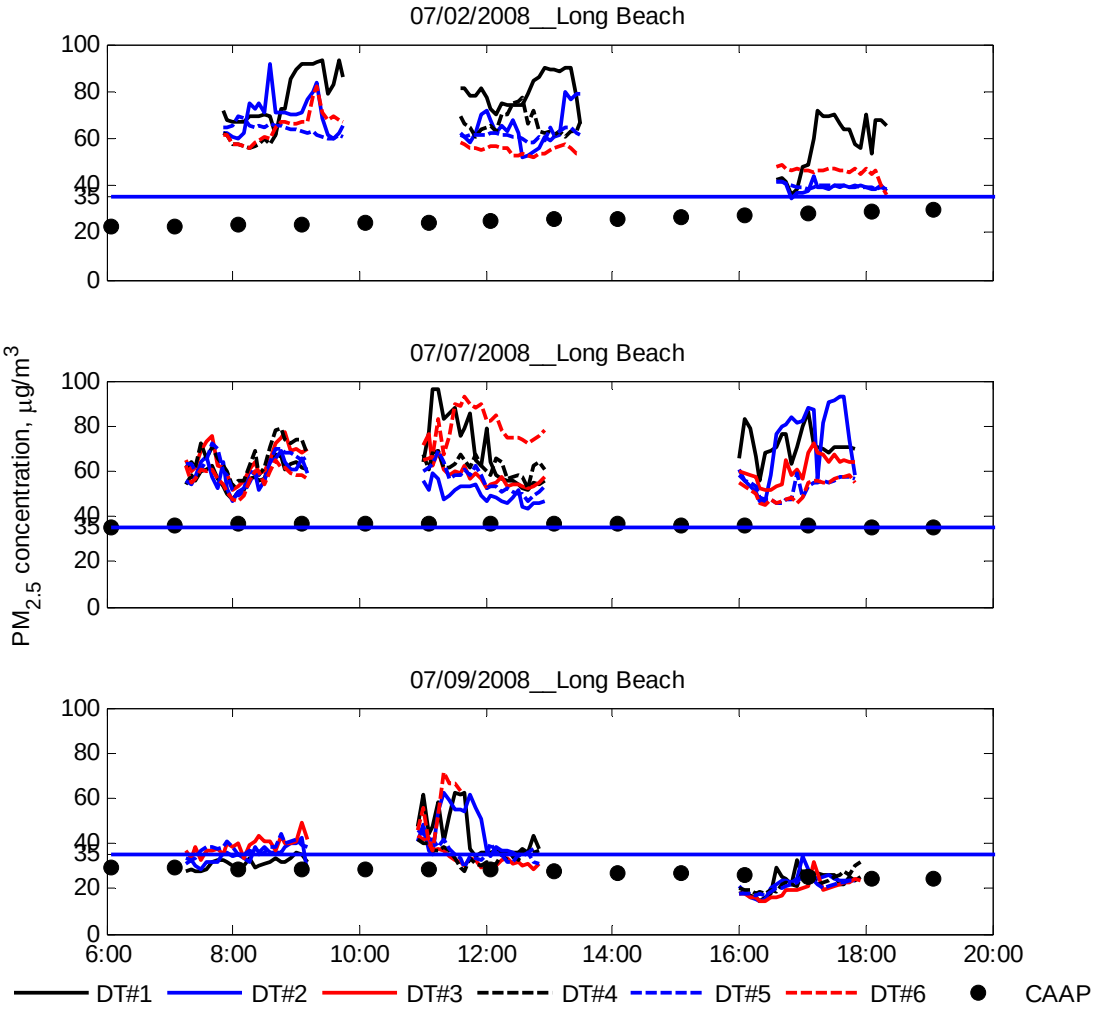

Figure 5.3 Three days of particulate measurements in Long Beach. The straight blue line represents national ambient Air Quality standards for $PM_{2.5}$ for 24-hour concentration (35 $\mu g/m^3$). DT stands for a DustTrak at the corresponding location. For the location map please refer to Appendix A. CAAP is routinely taken data. See text for details.

In Figure 5.3, CAAP stands for data taken from Clean Air Action Plan monitoring station, which is located at the inner port of Long Beach. On 07/09/2008, wind speed increased significantly (see Appendix E) between 14:00 and 16:00 hours, just before the sampling period started. It was the highest recorded wind in all three days (shown in Meteorological data plots, Appendix E.4), and it was southwesterly—from the ocean. The high wind speed bringing more fresh air from the ocean was one of the reasons causing low concentrations in the afternoon. Table 5.1 shows that 07/09/2008 had the lowest temperature and highest turbulent flux of the

three days. This made the overall concentration on 07/09/2008 lower than on 07/02/2008 and 07/07/2008.

Table 5.1 Meteorological statistics for Long Beach

Day	Temperature °C		Wind speed m/s		Turbulent flux M^2/s^2		Sensible heat flux W/m^2	
	MEAN	STDEV	MEAN	STDEV	MEAN	STDEV	MEAN	STDEV
07/02/2008	24.6	3.4	1.06	0.50	0.101	0.070	192	123
07/07/2008	22.6	2.5	0.78	0.44	0.105	0.069	227	113
07/09/2008	21.7	1.2	1.03	0.63	0.139	0.099	227	123

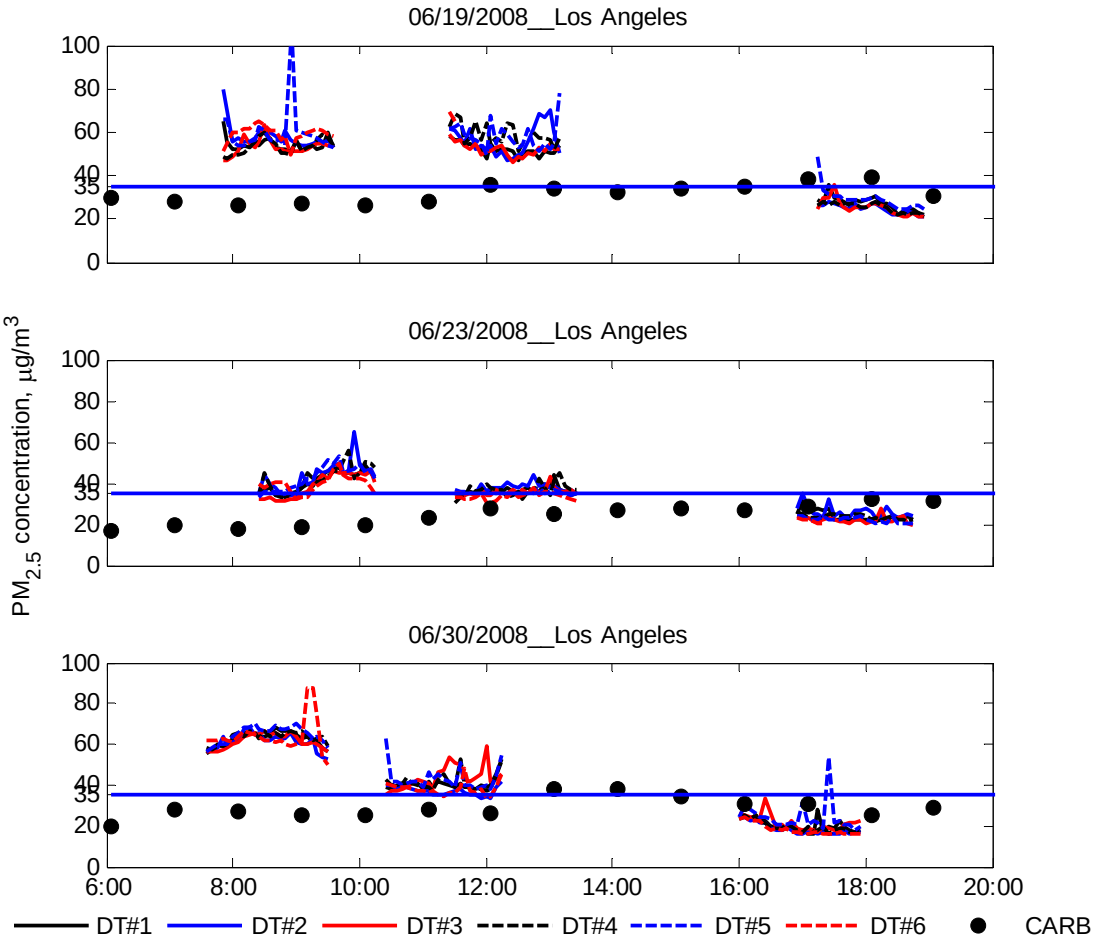

Figure 5.4 Three days of particulate measurements in Los Angeles. The straight blue line represents national ambient Air Quality standards for $PM_{2.5}$ for 24-hour concentration (35 $\mu g/m^3$). DT stands for a DustTrak at the corresponding location. For the location map please refer to Appendix A. CARB is routinely taken data. See text for details.

In Figure 5.4, CARB stand for data taken from California Air Resource Board monitoring station, which is located at North Main Street in Los Angeles. Site-related concentration variation was not obvious in Los Angeles. Meteorological data shows wind speed in this area

was quite low, mostly lower than 1 m/s, leading to uniform concentrations across all sites. As the boundary layer grows throughout the day, the street level concentrations are decreasing.

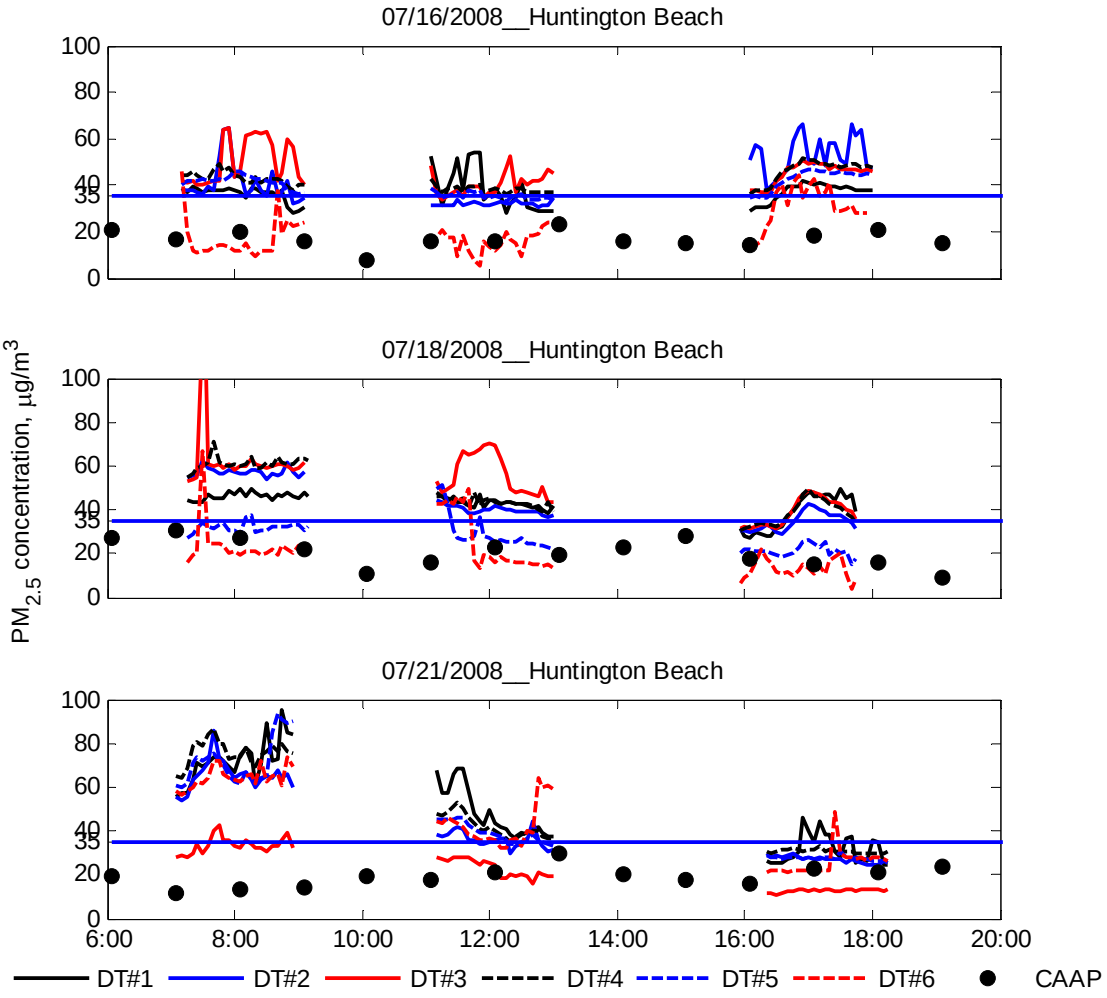

Figure 5.5 Three days of particulate measurements in Huntington Beach. The straight blue line represents national ambient Air Quality standards for $PM_{2.5}$ for 24-hour concentration (35 $\mu g/m^3$). DT stands for a DustTrak at the corresponding location. For the location map please refer to Appendix A. CAAP is routinely taken data. See text for details.

In Figure 5.5, CAAP stands for data taken from Clean Air Action Plan monitoring station, which is located at the inner port of Long Beach (closest station to Huntington Beach). Concentrations measured by DustTraks varied significantly from site to site. This variation was successfully reproduced in the QUIC model and is attributed to the morphology of Huntington Beach site (see Section 4).

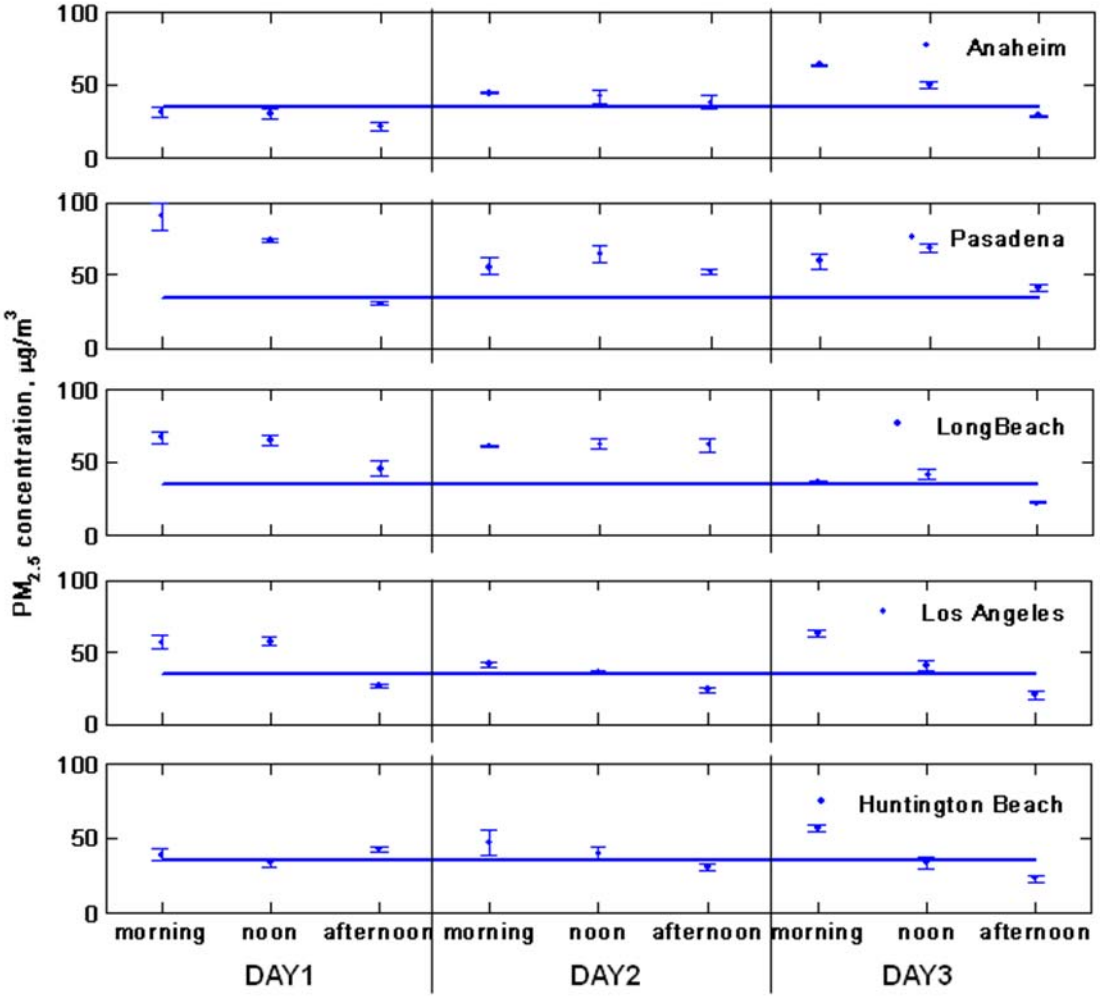

Figure 5.6 Three days of particulate measurements in all five sites averaged for each period over all measuring stations. The straight blue line represents national ambient Air Quality standards for $PM_{2.5}$ for 24-hour concentration (35 µg/m^3).

Figure 5.6 presents 3 days of data for all 5 sites averaged over all measured locations. Pasadena and Long Beach had the highest measured concentrations at the street level, and they were above the national standard.

5.2 Walkthrough DustTrak data

Members of the research team walked along designated routes within the study areas while measuring particulate matter concentration with a DustTrak. Each person carried a DustTrak in a backpack with a 32" aluminum tube attached to the DustTrak inlet protruding. The DustTrak data provide second-by-second measurements of particulate matter concentration. Route maps for each study area are shown in Figures 5.7 through 5.12, with median wind direction during each walkthrough time period indicated on the maps.

Members of the research team also recorded traffic conditions with a handheld video camera while walking the routes. We obtained traffic counts concurrent with the DustTrak readings from the resulting video files. We classified vehicles as cars, trucks, or buses to broadly account for the different emission factors of different classes of vehicles. The car category includes light trucks and smaller vehicles. The truck category includes delivery trucks and larger vehicles. We organized the counts into street segments and intersections. The endpoints of a street segment are the cross-streets at either end, and the count is the number of vehicles that passed along the adjacent street in either direction while the person walked from one endpoint to the other. The count for an intersection is the number of vehicles that passed through the intersection in any direction from the time the person reached the intersection to the time he or she reached the opposite side of the street. Thus, the intersection counts include both the time spent standing at the intersection, waiting to cross, and the time spent walking across the street. We obtained the time to the nearest second at each cutoff point from the video files.

We augmented the field data with building density measures obtained from parcel records for the three study areas in Los Angeles County. The parcel records contain the square feet of floor space in each parcel. We calculated the area of each parcel from the corresponding shapefile using ArcMap 9.2.

Figure 5.7 Map of walkthrough routes in Anaheim study area.

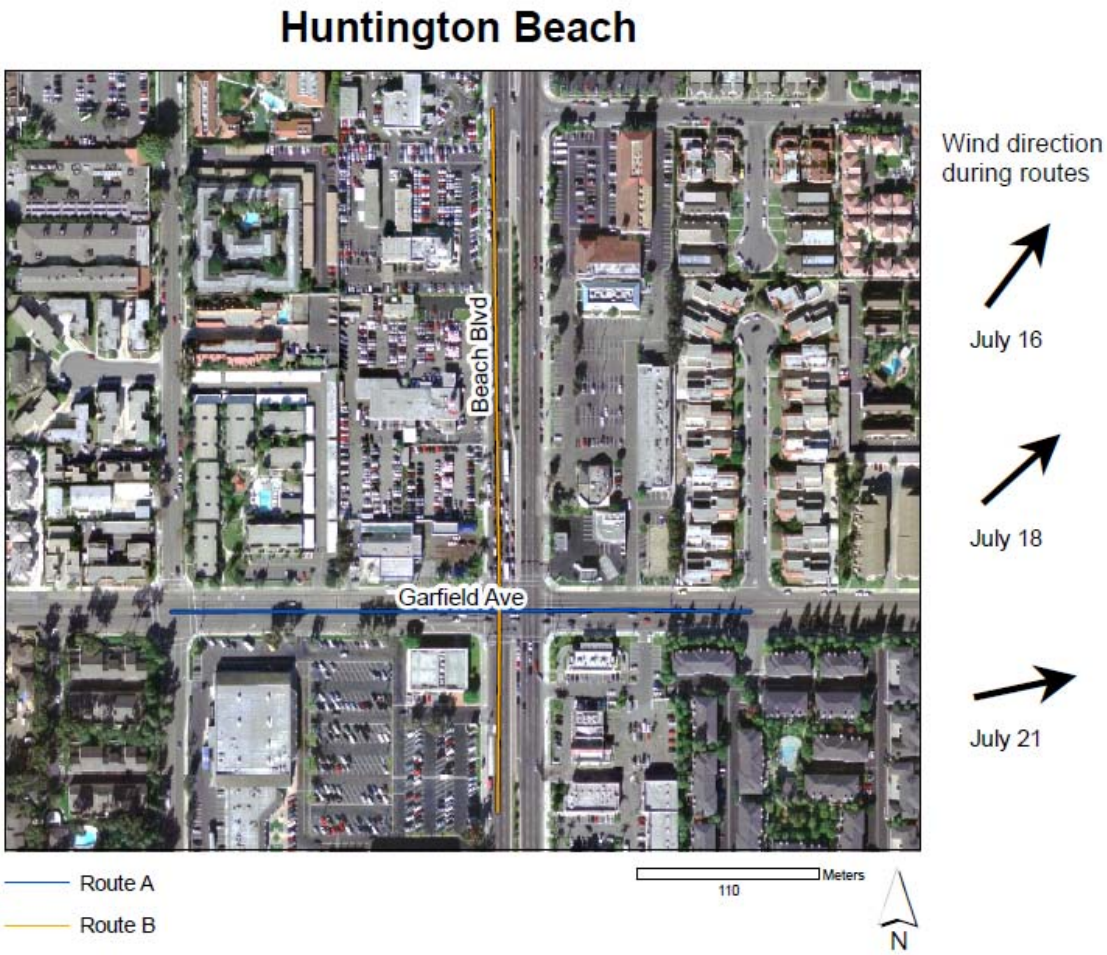

Figure 5.8 Map of walkthrough routes in Huntington Beach study area.

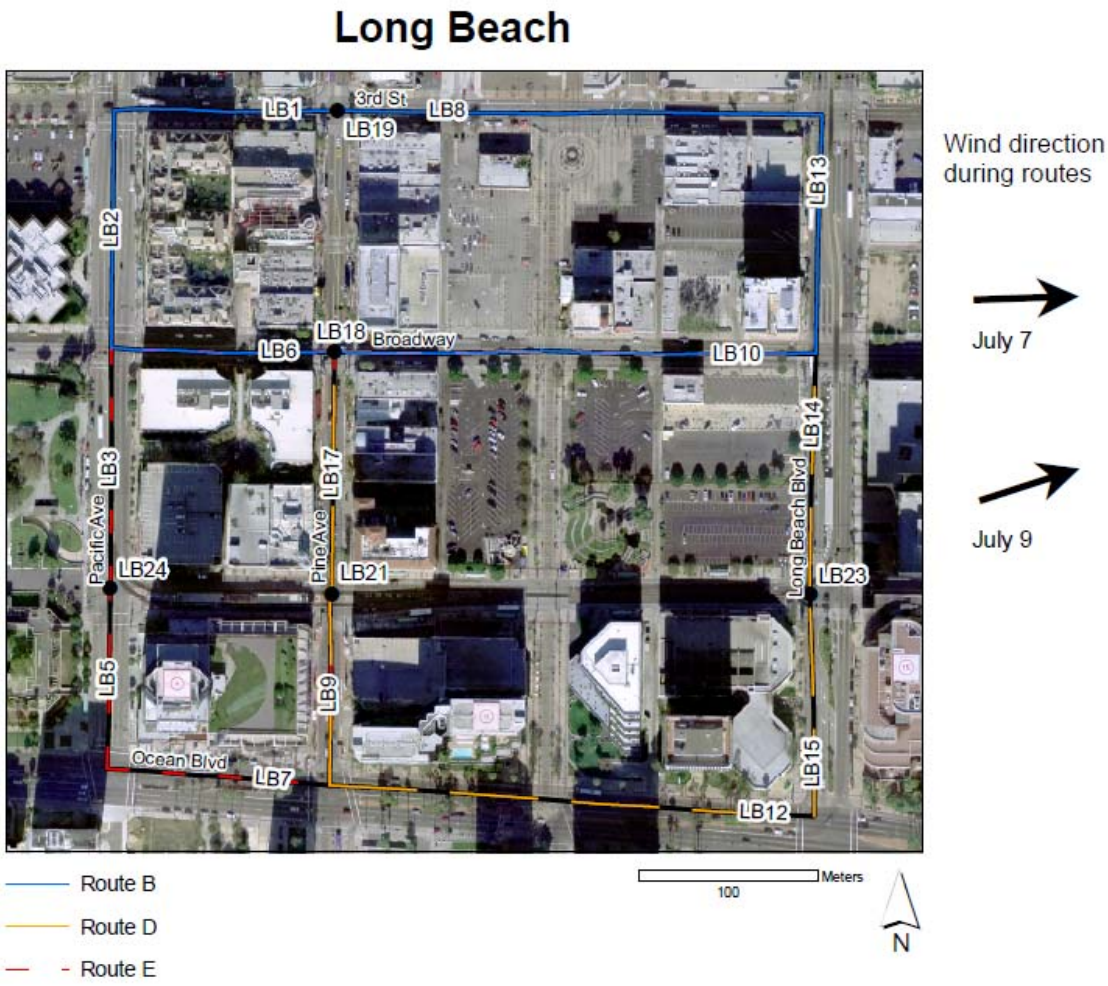

Figure 5.9 Map of walkthrough routes in Long Beach study area.

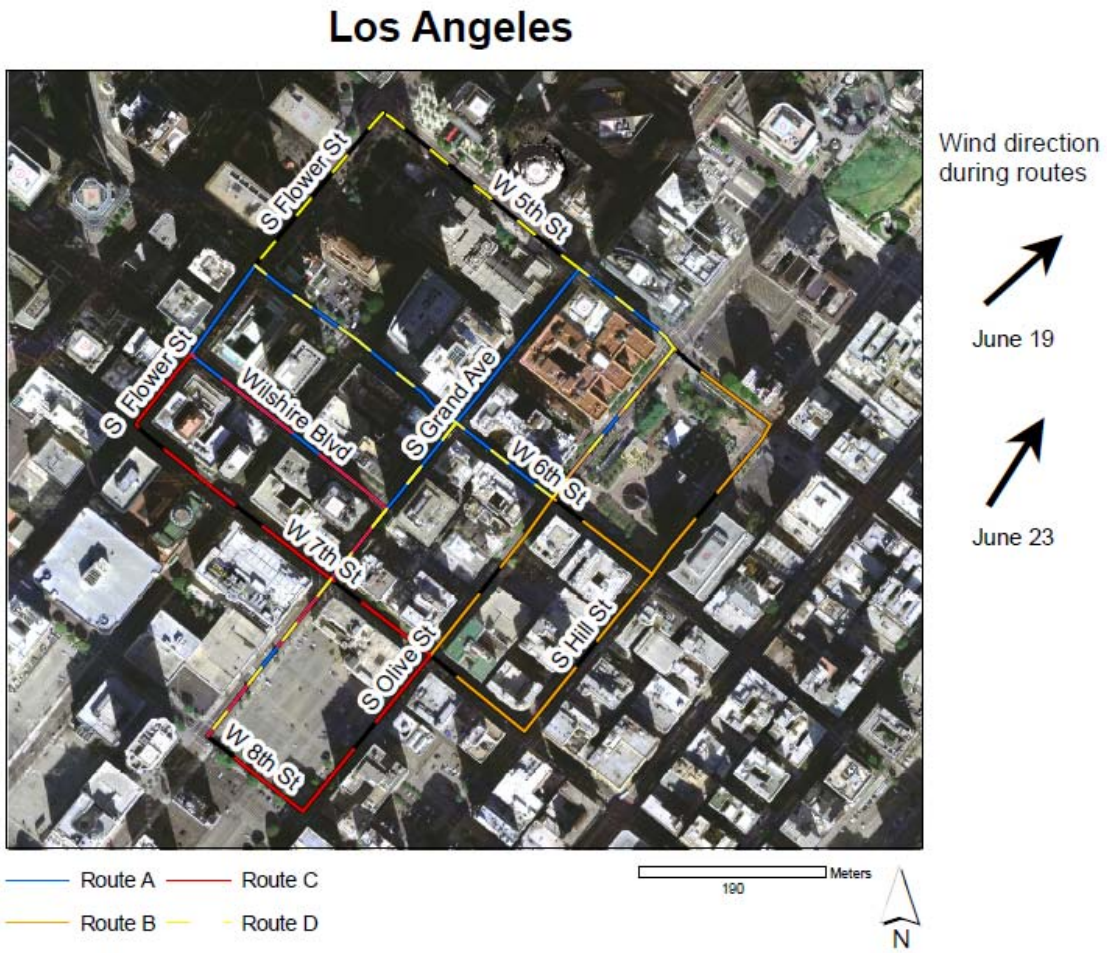

Figure 5.10 Map of walkthrough routes A through D in Los Angeles study area.

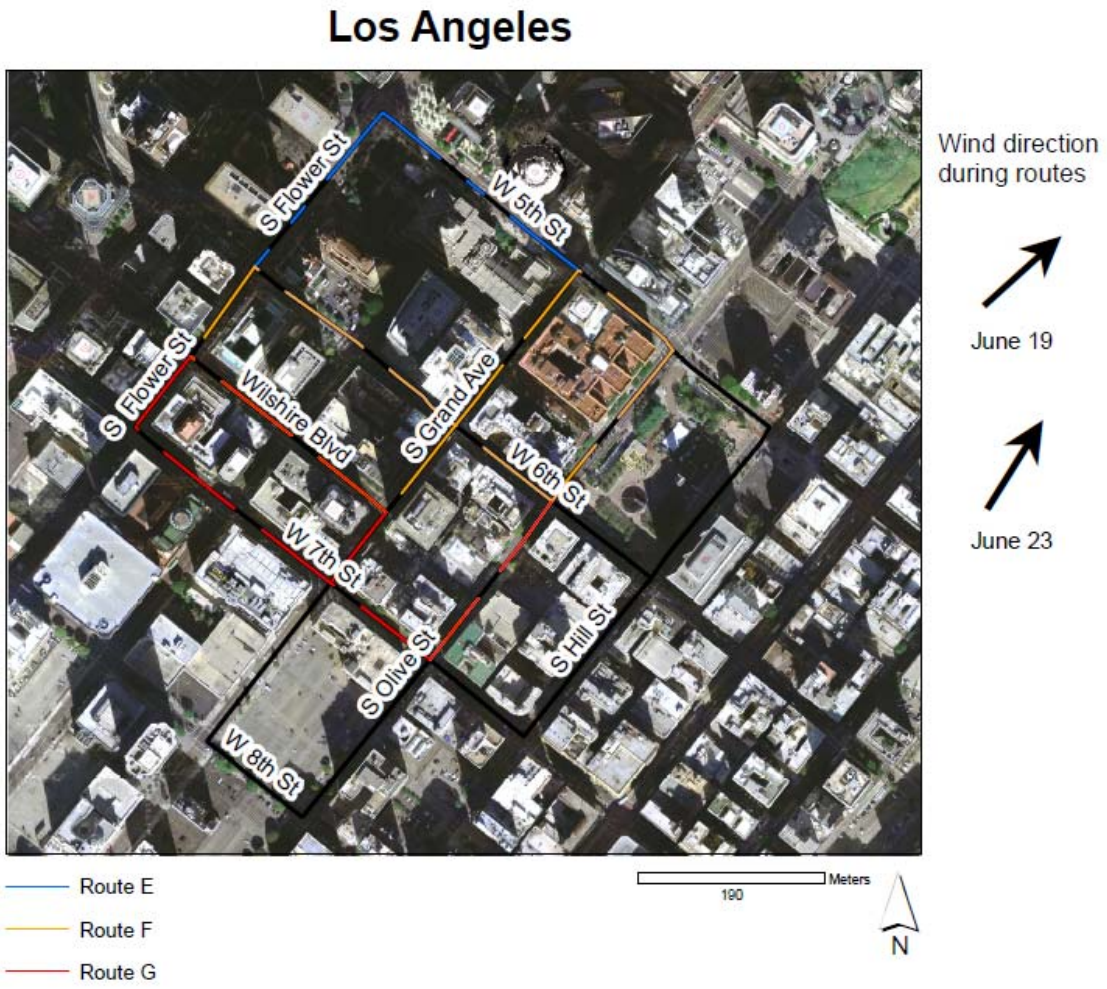

Figure 5.11 Map of walkthrough routes E, F, and G in Los Angeles study area.

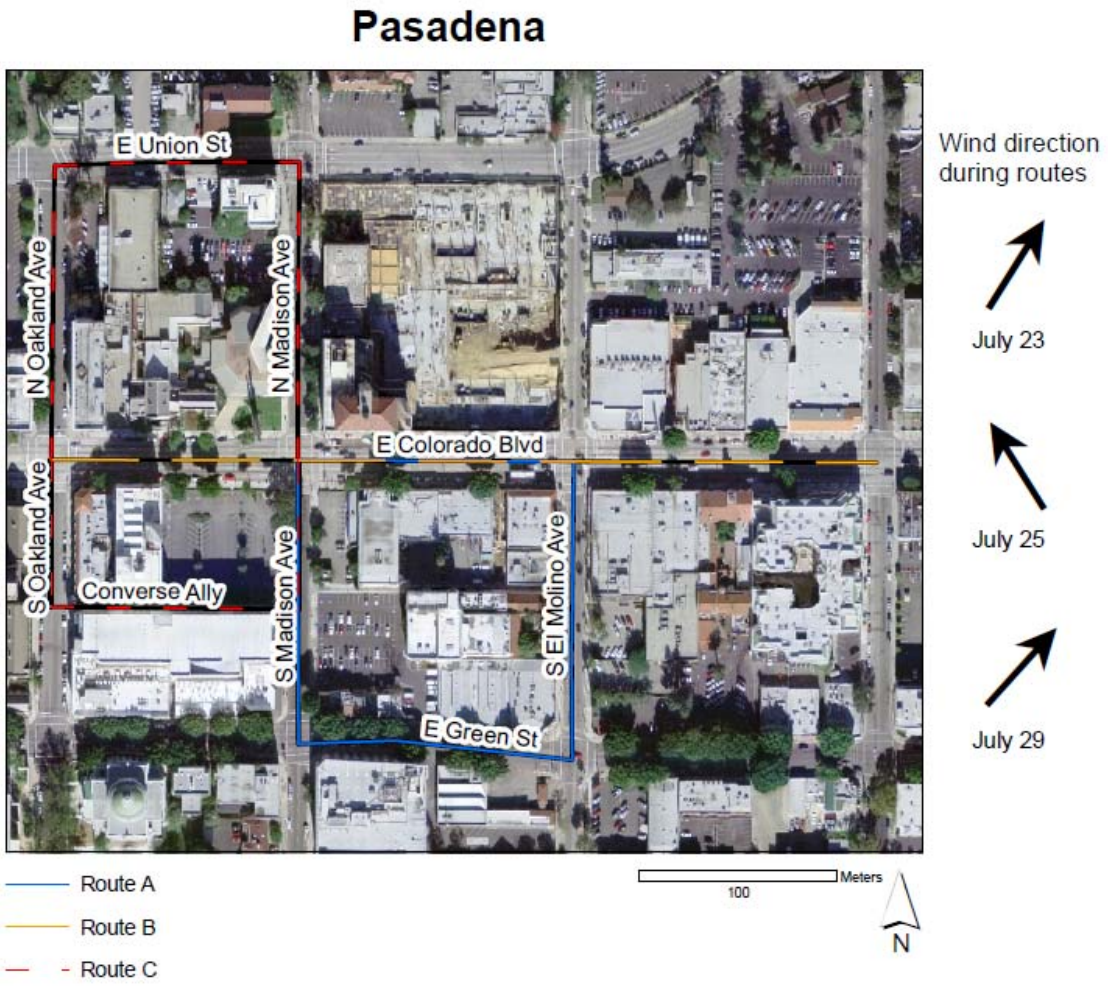

Figure 5.12 Map of walkthrough routes Pasadena study area.

Tables 5.2 through 5.5 contain summary statistics of one-second particulate matter concentrations, organized respectively by city, date, route, and date and route. In some cases, the minimum measured concentration is negative or the maximum measured concentration is much larger than the 99th percentile measurement. These are most likely measurement errors resulting from physical shock to the DustTrak.

Table 5.2 Summary statistics of one-second $PM_{2.5}$ concentrations ($\mu g/m^3$) encountered during walkthroughs, organized by city

City	n	Mean	Min[a]	1st Pctl.	25th Pctl.	50th Pctl.	75th Pctl.	99th Pctl.	Max
Anaheim	1,987	29.8	-7.3	14.7	26.1	28.6	30.8	46.3	1,874.1
Huntington Beach	13,262	31.4	12.0	17.0	28.0	31.8	35.0	46.8	554.9
Long Beach	8,072	36.6	12.5	15.3	19.7	45.2	49.7	60.4	304.3
Los Angeles	21,726	27.8	-8.2	18.4	24.4	27.0	29.6	50.8	1,418.3
Pasadena	13,097	53.0	26.8	44.1	49.8	52.5	55.2	68.4	1,315.8

Table 5.3 Summary statistics of one-second $PM_{2.5}$ concentrations ($\mu g/m^3$) encountered during walkthroughs, organized by date

City	Date	n	Mean	Min[a]	1st Pctl.	25th Pctl.	50th Pctl.	75th Pctl.	99th Pctl.	Max
Anaheim	7/30/08	1,038	28.9	-7.3	8.8	22.9	26.4	28.6	41.6	1,874.1
	7/31/08	949	30.8	21.6	23.7	28.6	29.9	31.9	46.3	88.5
Huntington	7/16/08	4,730	34.2	15.5	26.3	30.9	33.5	35.1	48.0	554.9
Beach	7/18/08	4,452	31.3	12.0	19.0	27.0	31.2	35.1	49.8	518.1
	7/21/08	4,080	28.2	15.5	16.3	20.7	28.4	32.9	43.0	60.2
Long Beach	7/7/08	4,436	49.6	29.6	41.0	46.7	49.0	51.9	64.9	197.1
	7/9/08	3,636	20.8	12.5	14.5	17.7	19.7	21.8	52.7	304.3
Los Angeles	6/19/08	8,657	25.4	-8.2	18.4	21.4	24.4	26.6	50.0	1,418.3
	6/23/08	13,069	29.3	6.6	22.9	26.1	28.1	30.2	51.0	387.0
Pasadena	7/23/08	3,688	56.6	42.7	48.1	53.5	55.4	58.1	73.4	1,315.8
	7/25/08	4,318	51.7	42.9	45.3	49.8	51.8	53.5	60.3	118.1
	7/29/08	5,091	51.7	26.8	41.8	48.4	51.0	54.0	68.6	167.9

Table 5.4 Summary statistics of one-second $PM_{2.5}$ concentrations ($\mu g/m^3$) encountered during walkthroughs, organized by route

City	Route	n	Mean	Min[a]	1st Pctl.	25th Pctl.	50th Pctl.	75th Pctl.	99th Pctl.	Max
Anaheim	A	985	30.2	-7.3	8.2	22.9	26.8	30.2	62.9	1874.1
	B	1,002	29.4	8.8	25.3	27.5	29.2	30.8	37.4	41.8
Huntington Beach	A	5,742	31.9	14.6	19.0	28.4	32.0	35.6	48.0	518.1
	B	7,520	31.0	12.0	17.0	27.3	31.6	34.9	44.5	554.9
Long Beach	B	4,220	35.6	12.5	14.5	18.7	44.0	49.7	59.8	304.3
	D	2,159	49.3	29.6	38.7	46.7	49.0	51.3	63.8	197.1
	E	1,693	22.9	13.1	15.3	18.6	20.8	23.0	49.1	147.7
Los Angeles	A	2,919	29.7	6.6	23.0	27.4	28.5	30.7	51.5	365.8
	B	2,742	30.5	17.2	21.7	26.9	29.0	31.2	57.0	387.0
	C	4,331	27.4	15.6	21.9	25.0	27.1	28.1	42.7	251.3
	D	3,136	30.5	15.0	24.0	28.0	29.0	32.0	57.0	188.0
	E	3,015	22.0	-8.2	17.4	20.4	21.4	22.5	40.8	161.3
	F	3,153	27.1	10.6	20.1	23.3	25.4	27.5	49.8	304.0
	G	2,430	27.6	20.2	21.1	23.9	25.7	27.5	60.6	1418.3
Pasadena	A	3,319	53.0	42.0	44.1	49.7	51.9	55.2	75.3	224.8
	B	6,846	53.8	37.8	44.3	50.8	53.5	56.0	68.4	1315.8
	C	2,932	51.2	26.8	40.7	48.8	50.8	53.6	64.3	79.3

Table 5.5 Summary statistics of one-second $PM_{2.5}$ concentrations ($\mu g/m^3$) encountered during walkthroughs, organized by route and date

City	Route	Date	n	Mean	Min[a]	1st Pctl.	25th Pctl.	50th Pctl.	75th Pctl.	99th Pctl.	Max
Anaheim	A	7/30/08	545	29.3	-7.3	4.1	21.2	22.9	25.3	79.2	1,874.1
	A	7/31/08	440	31.2	21.6	22.6	28.8	29.9	32.9	59.7	88.5
	B	7/30/08	493	28.4	8.8	24.2	27.5	28.6	29.7	35.2	37.4
	B	7/31/08	509	30.4	23.1	26.4	28.6	29.7	31.9	37.4	41.8
Huntington Beach	A	7/16/08	2,370	31.8	15.5	25.3	29.5	31.6	33.5	42.5	283.5
	A	7/18/08	1,748	30.5	14.6	18.3	21.9	32.9	36.3	54.4	518.1
	A	7/21/08	1,624	33.5	21.0	25.0	29.0	33.2	36.9	44.2	60.2
	B	7/16/08	2,360	36.6	27.5	29.9	32.8	34.7	36.3	58.5	554.9
	B	7/18/08	2,704	31.9	12.0	24.0	28.0	31.2	34.9	42.4	181.0
	B	7/21/08	2,456	24.6	15.5	16.3	19.2	25.0	29.5	37.5	57.9
Long Beach	B	7/7/08	2,212	50.2	40.6	42.9	47.4	49.7	51.9	66.6	126.5
	B	7/9/08	2,008	19.6	12.5	14.5	17.7	18.7	20.8	31.2	304.3
	D	7/7/08	2,088	49.2	29.6	38.7	46.7	49.0	51.3	64.9	197.1
	D	7/9/08	71	52.3	46.6	46.6	50.7	51.7	53.7	59.8	59.8
	E	7/7/08	136	45.7	41.3	41.3	44.2	45.2	47.2	52.1	54.1
	E	7/9/08	1,557	20.9	13.1	15.3	18.6	19.7	23.0	36.1	147.7
Los Angeles	A	6/23/08	2,919	29.7	6.6	23.0	27.4	28.5	30.7	51.5	365.8
	B	6/19/08	59	23.2	19.6	19.6	21.7	22.7	24.8	28.9	28.9
	B	6/23/08	2,683	30.6	17.2	22.6	26.9	29.0	31.2	58.1	387.0
	C	6/23/08	4,331	27.4	15.6	21.9	25.0	27.1	28.1	42.7	251.3
	D	6/23/08	3,136	30.5	15.0	24.0	28.0	29.0	32.0	57.0	188.0
	E	6/19/08	3,015	22.0	-8.2	17.4	20.4	21.4	22.5	40.8	161.3
	F	6/19/08	3,153	27.1	10.6	20.1	23.3	25.4	27.5	49.8	304.0
	G	6/19/08	2,430	27.6	20.2	21.1	23.9	25.7	27.5	60.6	1,418.3
Pasadena	A	7/23/08	1,156	55.5	45.0	47.0	52.3	55.4	57.5	71.1	224.8
	A	7/25/08	1,203	51.9	43.1	46.4	49.7	51.9	53.0	59.6	118.1
	A	7/29/08	960	51.5	42.0	44.1	47.4	49.5	52.7	95.8	167.9
	B	7/23/08	2,532	57.0	42.7	49.7	53.7	55.9	58.1	74.0	1,315.8
	B	7/25/08	1,792	52.3	44.5	46.6	50.0	52.3	54.0	60.3	88.9
	B	7/29/08	2,522	51.7	37.8	43.2	48.7	51.0	54.1	66.0	95.0
	C	7/25/08	1,323	50.7	42.9	44.9	48.8	50.8	52.8	60.8	77.7
	C	7/29/08	1,609	51.6	26.8	37.5	48.2	51.4	54.6	66.4	79.3

In four cases, two people walked the same route in tandem, one on each side of the street. Table 5.6 displays the results of two-sample t-tests comparing average particulate matter concentrations on opposite sides of the street for each case. The fifth column presents the sample difference in mean concentration and associated t-statistics for each route on each day. The sixth column displays the values of the same statistics obtained when we exclude the top one percent of measurements to eliminate possible influential measurement errors. The last two columns indicate the median wind direction and mean horizontal wind speed during each of the four cases.

Table 5.6 Results of t-tests comparing one-second $PM_{2.5}$ concentrations ($\mu g/m^3$) encountered on opposite sides of the street during parallel walkthroughs

City	Route	Date	n	Difference in mean conc. (t-statistic)	Difference in mean conc., highest 1% excluded (t-statistic)	High conc. side of street	Median wind direction	Mean horizontal wind speed (m/s)
Huntington Beach	A	7/16/08	2370	3.40 (11.77)	2.78 (24.46)	South	216˚ (SW)	1.41
	A	7/18/08	1748	13.52 (20.96)	14.35 (76.41)	South	228˚ (SW)	1.18
	A	7/21/08	1624	8.19 (52.74)	8.01 (56.57)	South	259˚ (W)	1.60
	B	7/16/08	2360	4.82 (5.25)	1.59 (12.73)	East	221˚ (SW)	1.32
	B	7/18/08	2704	6.82 (41.16)	6.45 (64.71)	East	228˚ (SW)	1.12
	B	7/21/08	2456	10.46 (98.09)	10.41 (117.27)	West	259˚ (W)	1.58
Pasadena	B	7/23/08	2532	2.51 (2.44)	1.05 (7.62)	North	212˚ (SW)	1.21
	B	7/25/08	1792	0.39 (2.65)	0.10 (0.81)	South	142˚ (SE)	0.80
	B	7/29/08	2522	2.40 (13.75)	2.10 (13.41)	South	220˚ (SW)	1.66

In addition to collecting data while walking, we also collected data for three two-hour periods each day at fixed locations. Table 5.7 displays results of two-sample t-tests comparing average particulate matter concentrations from sites on opposite sides of the street for three sites.

Table 5.7 Results of t-tests comparing one-second $PM_{2.5}$ concentrations ($\mu g/m^3$) at fixed locations on opposite sides of the street

City	Date	Street	n	Difference in mean conc. (t-statistic)	Difference in mean conc., highest 1% excluded (t-statistic)	High conc. side of street	Median wind direction	Mean horizontal wind speed (m/s)
Long Beach	7/2/08	Ocean Blvd.	42,668	14.64 (86.95)	14.79 (94.85)	S	262˚ (W)	1.10
	7/7/08	Ocean Blvd.	42,792	7.20 (50.65)	6.79 (50.54)	S	256˚ (W)	0.86
	7/9/08	Ocean Blvd.	42,612	11.09 (91.55)	11.30 (>100)	N	244˚ (SW)	1.05
Los Angeles	6/19/08	6th St.	26,340	6.15 (15.65)	4.25 (63.94)	SW	198˚ (S)	0.69
	6/23/08	6th St.	41,911	1.94 (14.37)	1.31 (15.68)	SW	216˚ (SW)	0.79
	6/30/08	6th St.	42,017	3.79 (6.90)	1.55 (8.69)	SW	207˚ (SW)	0.77
Pasadena	7/23/08	Colorado Blvd.	42,659	3.10 (0.25)	2.35 (9.35)	S	146˚ (SE)	1.04
	7/25/08	Colorado Blvd.	42,200	2.52 (10.55)	1.64 (27.64)	S	143˚ (SE)	0.74
	7/29/08	Colorado Blvd.	42780	3.29 (27.87)	2.93 (26.01)	S	171˚ (S)	0.92

Figures 5.13 through 5.21 are graphs of $PM_{2.5}$ concentrations measured on opposite sides of the streets during the parallel walkthroughs. Each graph plots particulate matter concentration versus time separately for each side of the street for comparison. We zeroed the time scale and eliminated gaps between repeated passes of the same route for the sake of presentation.

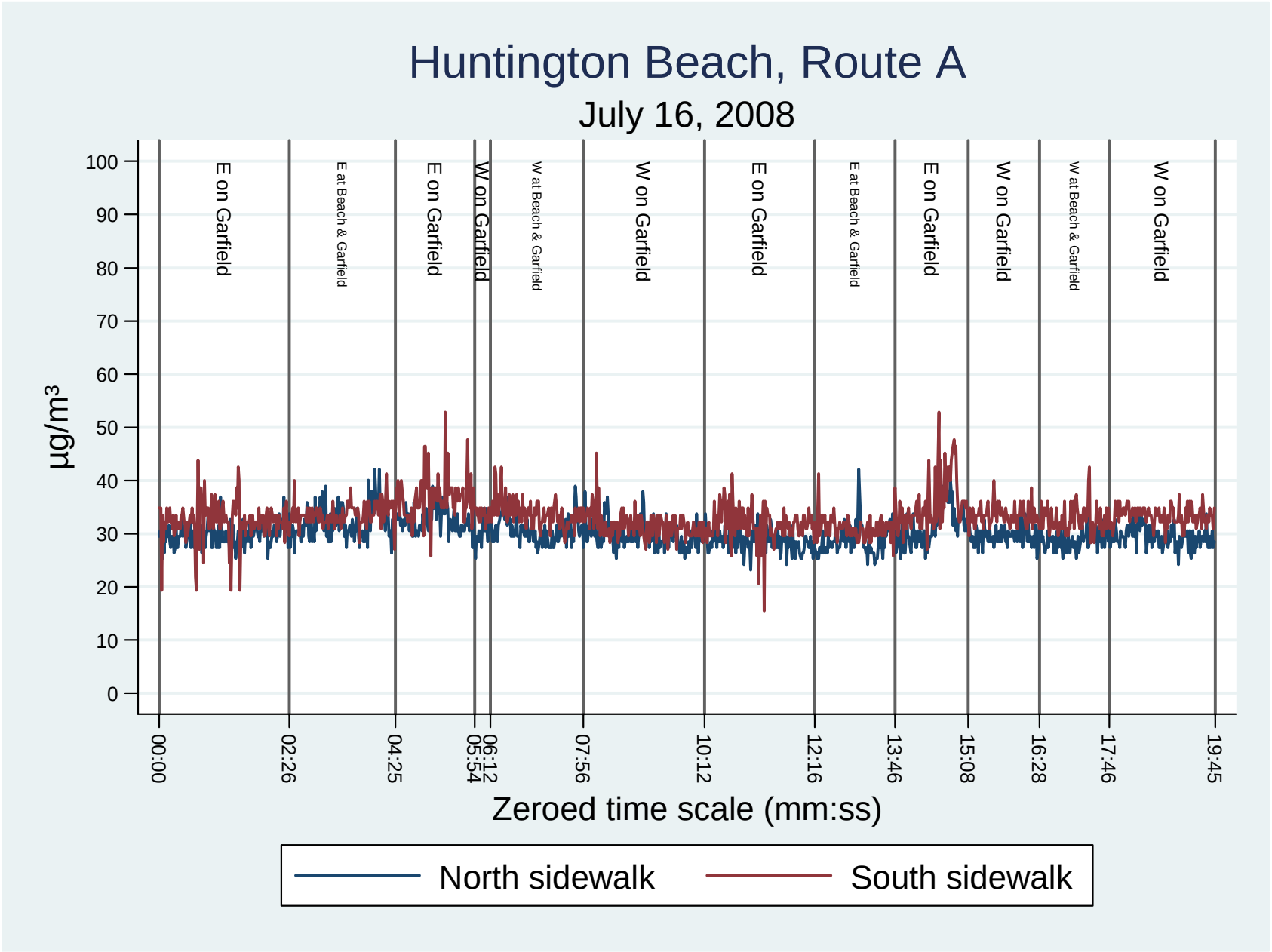

Figure 5.13 Plots of $PM_{2.5}$ concentrations on opposite sides of Garfield Ave. in Huntington Beach during July 16th walkthrough.

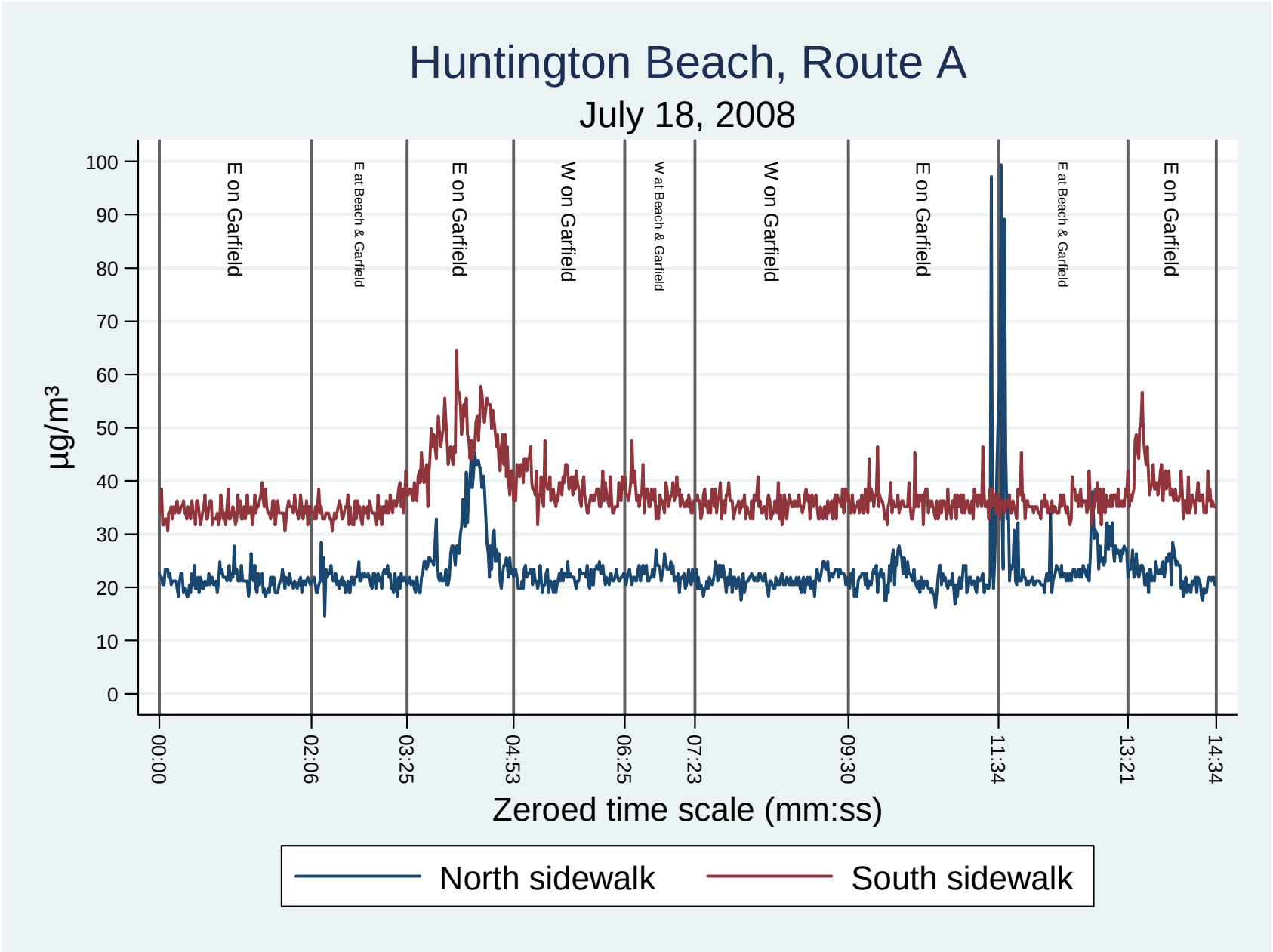

Figure 5.14 Plots of $PM_{2.5}$ concentrations on opposite sides of Garfield Ave. in Huntington Beach during July 18th walkthrough.

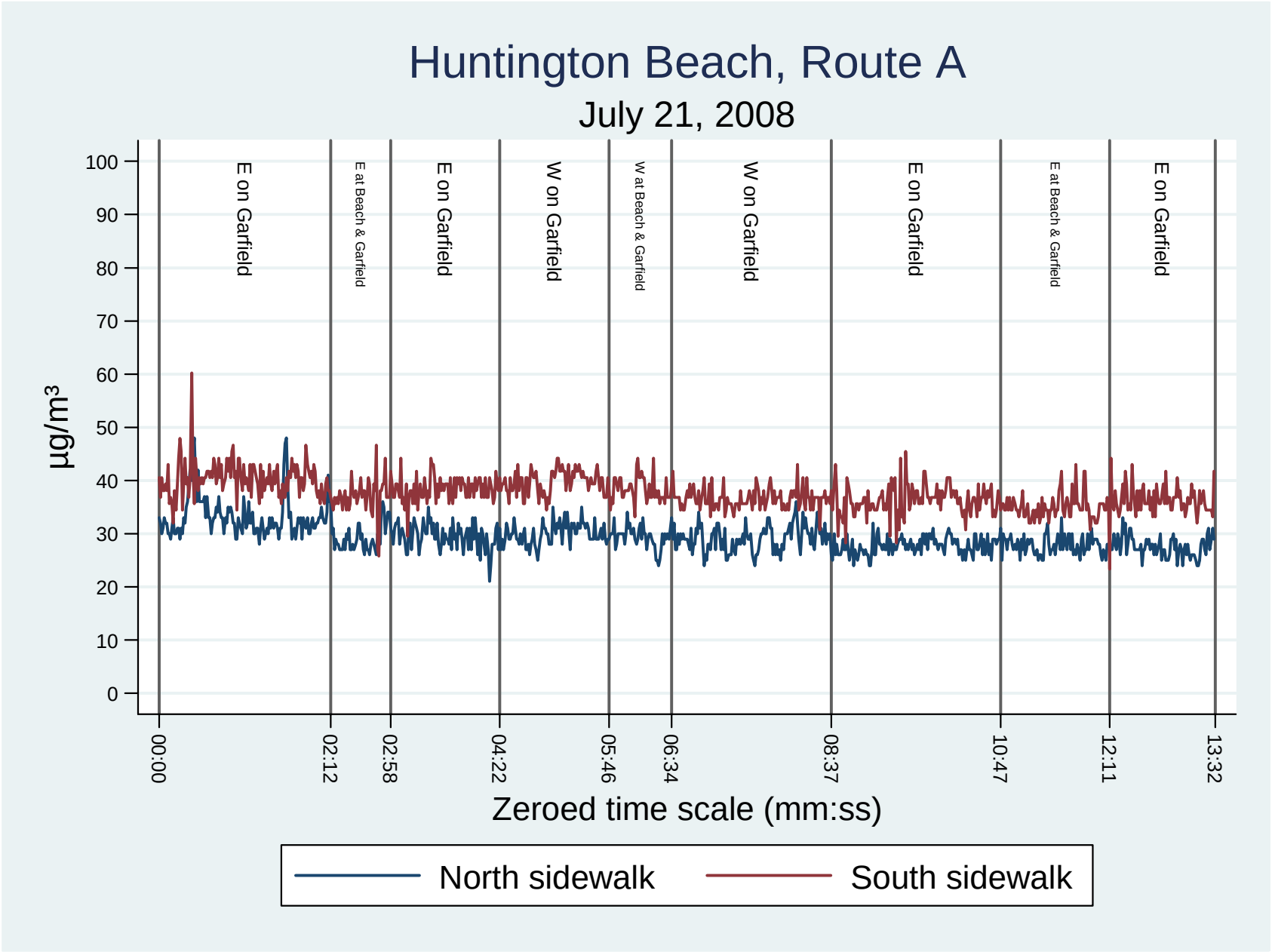

Figure 5.15 Plots of $PM_{2.5}$ concentrations on opposite sides of Garfield Ave. in Huntington Beach during July 21st walkthrough.

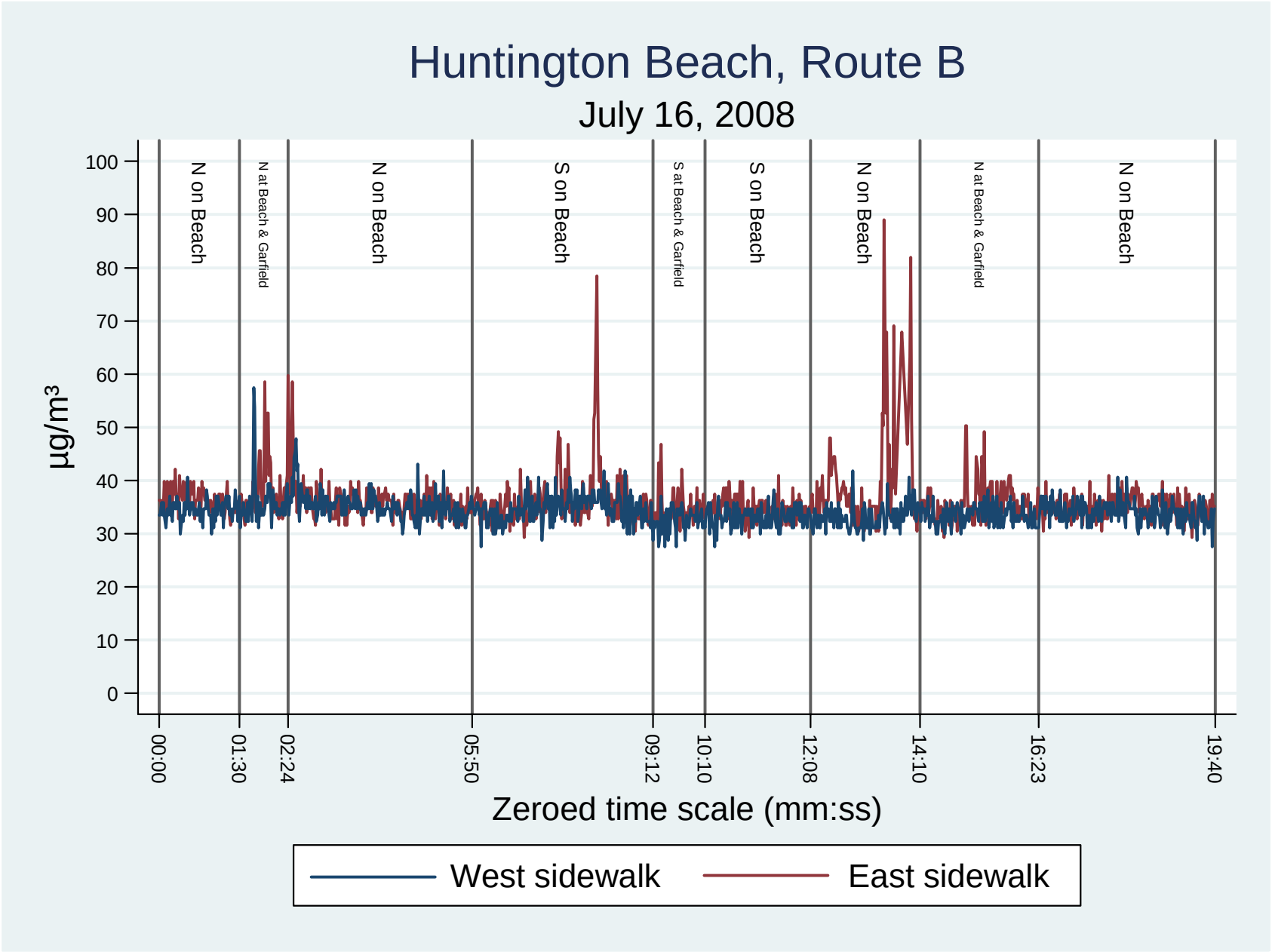

Figure 5.16 Plots of $PM_{2.5}$ concentrations on opposite sides of Beach Blvd. in Huntington Beach during July 16th walkthrough.

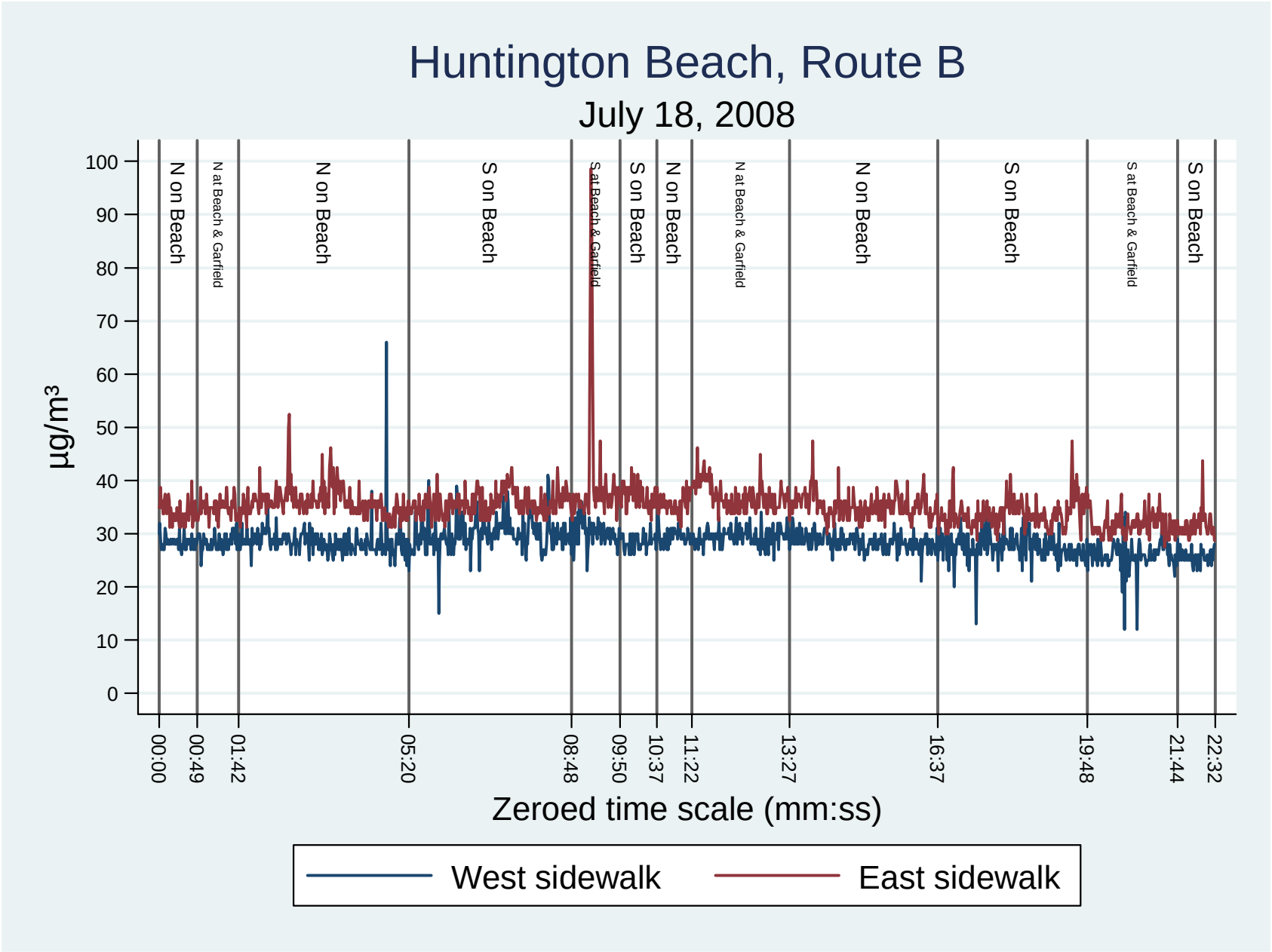

Figure 5.17 Plots of $PM_{2.5}$ concentrations on opposite sides of Beach Blvd. in Huntington Beach during July 18th walkthrough.

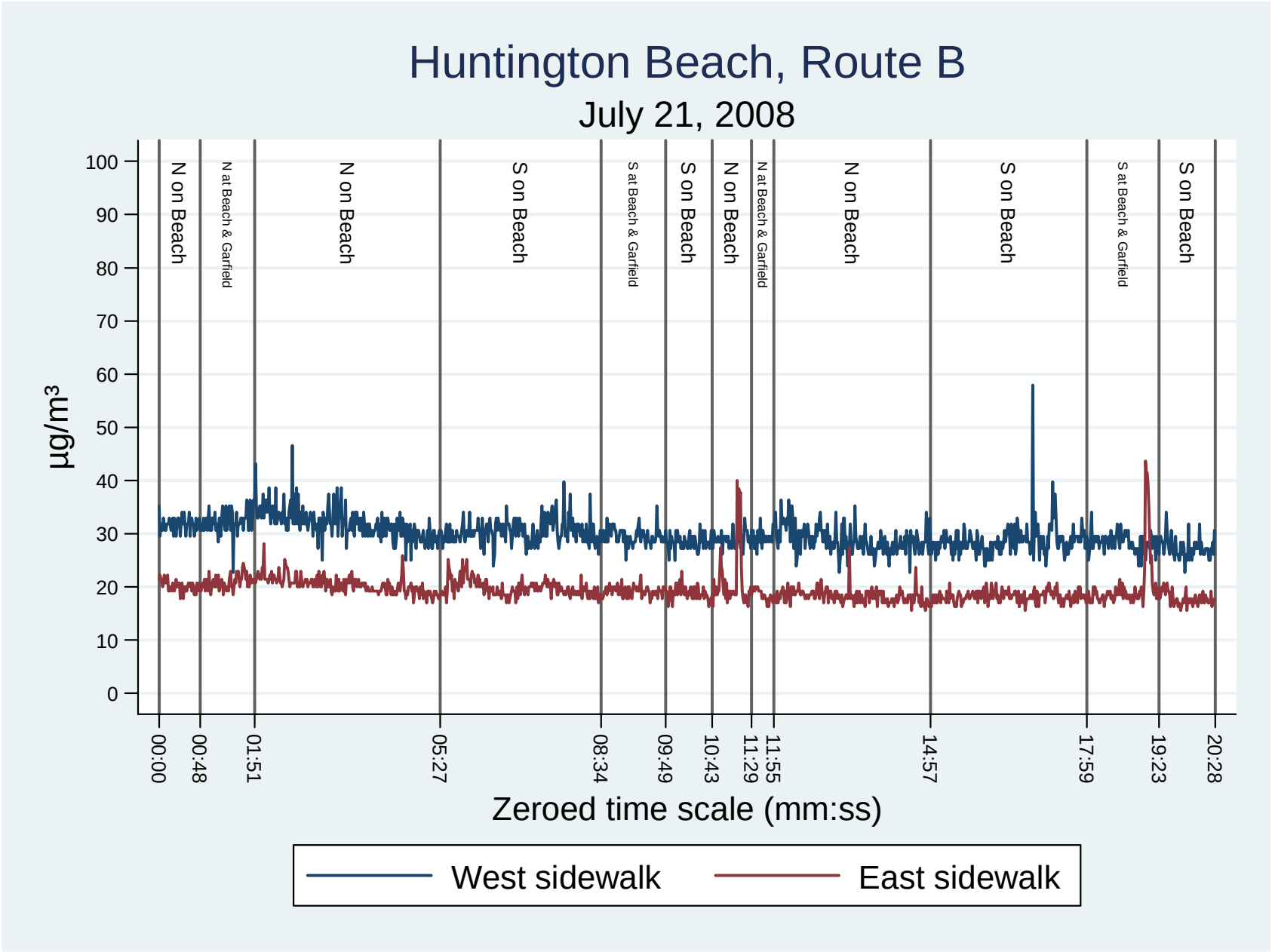

Figure 5.18 Plots of $PM_{2.5}$ concentrations on opposite sides of Beach Blvd. in Huntington Beach during July 21st walkthrough.

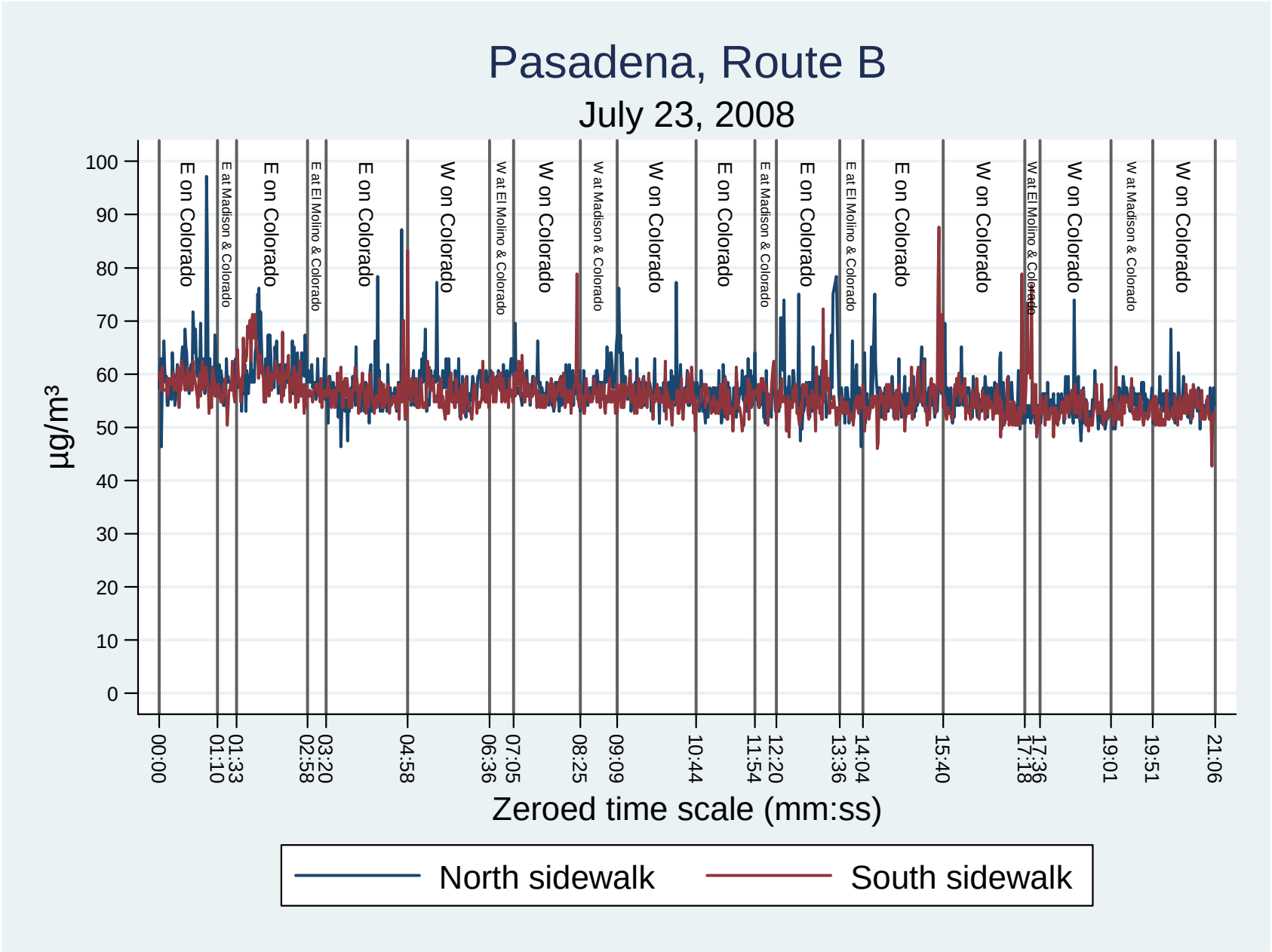

Figure 5.19 Plots of $PM_{2.5}$ concentrations on opposite sides of Colorado Blvd. in Pasadena during July 23rd walkthrough.

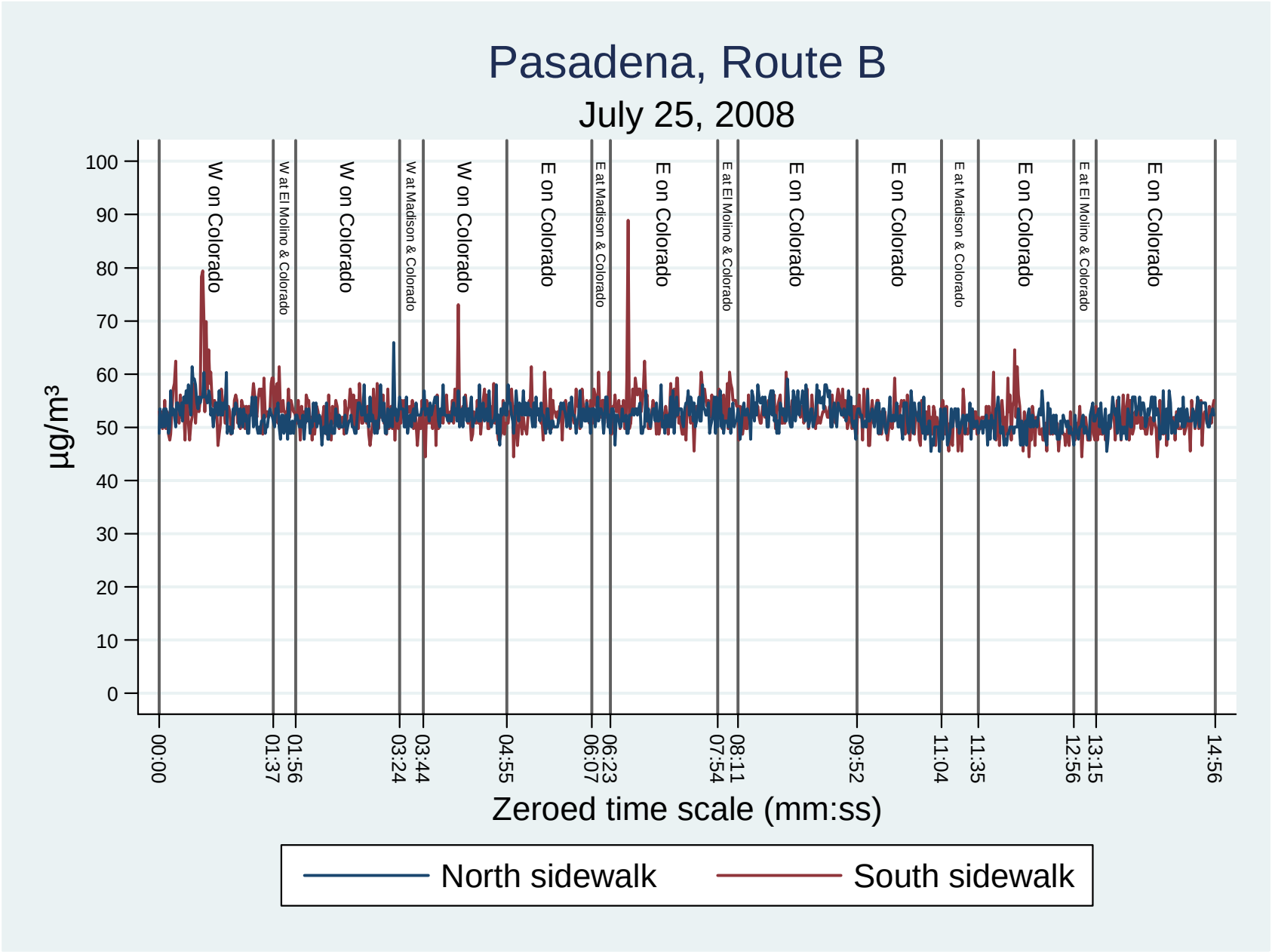

Figure 5.20 Plots of $PM_{2.5}$ concentrations on opposite sides of Colorado Blvd. in Pasadena during July 25th walkthrough.

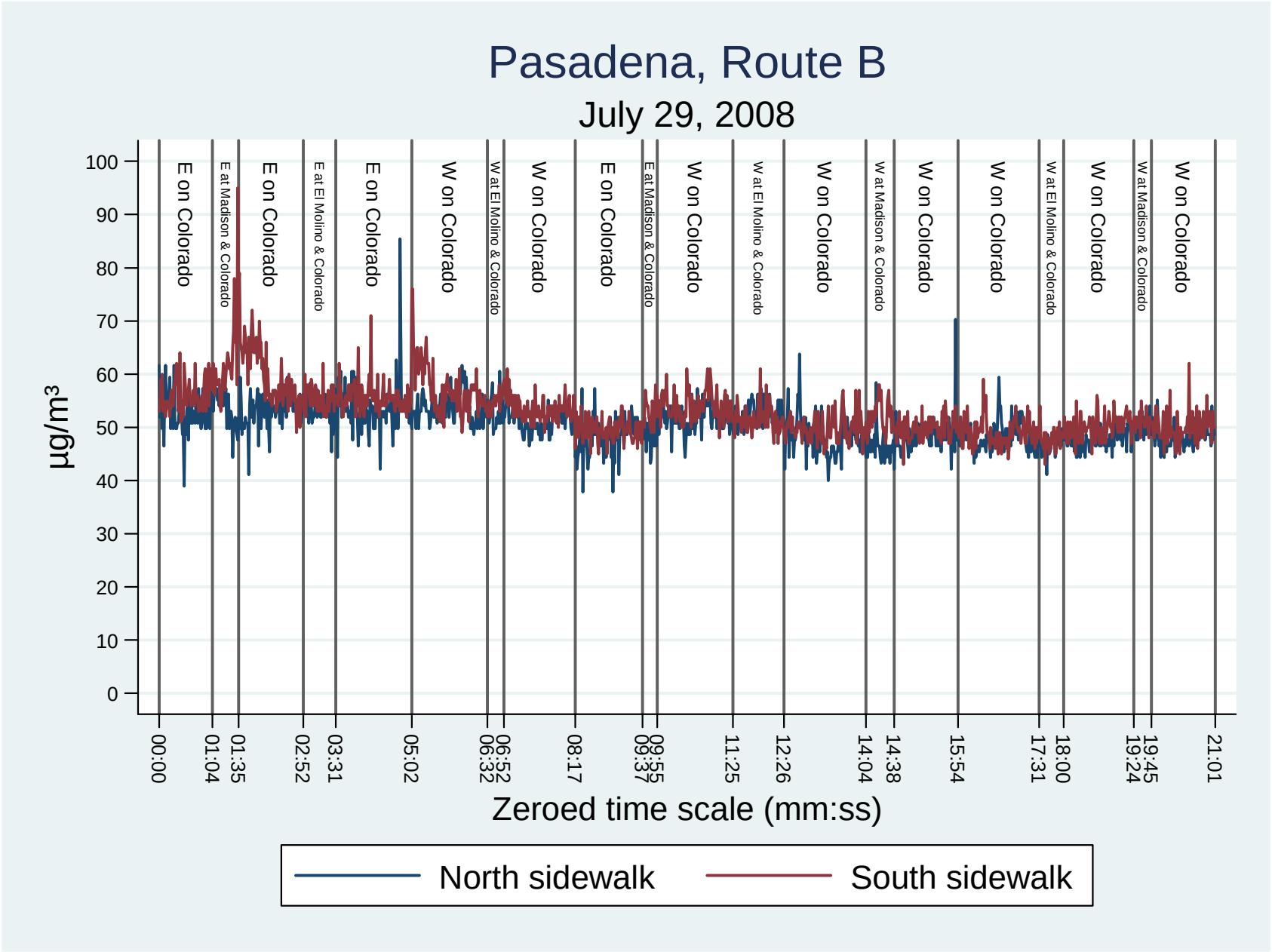

Figure 5.21 Plots of $PM_{2.5}$ concentrations on opposite sides of Colorado Blvd. in Pasadena during July 29th walkthrough.

We next ran several regressions using the data from three cities for which parcel data is available: Long Beach, Los Angeles, and Pasadena. The dependent variable is the average one-second particulate matter concentration for each traversal of a street segment or intersection. There are multiple observations for each street segment and intersection because team members traversed each route multiple times and some routes share common segments. To provide a buffer between street segments and adjacent intersections, we calculated the average for street segments using only readings from the middle 50% of the segment. The independent variables are:

- Cars per minute: Count of cars and light trucks divided by length of the traversal in minutes
- Heavy trucks per minute: Count of delivery trucks or larger vehicles (except buses) divided by length of the traversal in minutes
- Buses per minute: Count of buses divided by length of the traversal in minutes
- Floor-area-ratio: Sum of built square feet divided by sum of parcel square feet in parcels within 70ft for street segments or 100ft for intersections
- Indicator variables for city, date, and whether the observation corresponds to an intersection

Table 5.8 displays the results of the regressions. Huber-White standard errors are in parentheses. Specification (a) includes only the traffic flow variables, the floor-area ratio, and the intersection indicator. All of the variables except for car flow have the opposite of the expected sign, perhaps due to confounding variables that differ between cities. To control for this, we include city indicator variables in specification (b). As expected, the city indicator variables are significant, but the explanatory variables of interest are no longer significant. In specification (c) we attempt to control for unobserved factors more thoroughly by including indicator variables for each day in addition to each city. The coefficient on floor-area-ratio alone becomes significant, and it is positive.

Table 5.8 Results of regressions with average $PM_{2.5}$ concentration ($\mu g/m^3$) encountered along city blocks and intersections during walkthroughs as the dependent variable

Variable	(a)	(b)	(c)
Cars per minute	0.19***	0.03	0.02
	(0.04)	(0.03)	(0.02)
Heavy trucks per minute	-0.09	-0.23	0.12
	(0.62)	(0.36)	(0.15)
Buses per minute	-1.89***	-0.18	-0.06
	(0.32)	(0.13)	(0.10)
Floor-area-ratio	-1.45***	0.07	0.12*
	(0.11)	(0.06)	(0.06)
Intersection	-1.30	-0.45	-0.48
	(1.07)	(0.70)	(0.37)
Long Beach		7.31***	-8.38***
		(1.54)	(0.86)
Pasadena		24.97***	22.57***
		(0.59)	(0.56)
Date variables			3 of 4 significant at 0.001 level
Constant	41.20***	27.59***	28.73***
	(1.03)	(0.61)	(0.53)
n	654	654	654

*: $p < 0.05$; **: $p < 0.01$; ***: $p < 0.001$

5.3 Comparison of laboratory and numerical modeling

Figure 5.22 shows water channel simulation and QUIC modeling of Long Beach case with PIV/PLIF measurements in vertical plane. In both, model and laboratory, the pollution is trapped in the leeward side of building, producing concentrations much higher than at windward side. Due to big difference of building geometry between leeward side building and windward side building, the recirculating flow which is present within urban canopy with uniform building height is not formed here. The magnitude of mean velocity within the urban canopy is higher in the water channel experiment than in the QUIC modeling. The downdraft flow within the urban canopy measured in the laboratory (Figure 5.22a) is not reproduced by QUIC (Figure 5.22b). Also we can see higher mixing in laboratory (Figure 5.22a) where the street released plume is mixed all the way up to the building's roof level. However, in (Figure 5.22b), the vertical dispersion is less intense and pollutants are in higher concentration at the surface close to the leeward side.

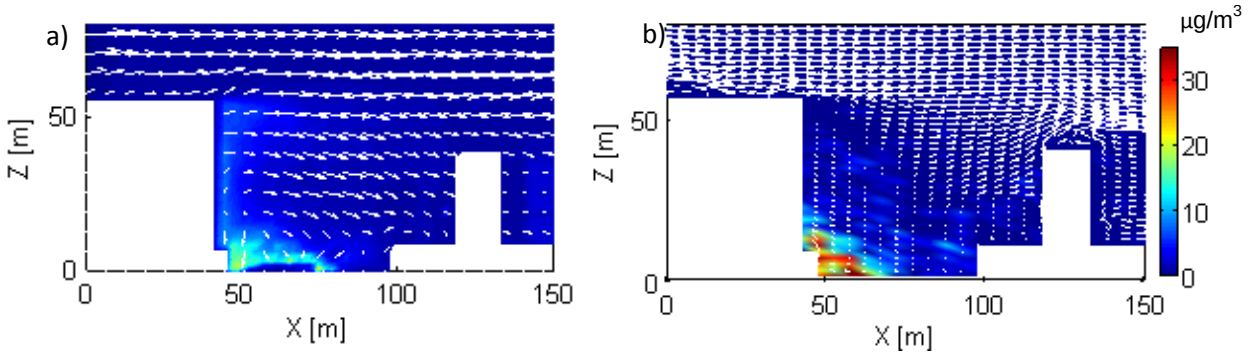

Figure 5.22 Velocity vectors (white arrows) and concentration distribution (color contours) of $PM_{2.5}$ in vertical plane: a) Water channel simulation, b) QUIC modeling.

References

Allwine, K. J., Leach, M., Stockham, L., et al. (2004) Overview of Joint Urban 2003 - An atmospheric dispersion study in Oklahoma City. Symposium on Planning, Nowcasting and Forecasting in the Urban Zone. American Meteorological Society, Januray 11-15, 2004, Seattle, Washington.

Allwine, K. J., Shinn, J. H., Streit, G. E., et al. (2002) Overview of URBAN 2000: A Multiscale Field Study of Dispersion through an Urban Environment. Bulletin of the American Meteorological Society. 83(4):521-536.

Ammann, C. (1999) On the applicablity of relaxed eddy accumulation and common methods for measuring trace gas surface fluxes. Thesis.

Bagal, N., Pardyjak,R.E. and Brown,J.M. (2003) Improved upwind cavity parameterization for a fast response urban wind model. AMS Conf.on Urban Zone,Seattle, WA.

Belcher, S. E. (2005) Mixing and transport in urban areas. Philosophical Transactions of the Royal Society A: Mathematical, Physical and Engineering Sciences. 363(1837):2947-2968.

Bottema, M. (1997) Urban roughness modelling in relation to pollutant dispersion. Atmospheric Environment. 31(18):3059-3075.

Britter, R. E. and Hanna, S. R. (2003) Flow and dispersion in urban areas. Annual Review of Fluid Mechanics. 35:469-496.

Cermak, J. E. (1984) Physical modelling of flow and dispersion over complex terrain. Boundary-Layer Meteorology. 30(1):261-292.

Coceal, O., Thomas, T., Castro, I., et al. (2006) Mean Flow and Turbulence Statistics Over Groups of Urban-like Cubical Obstacles. Boundary-Layer Meteorology. 121(3):491-519.

Counehan, J. (1971) Wind tunnel determination of the roughness length as a function of the fetch and the roughness density of three-dimensional roughness elements. Atmospheric Environment (1967). 5(8):637-642.

Dockery, D. W. a. P., C. A. (1994) Acute respiratory effects of particulate air pollution. Annual Review of Public Health. 15:107-132.

Eliasson, I., Offerle, B., Grimmond, C. S. B., et al. (2006) Wind fields and turbulence statistics in an urban street canyon. Atmospheric Environment. 40(1):1-16.

EPA, U. S. (2002) Air emission sources. http://www.epa.gov/air/emissions/pm.htm.

Gowardhan, A. A., Brown, M. J., DeCroix, D. S., et al. (2006a) Evaluation of the QUIC Pressure Solver Using Wind-Tunnel Data from Single and Multi-Building Experiments. 6th AMS Urban Environmental Symposium, Atlanta, GA.

Gowardhan, A. A., Brown, M. J., Williams, M. D., et al. (2006b) Evaluation of the QUIC Urban Dispersion Model using the Salt Lake City URBAN 2000 Tracer Experiment Data-IOP 10 6th AMS Urban Environmental Symposium, Atlanta, GA.

Grimmond, C. S. B. and Oke, T. R. (1999) Aerodynamic Properties of Urban Areas Derived from Analysis of Surface Form. Journal of Applied Meteorology. 38(9):1262-1292.

Grimmond, C. S. B. and Oke, T. R. (2002) Turbulent Heat Fluxes in Urban Areas: Observations and a Local-Scale Urban Meteorological Parameterization Scheme (LUMPS). Journal of Applied Meteorology. 41(7):792-810.

Hanna, S. R., Brown, M. J., Camelli, F. E., et al. (2006) Detailed simulations of atmospheric flow and dispersion in downtown Manhattan. Bulletin of the American Meteorological Society. 87(12):1713-1726.

Hanna, S. R. and Chang, J. C. (1992) Boundary-layer parameterizations for applied dispersion modeling over urban areas. Boundary-Layer Meteorology. 58(3):229-259.

Hanna, S. R., Reynolds, R. M., Heiser, J., et al. (2004) Plans for MSG04 tracer experiment in Manhattan. Fifth conference on urban environment. American Meteorological Society, August 23-26, 2004, Vancouver, Canada.

Hanna, S. R., Tehranian, S., Carissimo, B., et al. (2002) Comparisons of model simulations with observations of mean flow and turbulence within simple obstacle arrays. Atmospheric Environment. 36(32):5067-5079.

Hoydysh, W. G. and Dabberdt, W. F. (1988) Kinematics and dispersion characteristics of flows in asymmetric street canyons. Atmospheric Environment (1967). 22(12):2677-2689.

Kaimal, J. C. and Finnigan, J. J. (1994) Atmoshperic boundary layer flows.

Kastner-Klein, P., Berkowicz, R. and Britter, R. (2004) The influence of street architecture on flow and dispersion in street canyons. Meteorology and Atmospheric Physics. 87(1):121-131.

Kastner-Klein, P., Fedorovich, E. and Rotach, M. W. (2001) A wind tunnel study of organised and turbulent air motions in urban street canyons. Journal of Wind Engineering and Industrial Aerodynamics. 89(9):849-861.

Kastner-Klein, P. and Rotach, M. W. (2004) Mean Flow and Turbulence Characteristics in an Urban Roughness Sublayer. Boundary-Layer Meteorology. 111(1):55-84.

Kovar-Panskus, A., Louka, P., Sini, J.-F., et al. (2002) Influence of Geometry on the Mean Flow within Urban Street Canyons – A Comparison of Wind Tunnel Experiments and Numerical Simulations. Water, Air, and Soil Pollution. Focus 2:365–380.

Lettau, H. (1969) Note on Aerodynamic Roughness-Parameter Estimation on the Basis of Roughness-Element Description. Journal of Applied Meteorology. 8(5):828-832.

Lien, F.-S. and Yee, E. (2004) Numerical Modelling of the Turbulent Flow Developing Within and Over a 3-D Building Array, Part I: A High-Resolution Reynolds-Averaged Navier—Stokes Approach. Boundary-Layer Meteorology. 112(3):427-466.

Louka, P., Vachon, G., Sini, J. F., et al. (2002) Thermal Effects on the Airflow in a Street Canyon – Nantes'99 Experimental Results and Model Simulations. Water, Air, & Soil Pollution: Focus. 2(5):351-364.

MacDonald, R. W. (2000) Modelling The Mean Velocity Profile In The Urban Canopy Layer. Boundary-Layer Meteorology. 97(1):25-45.

MacDonald, R. W., Griffiths, R. F. and Hall, D. J. (1998a) A comparison of results from scaled field and wind tunnel modelling of dispersion in arrays of obstacles. Atmospheric Environment. 32(22):3845-3862.

MacDonald, R. W., Griffiths, R. F. and Hall, D. J. (1998b) An improved method for the estimation of surface roughness of obstacle arrays. Atmospheric Environment. 32(11):1857-1864.

Milliez, M. and Carissimo, B. (2007) Numerical simulations of pollutant dispersion in an idealized urban area, for different meteorological conditions. Boundary-Layer Meteorology. 122(2):321-342.

Nelson, M. A., Pardyjak, E. R., Klewicki, J. C., et al. (2007) Properties of the Wind Field within the Oklahoma City Park Avenue Street Canyon. Part I: Mean Flow and Turbulence Statistics. Journal of Applied Meteorology and Climatology. 46(12):2038-2054.

Oke, T. R. (1988) The urban energy balance. Progress in Physical Geography. 12:471-508.

Pardyjak, E. R., and Brown, M. (2002) Fast response modeling of a two building urban street canyon. 4th AMS Symp. Urban Env., Norfolk, VA.

Pardyjak, E. R., Bagal, N.L. and Brown, M.J. (2003) Improved velocity deficit parameterizations for a fast response urban wind model. AMS Conf. on Urban Zone, Seattle, WA.

Pardyjak, E. R. and Brown, M. J. (2001) Evaluation of a Fast-Response Urban Wind Model-Comparison to Single-Building Wind Tunnel Data. International Symposium on Environmental Hydraulics. Tempe, Arizona.

Pascheke, F., Barlow, J. and Robins, A. (2008) Wind-tunnel Modelling of Dispersion from a Scalar Area Source in Urban-Like Roughness. Boundary-Layer Meteorology. 126(1):103-124.

Randall, D. A. (2003) Dimensional Analysis, scale analysis, and similarity analysis. http://kiwi.atmos.colostate.edu/group/dave/teaching.html.

Raupach, M. R. (1994) Simplified expressions for vegetation roughness length and zero-plane displacement as functions of canopy height and area index. Boundary-Layer Meteorology. 71(1):211-216.

Raupach, M. R. and Legg, B. J. (1984) The uses and limitations of flux-gradient relationships in micrometeorology. Agricultural Water Management. 8(1-3):119-131.

Raupach, M. R., Thom, A. S. and Edwards, I. (1980) A wind-tunnel study of turbulent flow close to regularly arrayed rough surfaces. Boundary-Layer Meteorology. 18(4):373-397.

Rockle, R. (1990) Bestimmung der Stomungsverhaltnisse im Bereich komplexer Bebauungsstrukturen. Ph.D. thesis, Vom Fachbereich Mechanik,der Technischen Hochschule Darmstadt, Germany, .

Roth, M. (2000) Review of atmospheric turbulence over cities. Quarterly Journal of the Royal Meteorological Society. 126(564):941-990.

Schatzmann, M., Leitl, B. and Liedtke, J. (2000) Dispersion in Urban Environments; Comparison of Field Measurements with Wind Tunnel Results. Environmental Monitoring and Assessment. 65(1):249-257.

Simoëns, S., Ayrault, M. and Wallace, J. M. (2007) The flow across a street canyon of variable width--Part 1: Kinematic description. Atmospheric Environment. 41(39):9002-9017.

Simoëns, S. and Wallace, J. M. (2008) The flow across a street canyon of variable width--Part 2:: Scalar dispersion from a street level line source. Atmospheric Environment. 42(10):2489-2503.

So, E. S. P., Chan, A. T. Y. and Wong, A. Y. T. (2005) Large-eddy simulations of wind flow and pollutant dispersion in a street canyon. Atmospheric Environment. 39(20):3573-3582.

Vachon, G., Louka, P., Rosant, J. M., et al. (2002) Measurements of Traffic-Induced Turbulence within a Street Canyon during the Nantes'99 Experiment. Water, Air, & Soil Pollution: Focus. 2(5):127-140.

Vardoulakis, S., Fisher, B. E. A., Pericleous, K., et al. (2003) Modelling air quality in street canyons: a review. Atmospheric Environment. 37(2):155-182.

Venkatram, A. (2008) New Directions: The future modelling requirements to inform policy and legislation of urban air abatement. Atmospheric Environment. 42(16):3906-3907.

Williams, M. D., Brown, M. J., Boswell, D., et al. (2004a) Testing of the QUIC-PLUME Model with wind-turnnel measurements for a high-rise building. 5th AMS Urban Environmental Symposium, Vancouver, B. C., Canada.

Williams, M. D., Brown, M. J., Singh, B., et al. (2004b) QUIC-PLUME Theory Guide. Los Alamos National Laboratory.

Yee, E., Gailis, R., Hill, A., et al. (2006) Comparison of Wind-tunnel and Water-channel Simulations of Plume Dispersion through a Large Array of Obstacles with a Scaled Field Experiment. Boundary-Layer Meteorology. 121(3):389-432.

Williams, M. D., Brown, M. J., Boswell, D., et al. (2004a) Testing of the QUIC-PLUME Model with wind-turnnel measurements for a high-rise building. 5th AMS Urban Environmental Symposium, Vancouver, B. C., Canada.

Williams, M. D., Brown, M. J., Singh, B., et al. (2004b) QUIC-PLUME Theory Guide. Los Alamos National Laboratory.

Appendix A – Instrumentation Locations for five field studies

1. Low-density settlement – Anaheim

A typical residential area in the city of Anaheim, measuring 460 m × 323 m, was selected as the low-density settlement. The heights of buildings are from 3 m to 4 m. Figure A.1 shows the positions of the 6 measurement sites in this area. Table A.1 gives the latitude and longitude of each site, available instrument at the location and which road was recorded by video camera. The wind direction of the area in summertime is usually southwesterly, approximately 45° to the arterial, Harbor Blvd. Site 6, with the sonic anemometer, was located in the parking lot close to Lampson Avenue and had a relatively open view from the upwind direction. The height of the sonic anemometer was 1.4 m from the ground. Both Harbor Blvd. and Lampson Ave. are two-way roads.

Main Arterial: Harbor Blvd/ Lampson Avenue
Domain size: 460 m × 323 m

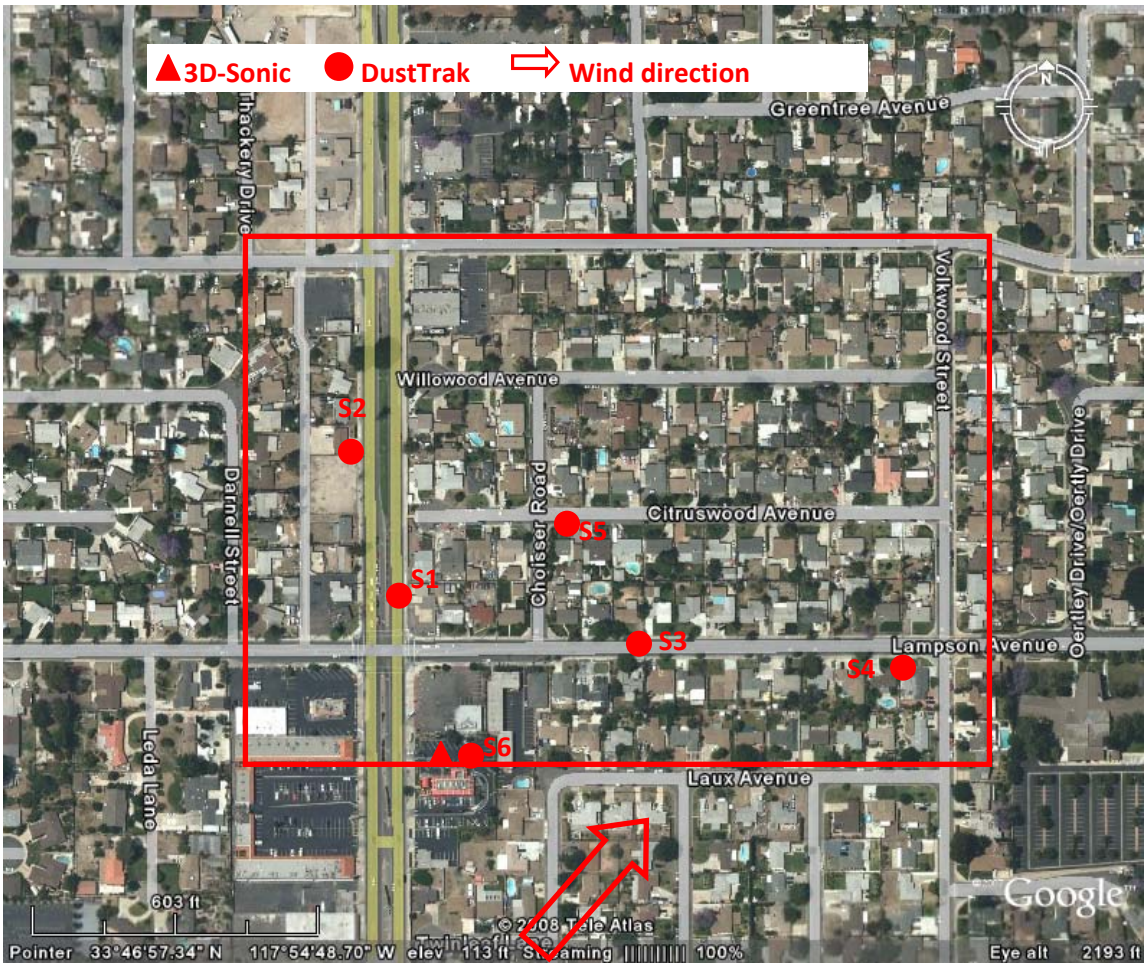

Figure A.1 Measurement domain and instrumentation in Anaheim.

Table A.1 Locations of instrumentation in Anaheim

Site No.	Longitude	Latitude	Instrument	Recording Road
S1	W 117°54'52"	N 33°46'55"	DustTrak1, Camera1	Harbor Blvd.
S2	W 117°54'54"	N 33°46'58"	DustTrak2, Camera2	Harbor Blvd.
S3	W 117°54'48"	N 33°46'54"	DustTrak3, Camera3	Lampson Ave.
S4	W 117°54'41"	N 33°46'54"	DustTrak4	
S5	W 117°54'49"	N 33°46'56"	DustTrak5	
S6	W 117°54'52"	N 33°46'52"	DustTrak6, 1 Sonic	

2. Low-rise settlement - Pasadena

A 423 m × 350 m area in the city of Pasadena was selected as the low-rise settlement. The heights of buildings are in range from 10 m to 20 m. The positions and descriptions of the 6 measurement sites in this area are shown in Figure A.2 and Table A.2. The wind direction of the area in summer is usually southwesterly, which is close to perpendicular to the arterial, East Colorado Blvd. Site 6, with the sonic anemometer, was located on the roof of a 4 story parking garage. The height of the sonic anemometer was 16 m from the ground. Both East Colorado Blvd. and El Molino Ave. are two-way roads. Madison Ave. is a one-way road.

Main Arterial: East Colorado Blvd/ El Molino Ave
Domain size: 423 m × 350 m

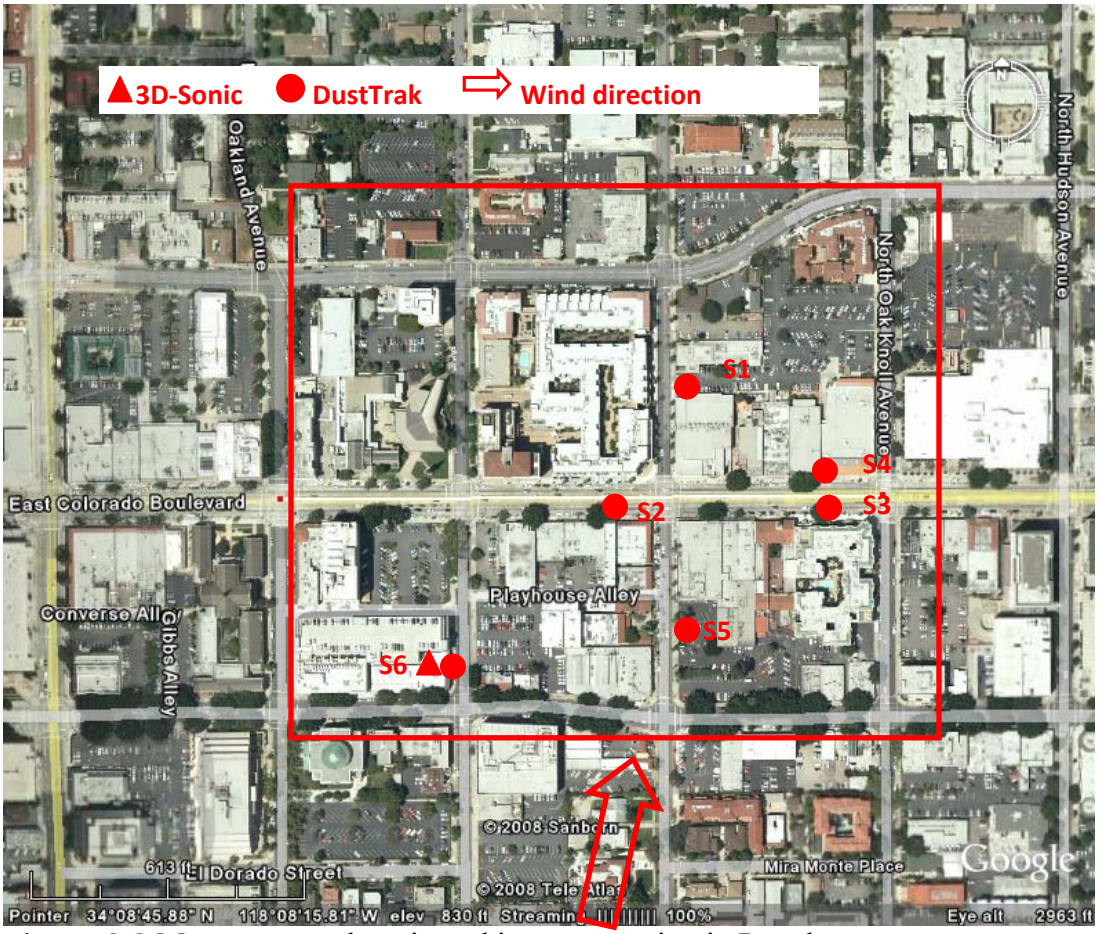

Figure A.2 Measurement domain and instrumentation in Pasadena.

Table A.2 Locations of instrumentation in Pasadena

Site Number	Longitude	Latitude	Instrument	Recording Road
S1	W 118°08'13"	N 34°08'43"	DustTrak1	
S2	W 118°08'17"	N 34°08'50"	DustTrak2, Camera1	East Colorado Blvd.
S3	W 118°08'14"	N 34°08'45"	DustTrak3, Camera2	East Colorado Blvd.
S4	W 118°08'18"	N 34°08'47"	DustTrak4, Camera3	El Molino Ave.
S5	W 118°08'14"	N 34°08'50"	DustTrak5	
S6	W 118°08'22"	N 34°08'41"	DustTrak6, 1 Sonic	

3. Mid-rise settlement - Long Beach

A 406 m × 512 m area in downtown Long Beach was selected as the mid-rise settlement. The heights of buildings are in range from 20 m to 80 m. The positions and descriptions of the 6 measurement sites in this area are shown in Figure A.3 and Table A.3. The wind direction of the area in summer is usually southerly, which is perpendicular to the arterial, East Ocean Blvd. Site 6, with the sonic anemometer, was located on the roof of a 6 story parking garage. The height of sensor was 24 m from the ground. East Ocean Blvd is a two-way road. Both Broadway and Pine Ave. are one-way roads.

Main Arterial: East Ocean Blvd
Domain size: 406 m × 512 m

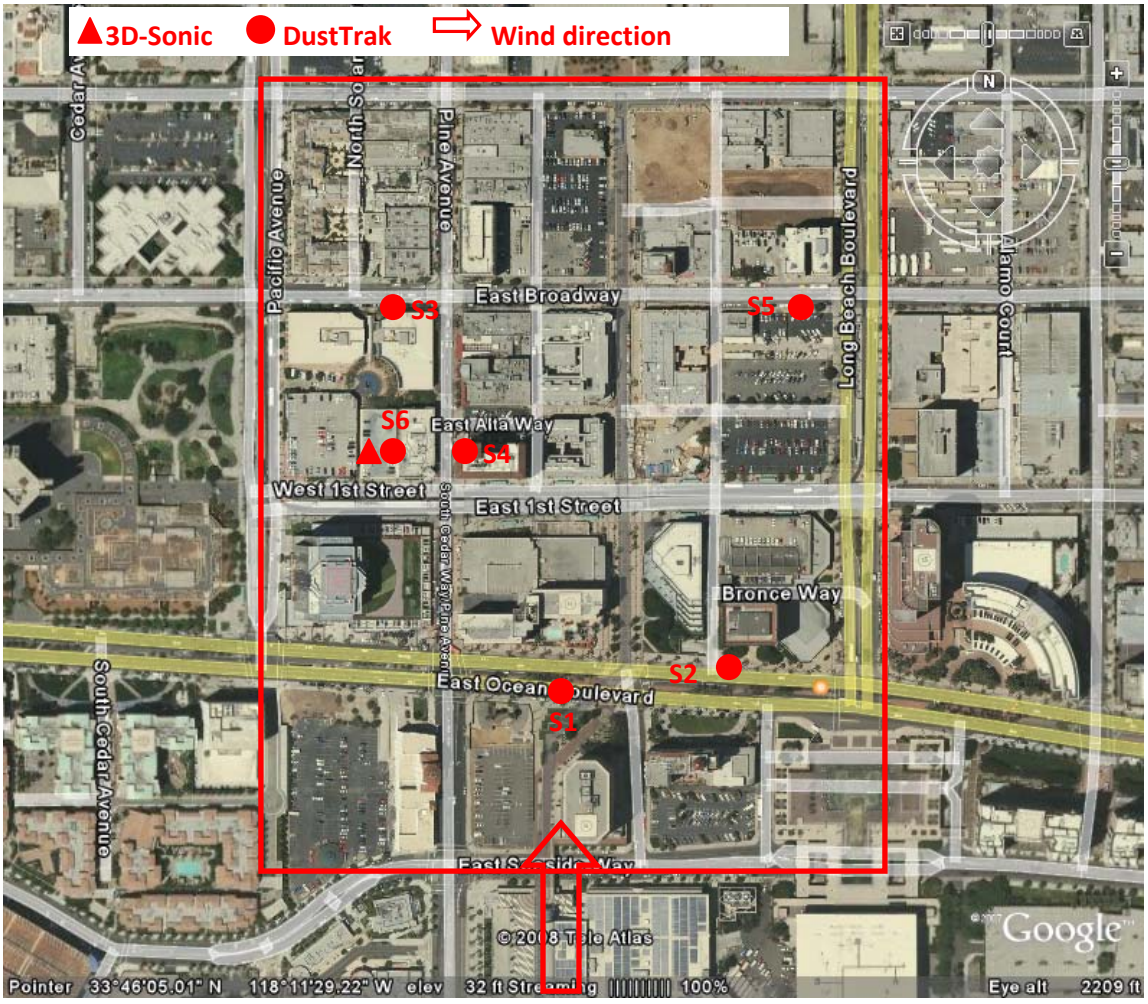

Figure A.3 Measurement domain and instrumentation in Long Beach.

Table A.3 Locations of instrumentation in Long Beach

Site Number	Longitude	Latitude	Instrument	Recording Road
S1	W 118°11'28"	N 33°46'01"	DustTrak1	
S2	W 118°11'26"	N 33°46'02"	DustTrak2, Camera1	East Ocean Blvd.
S3	W 118°11'34"	N 33°46'09"	DustTrak3	
S4	W 118°11'32"	N 33°46'06"	DustTrak4, Camera2	Pine Ave.
S5	W 118°11'24"	N 33°46'09"	DustTrak5, Camera3	Broadway
S6	W 118°11'35"	N 33°46'06"	DustTrak6, 1 Sonic	

4. High-rise settlement - Los Angeles

A 512 m × 466 m area in the downtown Los Angeles was selected as the high-rise settlement. The heights of buildings are in a range from 9 m to 258 m. The positions and descriptions of the 6 measurement sites in this area are shown in Figure A.4 and Table A.4. The wind direction of the area in summer is usually southwesterly, which is perpendicular to the arterial, 6th Ave. Site 6, with sonic anemometer, was located in the Pershing Square. The height of sonic anemometer is 1.4 m from the ground. Except for Hope St., Wilshire Blvd. and Hill St., which are two-way roads, all streets are one-ways. Site 7, which is on the roof of a 5 story parking garage, was added so that after each 2 hour measurement, DustTrak 5 was moved to this site to measure 10 minutes for the background measurement.

Main Arterial: 6th Ave / Grand Ave
Domain size: 512 m × 466 m

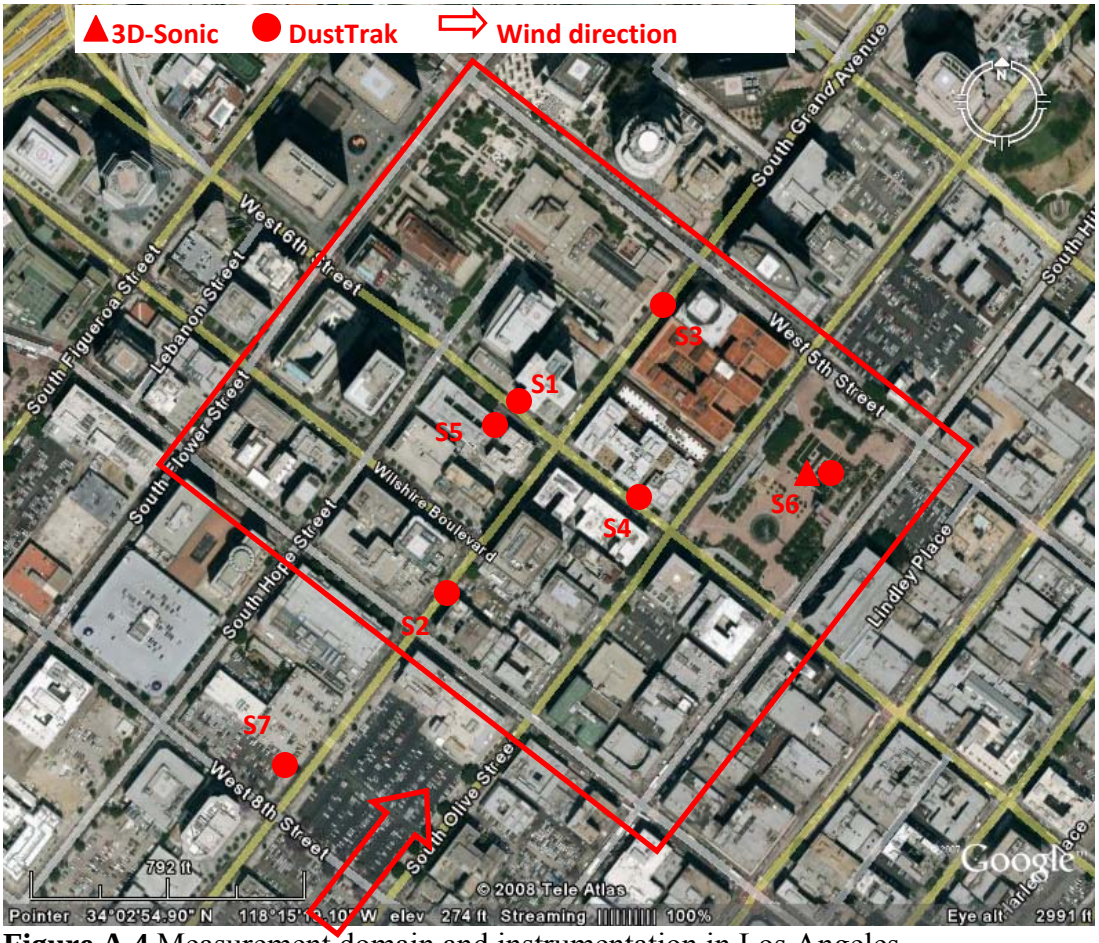

Figure A.4 Measurement domain and instrumentation in Los Angeles.

Table A.4 Locations of instrumentation in Los Angeles

Site Number	Longitude	Latitude	Instrument	Recording Road
S1	W 118°15'21"	N 33°02'57"	DustTrak1, Camera1	6th St.
S2	W 118°15'21"	N 33°02'53"	DustTrak2, Camera2	Grand Ave.
S3	W 118°15'16"	N 33°02'59"	DustTrak3, Camera3	Grand Ave.
S4	W 118°15'17"	N 33°02'55"	DustTrak4, Camera4	6th St.
S5	W 118°15'20"	N 33°02'56"	DustTrak5	
S6	W 118°15'10"	N 33°02'55"	DustTrak6, 1 Sonic	
S7	W 118°15'25"	N 33°02'50"	DustTrak5	

5. Strip mall - Huntington Beach

A 354 m × 500 m area in Huntington Beach was selected as the strip mall area. The heights of buildings are in a range from 3 m to 16 m. The positions and description of the 6 measurement sites in this area are shown in Figure A.5 and Table A.5. The wind direction of the area in summer is usually southwesterly, which has an approximate angle of 45° with the arterial, Beach Blvd. Site 6, with the sonic anemometer, was located in the parking lot close to the southern boundary of the domain, and it has a relatively open view from the upwind direction. The height of sonic anemometer was 1.4 m from the ground. All roads in this area are two-ways.

Main Arterial: Beach Blvd / Lampson Ave.
Domain size: 354 m × 500 m

Table A.5 Locations of instrumentation in Huntington Beach

Site Number	Longitude	Latitude	Instrument	Recording Road
S1	W 117°59'22"	N 33°41'13"	DustTrak1	
S2	W 117°59'18"	N 33°41'12"	DustTrak2, Camera1	Garfield Ave.
S3	W 117°59'20"	N 33°41'15"	DustTrak3, Camera2	Beach Blvd.
S4	W 117°59'19"	N 33°41'18"	DustTrak4, Camera3	Beach Blvd.
S5	W 117°59'21"	N 33°41'20"	DustTrak5	
S6	W 117°59'19"	N 33°41'13"	DustTrak6, 1 Sonic	

Figure A.5 Measurement domain and instrumentation in Huntington Beach.

Appendix B – Laboratory Setup

The re-circulating water channel (Figure B.1), which has a test section of 1.5 m long, 1 m wide and 0.5 m deep, was designed in the laboratory for Environmental Flow Modeling (LEFM) at the University of California, Riverside. Two 0.5 m thick honeycombs with perforated screens between them are placed at the entrance to the channel to reduce the turbulence level and adjust the flow to the desired logarithmic profile. The axial pump (Carry Manufacturing, Inc., 15HP, 8" in diameter) drives the flow from the settling tanks. The pump can produce a maximum mean velocity of 0.5 m/s in the test section. A variable frequency controller (AC Tech 20HP) allows pump control with a resolution of 1/100 Hz, which corresponds to the mean velocity change of 0.1 mm/s.

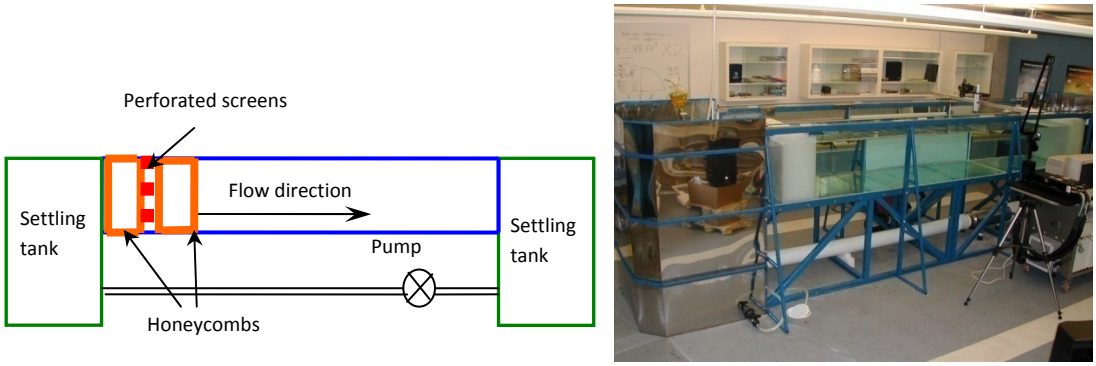

Figure B.1 Water channel schematic (left) and picture (right).

TSI Particle Image Velocimetry (PIV) system was used to measure the velocity field, and Planar Laser Induced Fluorescence (PLIF) was used for concentration measurements. The PIV system includes a 400 mJ Nd-YAG laser (Big Sky Laser Technologies, Inc), a LASERPULSE Synchronizer (TSI Inc.), and a PowerView Plus 2M camera with CameraLink frame grabber (TSI Inc.). Particles (specific gravity 1.02) used to seed the channel were Pliolite Ultra 100 (Eliokem). Insight 3G (TSI Inc.) software was utilized for data collection and TecPlot (TecPlot, Inc.) and the MatLab were used for the velocity and concentration field visualizations.

Downtown models were created using highly polished acrylic models to minimize effects of refraction and attenuation of the laser sheet utilized for the PIV/PLIF measurements (Figure B.2). Velocity and concentration fields were measured in horizontal and vertical planes, as presented in Figure B.3.

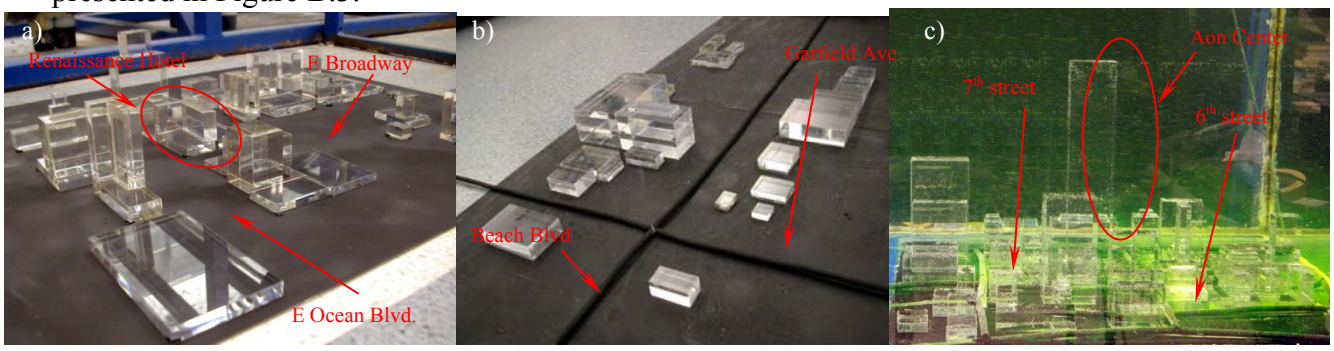

Figure B.2 Laboratory model setup for a) Long Beach in scale 1:800; b) Huntington Beach strip mall in scale 1:400; and c) Los Angeles downtown in scale 1:800.

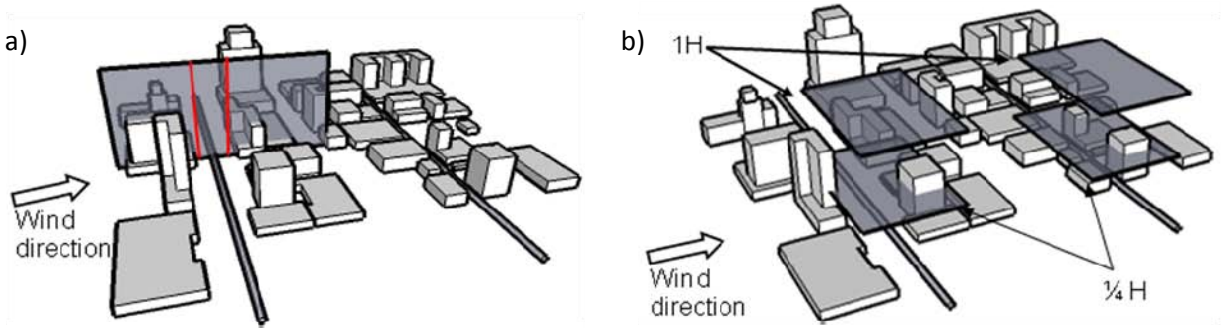

Figure B.3 PIV/PLIV laser sheet for measurements in a) vertical plane and b) horizontal plane.

Approaching flow profile was made logarithmic (Figure B.4a) and a sufficient level of turbulence was formed in the water channel (Figure B.4b).

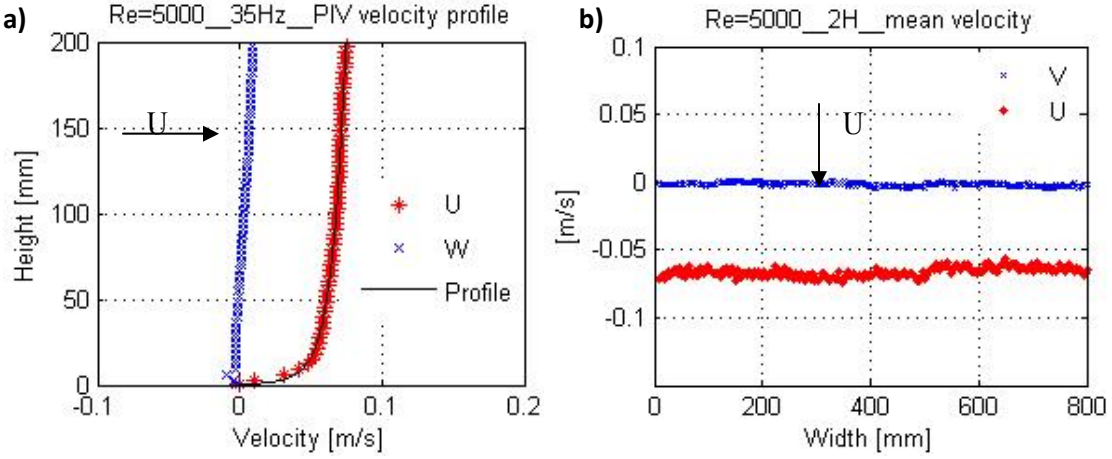

Figure B.4 Mean velocity (u, v, w) of the initial flow: a) velocity profile on the vertical plane; b) velocity profile on the horizontal plane.

The planar laser induced fluorescence (PLIF) technique was applied for the measurement of the concentration distribution in the street network. As the fluorescent tracer, Rhodamine 610 Chloride dye was used.

Scaling parameters

Dimensionless length scale factor Φ_L is defined as

$$\Phi_L = \frac{[L]_{field}}{[L]_{lab}} \qquad \text{B.1}$$

where L is length scale, [m].

Considering kinematic similarity, or equality of time scales $t^* = tU/L$, the dimensionless time scale factor Φ_T is defined as

$$\Phi_T = \frac{[t]_{field}}{[t]_{lab}} = \frac{\left[\frac{L}{U_e}\right]_{field}}{\left[\frac{L}{U_e}\right]_{lab}} = \frac{[L]_{field}}{[L]_{lab}} \frac{[U_e]_{lab}}{[U_e]_{field}} = \frac{\Phi_L}{\Phi_U} \qquad \text{B.2}$$

where U_e is velocity of ambient flow, [m/s]; Φ_U is velocity scale factor.

The ambient concentration, C_e, of well mixed passive contaminants could be written as

$$C_e = \frac{\dot{m}_s \cdot t}{Volume} \qquad \text{B.3}$$

where $\dot{m}_s$ is mass flow rate of source, [mg/s]; t is the travel time of passive contaminant, [s].

Now the dimensionless concentration scale factor is introduced as

$$\Phi_C = \frac{[C_e]_{field}}{[C_e]_{lab}} = \frac{\left[\frac{\dot{m}_s \cdot t}{Volume}\right]_{field}}{\left[\frac{\dot{m}_s \cdot t}{Volume}\right]_{lab}} = \frac{\left[\frac{\dot{m}_s \cdot t}{L^3}\right]_{field}}{\left[\frac{\dot{m}_s \cdot t}{L^3}\right]_{lab}} = \frac{[\dot{m}_s]_{field}}{[\dot{m}_s]_{lab}} \frac{\Phi_T}{\Phi_L^3} = \frac{[\dot{m}_s]_{field}}{[\dot{V}_s \cdot C_s]_{lab}} \frac{\Phi_T}{\Phi_L^3} \qquad \text{B.4}$$

where $\dot{V}_s$ is volumetric flow rate of source, [m^3/s]; C_s is source concentration, [mg/m^3]. Φ_C is used as a multiplying factor by which the ambient concentration of passive contaminant observed in the laboratory is scaled to that in the field.

Appendix C – Numerical Model

QUIC (Quick Urban and Industrial Complex), which is composed of a wind model, QUIC-URB, and a dispersion model, QUIC-PLUME, is used to simulate both velocity field and concentration distribution in all five areas.

QUIC-URB is a fast response model developed by Los Alamos National Laboratory for computing flow around buildings. It uses empirical algorithms and mass conservation to quickly compute 3D flow fields around building complexes. The underlying code is based on the work of Rockle (1990). Improvements to the original model are described by Bagal et al. (2003) and Pardyjak et al. (2003). Additional evaluation studies of QUIC-URB have been performed by Pardyjak and Brown (2002).

The model constructs the flow field around a cluster of buildings, and uses this information in a particle dispersion model to estimate the concentration filed associated with a release among the buildings. Mass conservation method is composed of two main steps: 1) interpolation, in which an interpolated mean wind field is obtained from the existing wind data, and 2) mass consistency enforcement, in which the interpolated wind field is used as a first guess, and then it is adjusted with minimal corrections in order to satisfy the continuity equation.

The QUIC-PLUME model is a Lagrangian dispersion model that uses the mean wind fields from QUIC-URB and turbulent winds computed internally using the Langevin random walk equations. Gradients in the wind fields are used to estimate the turbulence parameters. It includes reflection terms for building and street surfaces. The dispersion of aerosols and gases can be simulated. Lagrangian particle models describe dispersion by simulating the releases of particles and moving them with an instantaneous wind composed of a mean wind plus a turbulent wind. The theory of QUIC-PLUME is described by Williams et al. (2004b).

Appendix D – Urban boundary layer structure and urban morphometry

Figure D.1 was created after Oke (1988) and Bottema (1997). The two-layer model recognizing the urban canopy layer (UCL) and urban boundary layer (UBL) was first proposed by Oke (1976). Furthermore, three distinct regions, roughness sub-layer (RSL), inertial sub-layer (ISL) and mixed layer (ML) were proposed by Grimmond and Oke (2002). Roth (2000) discussed each layer as following: UCL is produced by microscale effects of site characteristics. Here dynamic and thermal processes are dominated by the immediate surroundings; flow and scalar structure are generally very complex. RSL is also called the transition layer, interfacial layer or wake layer, includes UCL. It is mechanically and thermally influenced by the length-scales associated with the roughness and is thought of as a region in which the underlying buildings lead to a spatial horizontal inhomogeneity of the flow (Britter and Hanna, 2003). ISL is also called the constant-flux layer and for neutral stratification a mean velocity profile follows a logarithmic wind law.

The depth of RSL, z_*, is usually related to the values of roughness element's height, z_H. Wind tunnel experiments and field observations found that z_* / z_H are in the range of 2-5 for momentum RSL and about 10 for heat RSL (Raupach and Legg, 1984).

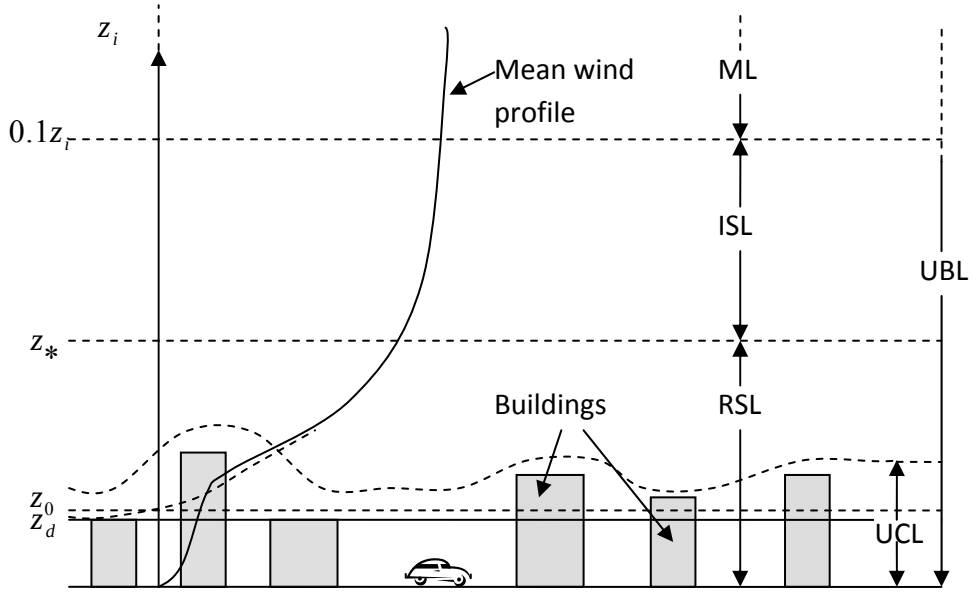

Figure D.1 Structure of urban boundary layer. Modified after Oke (1988) and Bottema (1997).

Aerodynamic properties, such as roughness length (z_0) and displacement height (z_d) were originally used over vegetated surfaces. z_0 describes the height above displacement level where the downward extrapolated wind speed profiles reach zero (Ammann, 1999). z_d represents the asymptotic lower limit, where the near-logarithmic profiles of atmospheric quantities (concentrations, temperature, wind speed, etc.) of the inertial sub-layer converge to, if they are extrapolated downwards into the roughness sub-layer or canopy layer (Ammann, 1999). The effective aerodynamic height (z) of roughness elements is described by $z = z_H - z_d$. In order to

make the published data from sites with different surface characteristics comparable, Roth (2000) suggested that all work should include a detailed description of the overall setting of the observation site and the characteristics of the fetch (average height of buildings, aerodynamic roughness length and zero-plane displacement height as a minimum).

Two classes of approach are available to assign values of z_0 and z_d: morphometric methods and micrometeorological methods (Grimmond and Oke, 1999). Morphometric methods were used widely because values can be achieved without field observations of wind or turbulence from tall meteorological towers. The dimensions used to characterize the surface geometry in the morphometric methods are defined in Figure D.2 and nondimensional ratios are defined as follow:

$$\overline{\lambda_P} = \overline{A_P} / \overline{A_T} = \overline{L_x L_y} / \overline{D_x D_y} \quad \text{D.1}$$

$$\overline{\lambda_F} = \overline{A_F} / \overline{A_T} = \overline{z_H L_y} / \overline{D_x D_y} \quad \text{D.2}$$

$$\overline{\lambda_S} = \overline{z_H} / \overline{W_x} = \overline{z_H} / \overline{(D_x - L_x)} \quad \text{D.3}$$

$$\overline{\lambda_C} = \left[\overline{L_x L_y} + 2\left(\overline{L_y z_H}\right) + 2\left(\overline{L_x z_H}\right)\right] / \overline{D_x D_y} \quad \text{D.4}$$

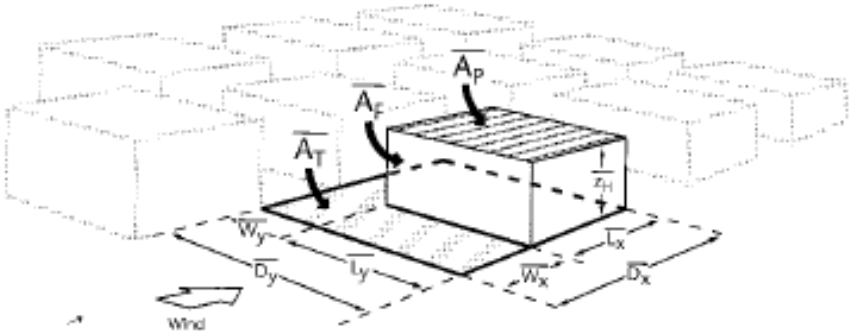

Figure D.2 Definition of surface dimensions used in morphometric analysis (Grimmond and Oke, 1999).

There are several morphometric methods, such as height-based approach (Hanna and Chang, 1992), methods that use height and plan area fraction (λ_P) (Counehan, 1971) and methods that consider height and frontal area fraction (λ_F) (Lettau, 1969; Raupach, 1994; Bottema, 1997; MacDonald et al., 1998b). MacDonald's model (MacDonald et al., 1998b) is an attractive alternative given its good performance and more readily available data requirements (Grimmond and Oke, 1999).

The plan area fraction and frontal area fraction for all buildings are calculated based on Equation D.1-D.4 and Figure D.2. For the buildings which have more complicated geometries than Figure D.2, A_P indicates the projection of plan area on the ground and A_F indicates the projection of frontal area on the vertical plane which is facing the wind direction (as shown in

Figure D.3). For the case that the building has a complex roof shape, e.g. steep roof, we calculate the building height z_H as the approximate level where the roof pitch changes from steep to flat (Eliasson et al., 2006).

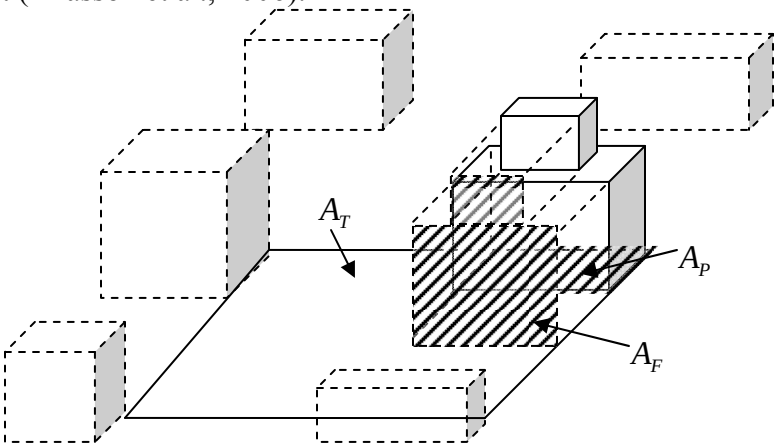

Figure D.3 Definition of A_P, A_F and A_T

We use the Ma method (MacDonald et al., 1998b) in our study to calculate roughness, z_0, and displacement height, z_d, as

$$\frac{z_d}{z_H} = 1 + \alpha^{-\lambda_P}\left(\lambda_P - 1\right), \qquad \text{D.5}$$

$$\frac{z_0}{z_H} = \left(1 - \frac{z_d}{z_H}\right)\exp\left\{-\left[0.5\beta\frac{C_D}{k^2}\left(1 - \frac{z_d}{z_H}\right)\lambda_F\right]^{-0.5}\right\}, \qquad \text{D.6}$$

where α is an empirical coefficient, C_D is a drag coefficient (1.2), k is von Karman's constant (1.4), and β is a correction factor for the drag coefficient (the net correction for several variables, including velocity profile shape, incident turbulence intensity, turbulence length scale, and incident wind angle, and for rounded corners). Macdonald (1998b) provides a graphical sensitivity analysis that demonstrates responses to changes in these values. For square arrays of cubes, α =2.3 and β=0.55. For staggered arrays, α =4.43 and β=1.0.

Appendix E – Detailed Measured Meteorology

E.1 Los Angeles Downtown

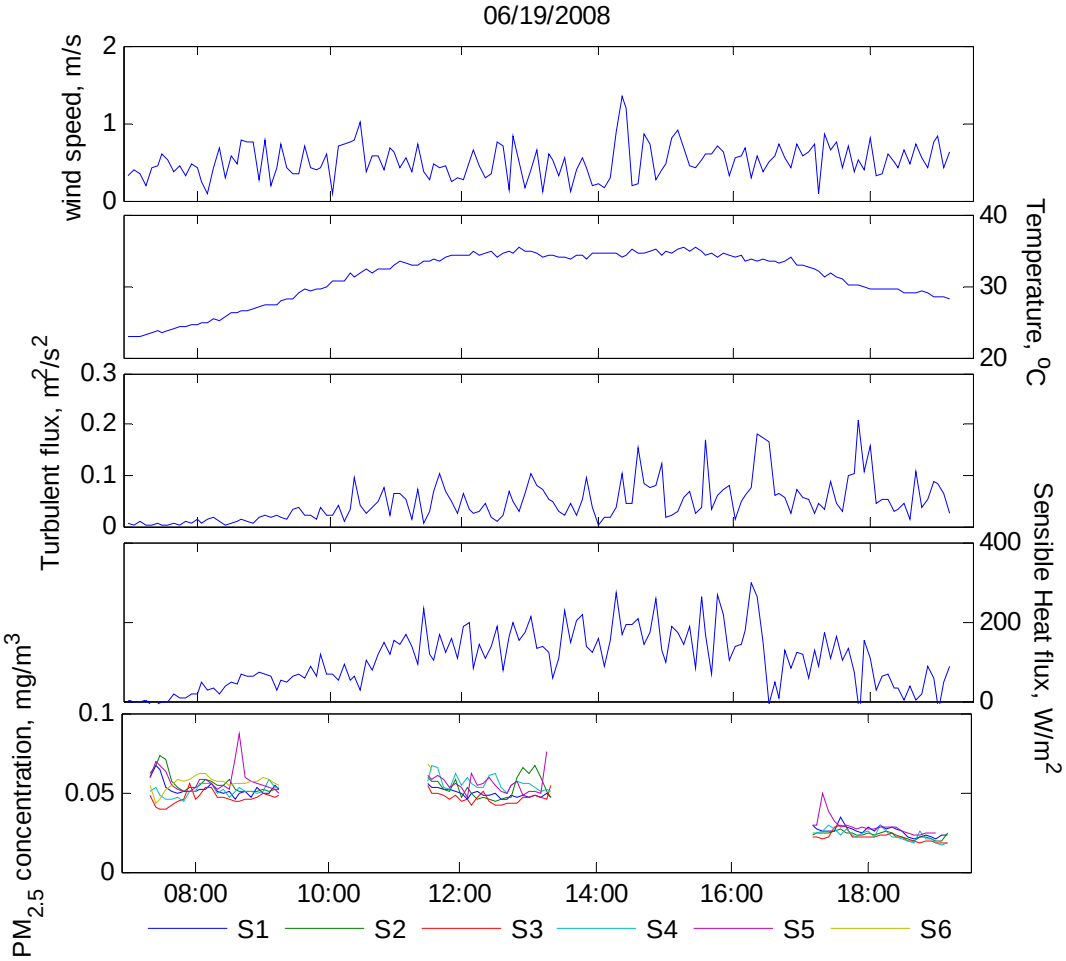

Figure E.1 Meteorological data and $PM_{2.5}$ concentrations on 06/19/2008.

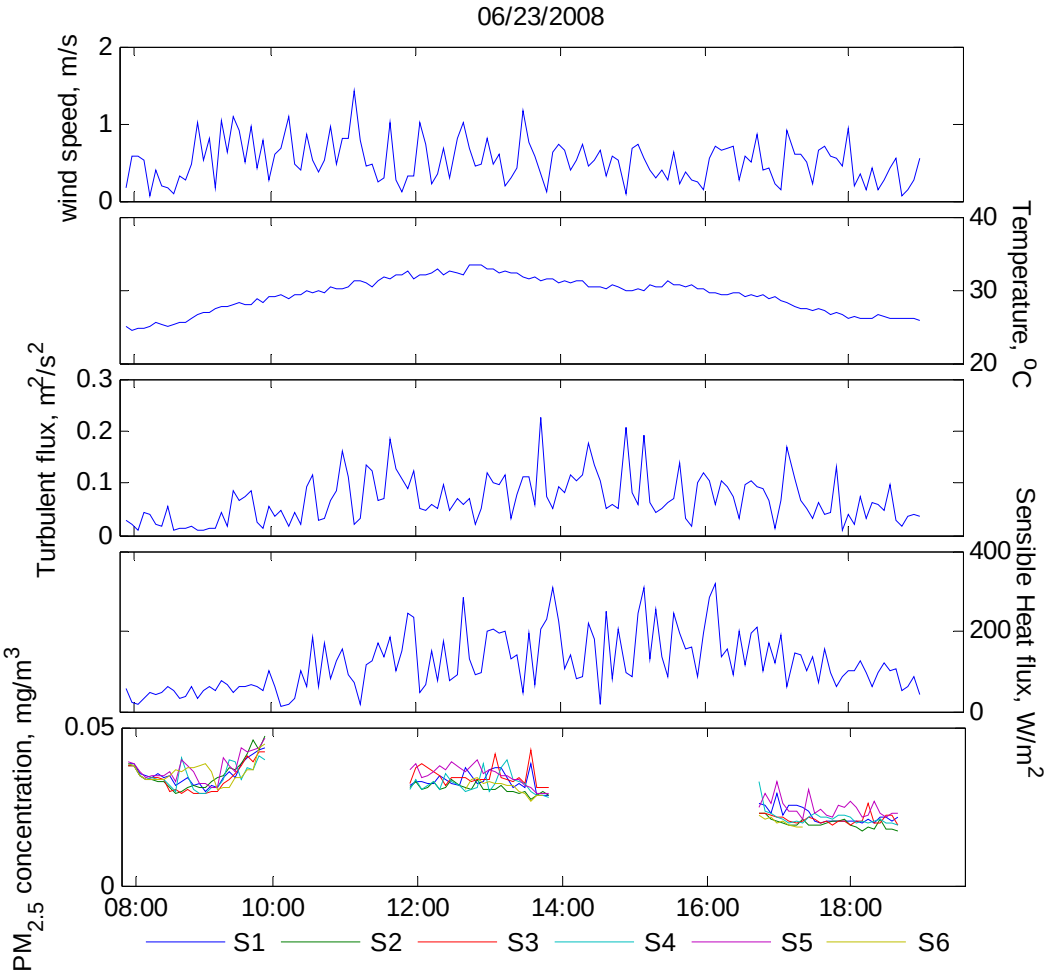

Figure E.2 Meteorological data and $PM_{2.5}$ concentrations on 06/23/2008.

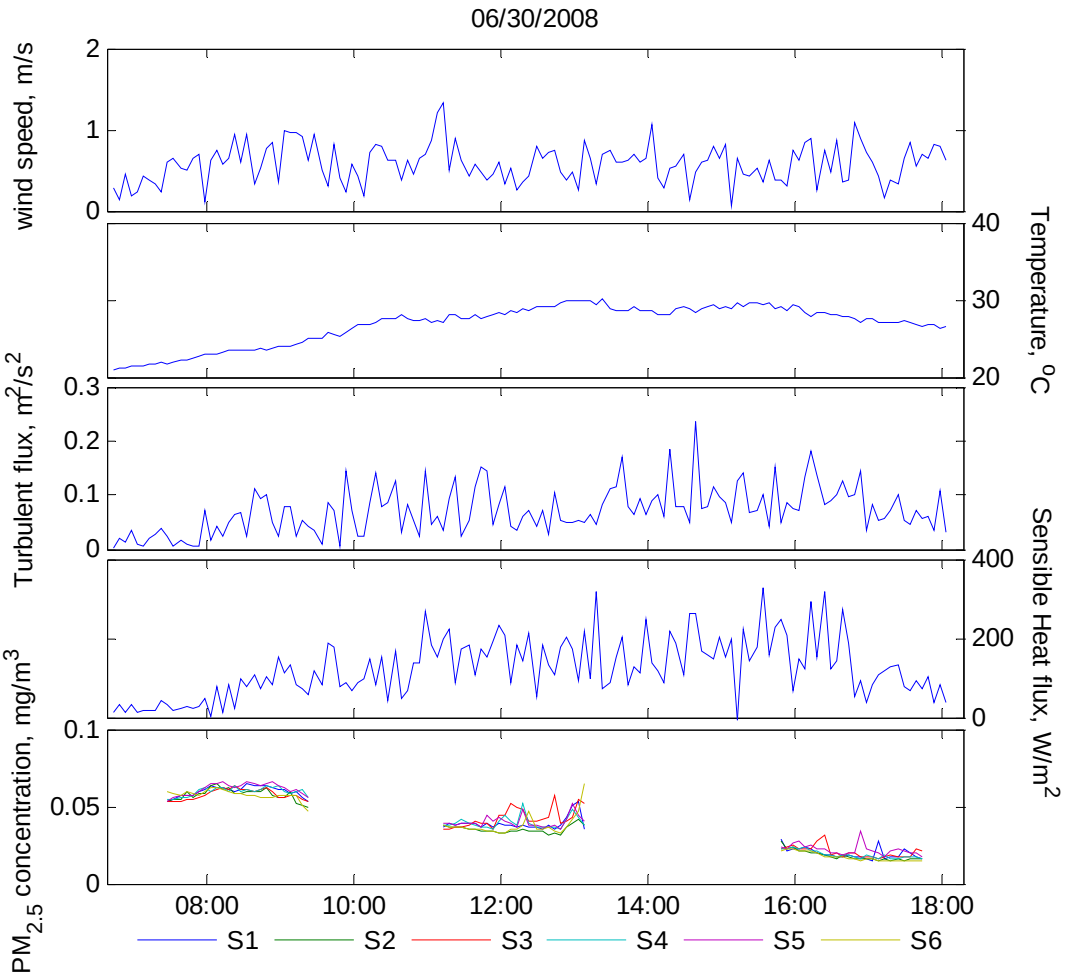

Figure E.3 Meteorological data and $PM_{2.5}$ concentrations on 06/30/2008.

Figure E.1, E.2 and E.3 show the comparison of $PM_{2.5}$ concentrations at site S1, S4 and S5 for all three measurement days. All sites are on 6th street (as shown in Figure A.4). S1 and S5 are crossing each, where S1 is at windward side of street and S5 is at leeward side of street. The buildings height of windward side is 3 times of that of leeward side. S4 is also at the windward side but the buildings height is a quarter of that of site 1.

Comparing the concentration of leeward side S1 and windward side S5, we find that during the morning, the variations of concentrations on both sides are consistent with each other. During the afternoon, the peak concentration for each side appears at different time. For all three days, the leeward side always experienced higher concentrations.

Comparing the concentration of S1 and S4, both of which are on the windward side but have different buildings height, we find that on 06/19/2008 (Figure E.4), site S1, which is on the windward side of higher buildings, has much lower concentration than site S4 during the noon. However, no such difference is observed during other time periods. From Figure E.4, E.5 and E.6, we can see that relatively high concentration fluctuations are observed during the noon time for all three days.

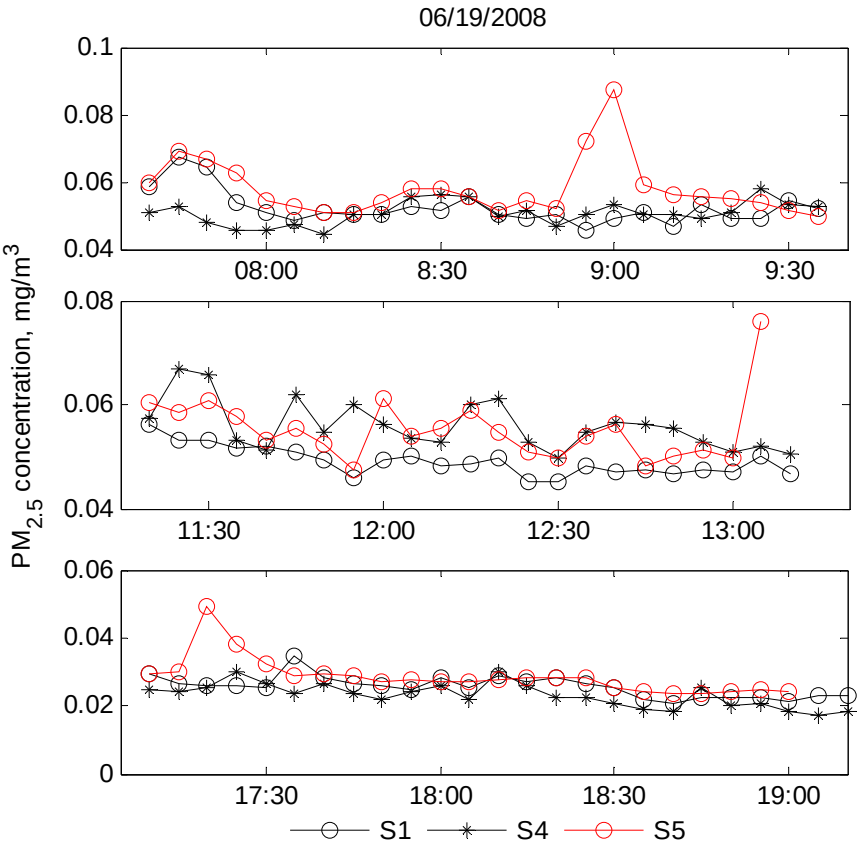

Figure E.4 Comparison of $PM_{2.5}$ concentrations at S1, S4 and S5 on 06/19/2008.

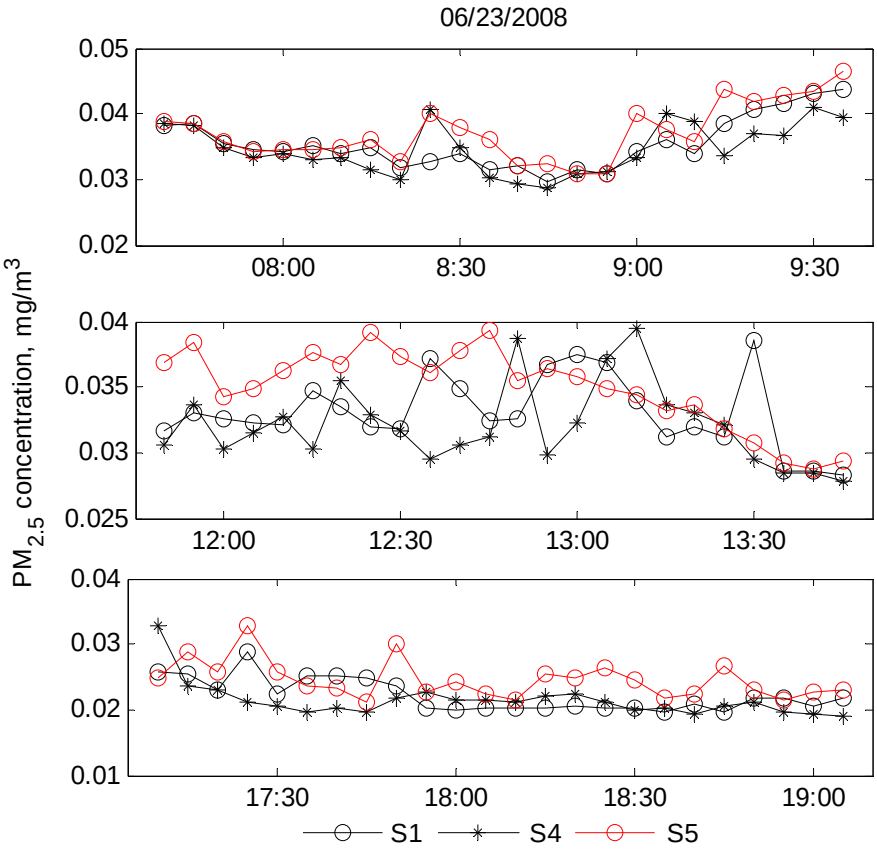

Figure E.5 Comparison of $PM_{2.5}$ concentrations at S1, S4 and S5 on 06/23/2008.

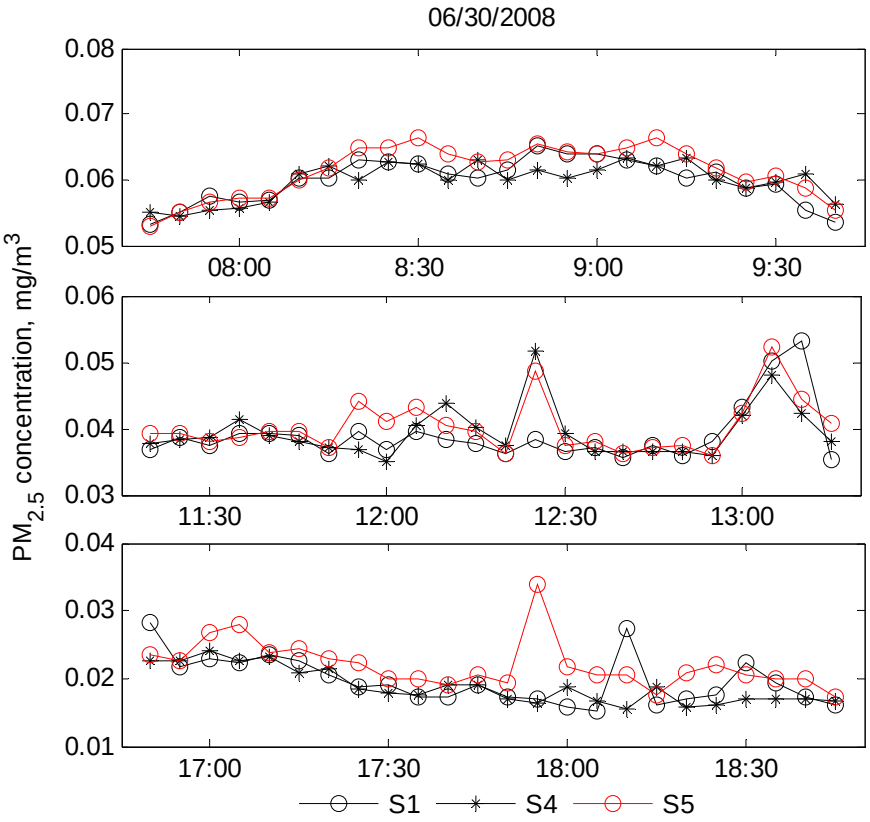

Figure E.6 Comparison of $PM_{2.5}$ concentrations at S1, S4 and S5 on 06/30/2008.

Figures E.7, E.8 and E.9 compare the concentration measured at site S2 and S3, which are on the street approximately parallel to wind direction. S2 is close to the upwind boundary of the domain, out of which are lower height buildings and open areas. S3 are close to the downwind boundary of the domain, with high-rise buildings at the upwind direction of it. From Figure E.8 and E.9, we can see that the variation of concentration at S2 and S3 during the morning period is small. Several peaks appear at S3 during the noon and afternoon. Site 3 is much easier to be influenced by local traffic emissions when turbulence is stronger.

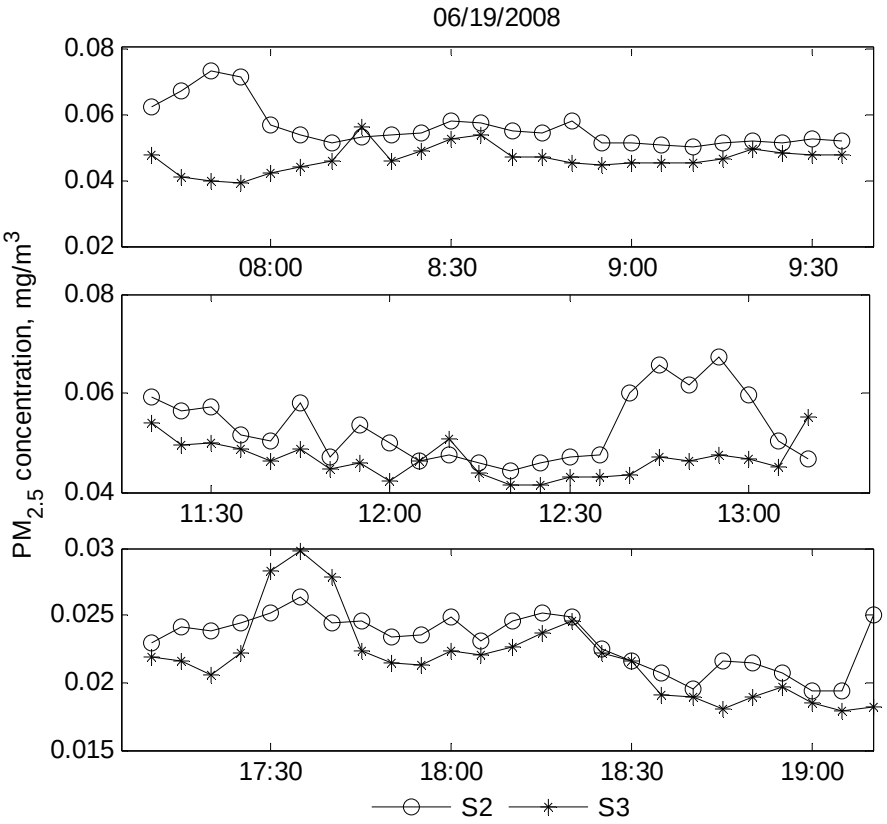

Figure E.7 Comparison of $PM_{2.5}$ concentrations at S2 and S3 on 06/19/2008.

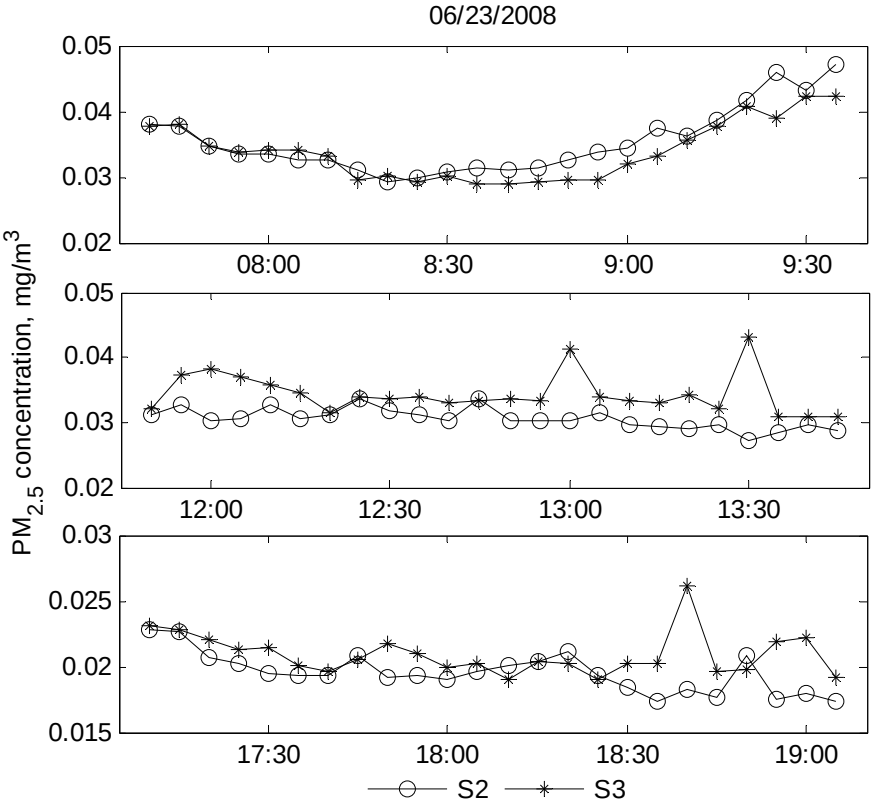

Figure E.8 Comparison of $PM_{2.5}$ concentrations at S2 and S3 on 06/23/2008.

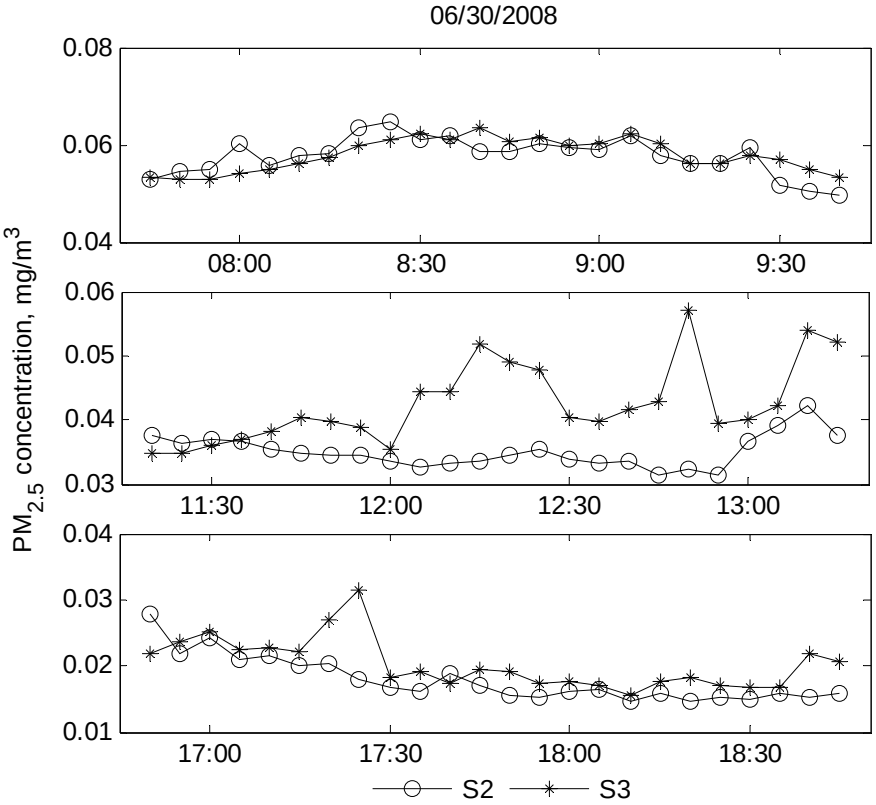

Figure E.9 Comparison of $PM_{2.5}$ concentrations at S2 and S3 on 06/30/2008.

Table E.1 Mean and standard derivation of $PM_{2.5}$ concentration on 06/19/2008

		S1	S2	S3	S4	S5	S6
Morning	mean	0.052	0.056	0.046	0.051	0.058	0.056
	std	0.005	0.006	0.004	0.004	0.009	0.004
Noon	mean	0.049	0.053	0.045	0.056	0.055	0.063
	std	0.003	0.007	0.004	0.005	0.006	0.003
Afternoon	mean	0.026	0.023	0.033	0.023	0.029	NaN
	std	0.003	0.002	0.003	0.004	0.006	NaN

Table E.2 Mean and standard derivation of $PM_{2.5}$ concentration on 06/23/2008

		S1	S2	S3	S4	S5	S6
Morning	mean	0.036	0.036	0.035	0.036	0.039	0.036
	std	0.004	0.005	0.005	0.006	0.007	0.004
Noon	mean	0.033	0.031	0.034	0.032	0.035	0.031
	std	0.003	0.002	0.003	0.003	0.003	0.002
Afternoon	mean	0.022	0.020	0.021	0.022	0.025	0.020
	std	0.003	0.002	0.002	0.003	0.003	0.002

Table E.3 Mean and standard derivation of $PM_{2.5}$ concentration on 06/30/2008

		S1	S2	S3	S4	S5	S6
Morning	mean	0.060	0.058	0.058	0.060	0.061	0.057
	std	0.003	0.004	0.003	0.003	0.004	0.003
Noon	mean	0.039	0.035	0.043	0.040	0.040	0.038
	std	0.004	0.003	0.006	0.004	0.004	0.007
Afternoon	mean	0.020	0.018	0.020	0.019	0.022	0.017
	std	0.004	0.003	0.004	0.003	0.004	0.003

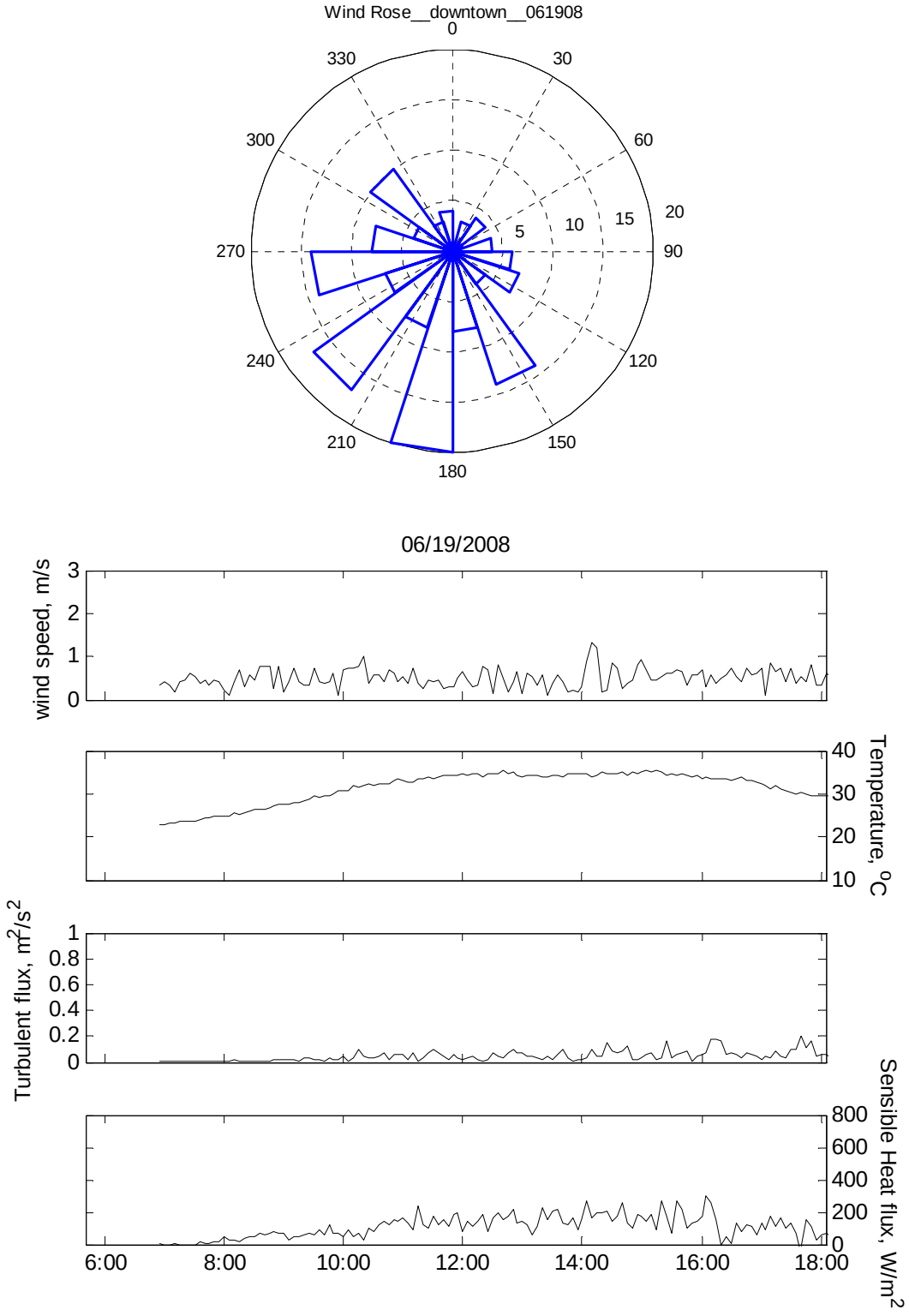

Figure E.10 Meteorological variables observed in Los Angeles on 06/19/2008.

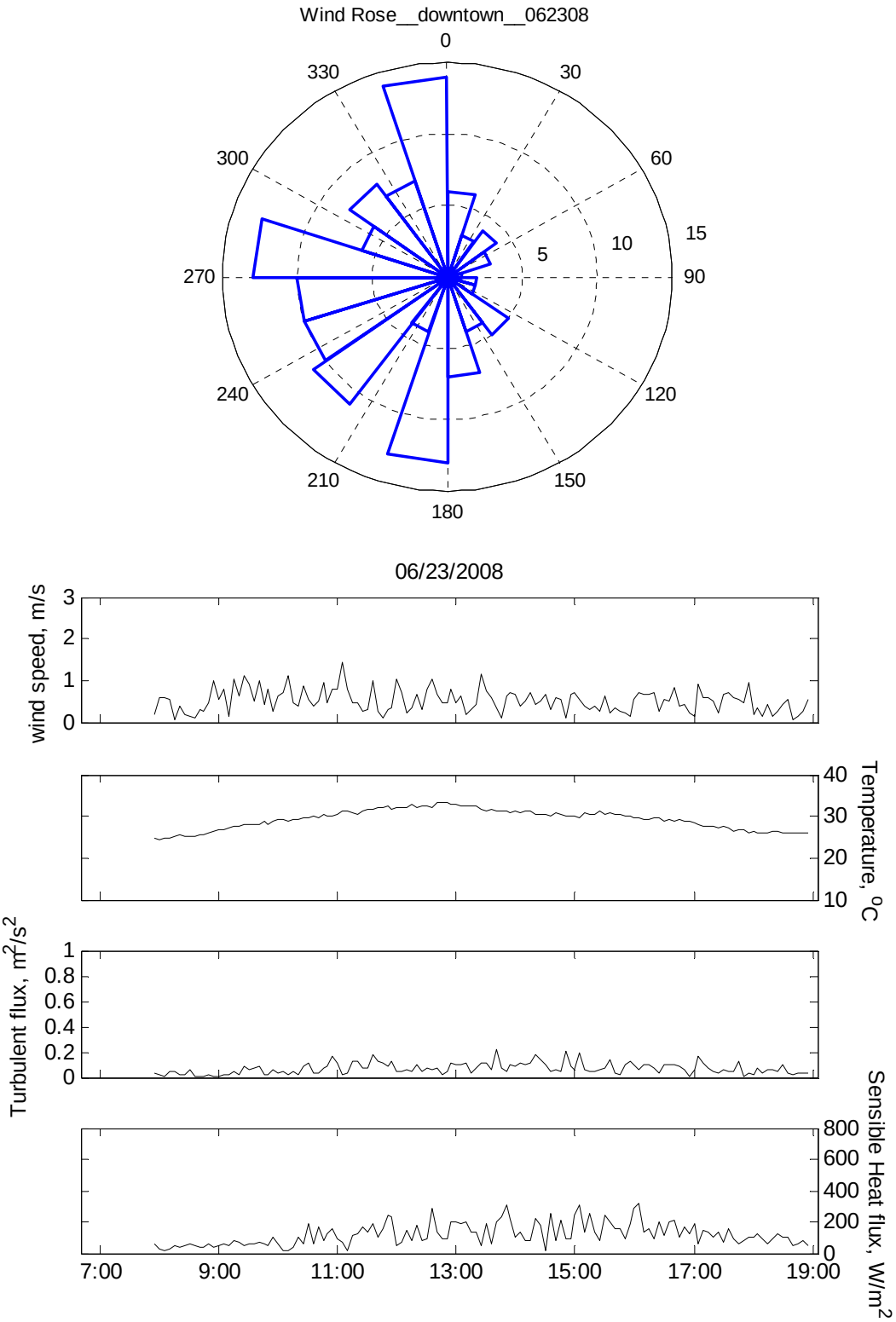

Figure E.11 Meteorological variables observed in Los Angeles on 06/23/2008.

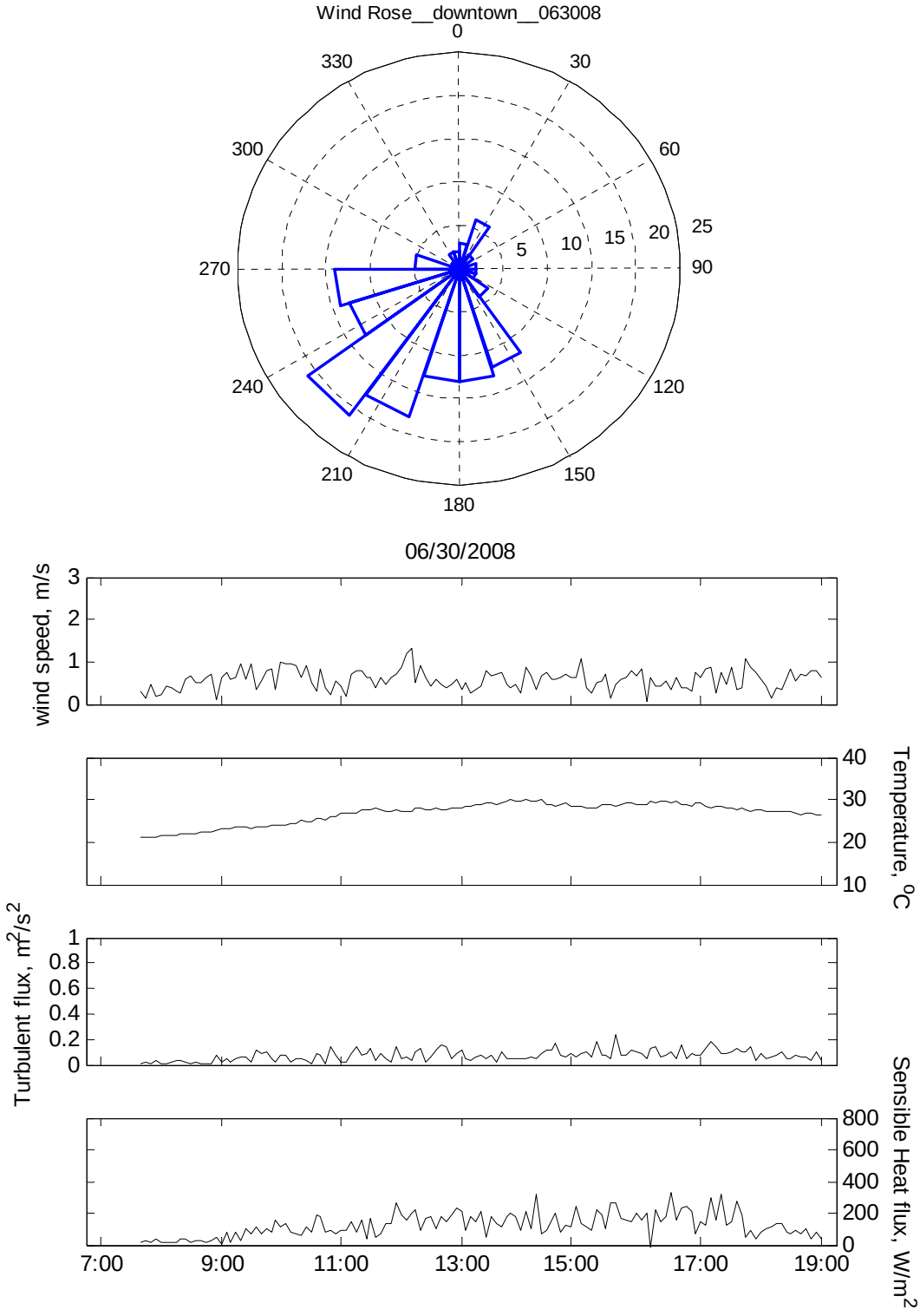

Figure E.12 Meteorological variables observed in Los Angeles on 06/30/2008.

E.2 Anaheim

Figure E.13, E.14 and E.15 present the observations of wind direction, wind speed, air temperature, turbulent flux and sensible heat flux of Anaheim on 07/30/2008, 07/31/2008 and 08/01/2008. The mean wind speeds were 1.02±0.58, 1.15±0.59 and 1.33±0.48 m/s, respectively. The turbulent fluxes were 0.035±0.022, 0.064±0.042 and 0.055±0.020 m/s, respectively. The heat fluxes were 114±61, 193±114 and 161±94 m/s, respectively.

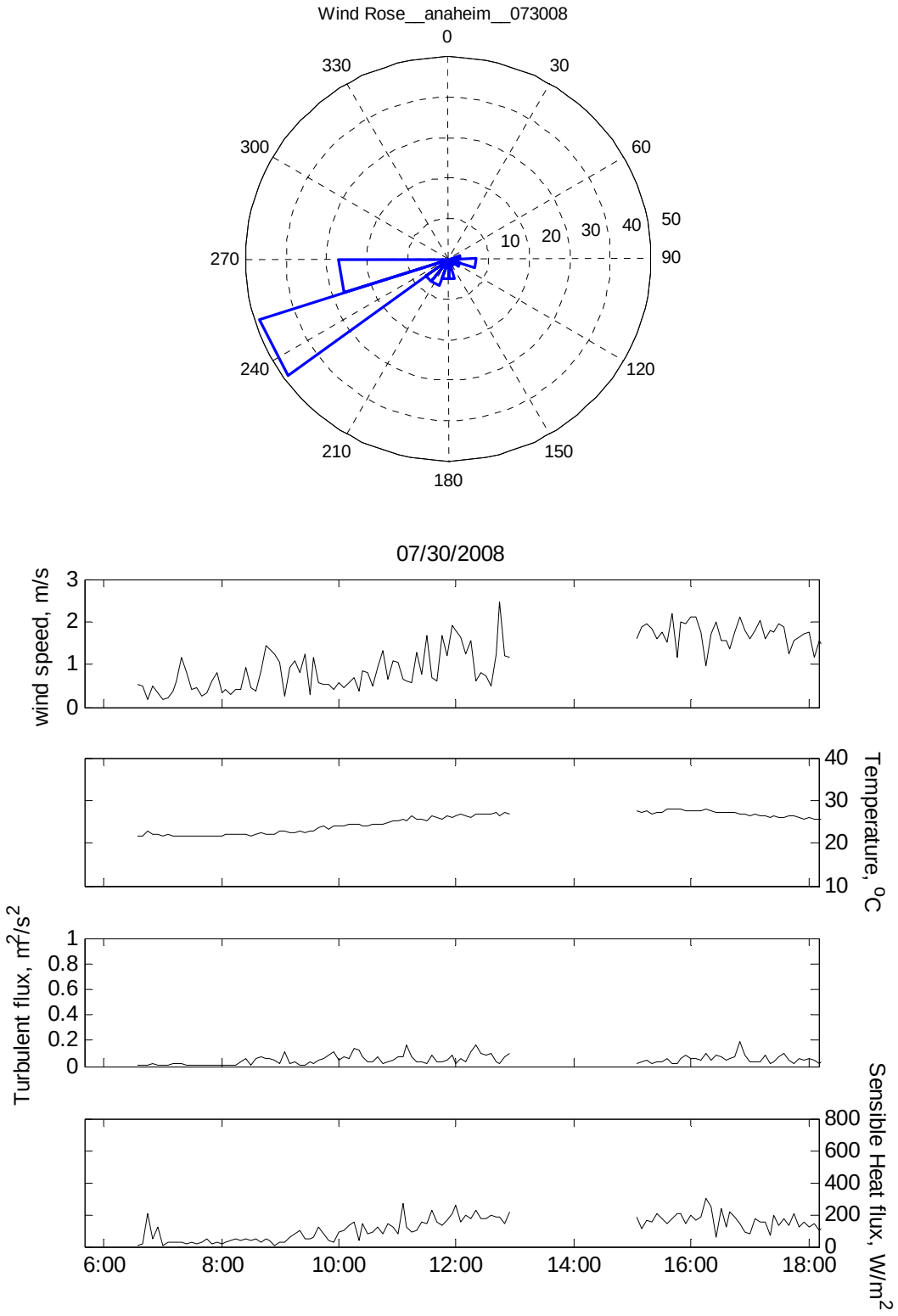

Figure E.13 Meteorological variables observed in Anaheim on 07/30/2008.

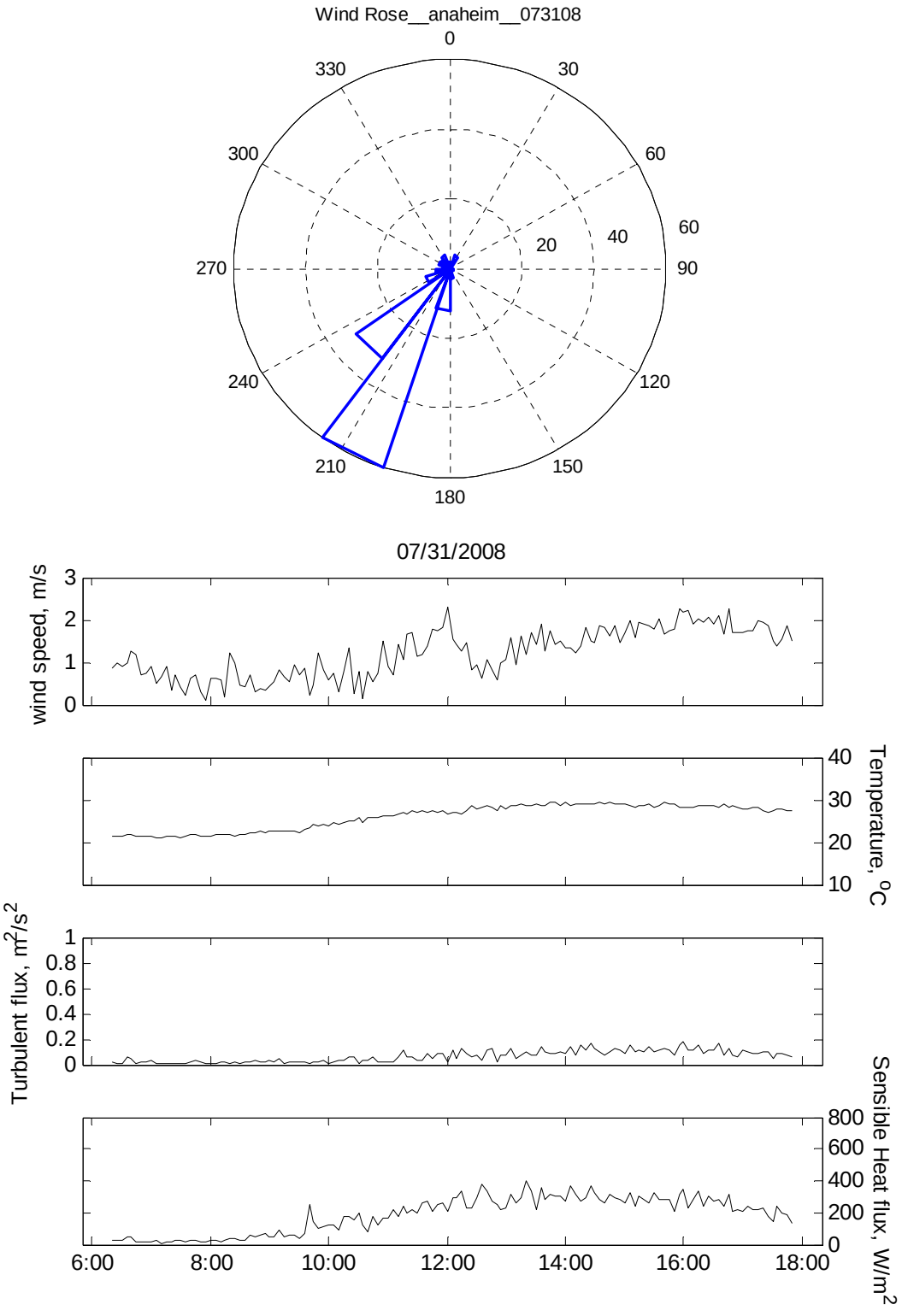

Figure E.14 Meteorological variables observed in Anaheim on 07/31/2008.

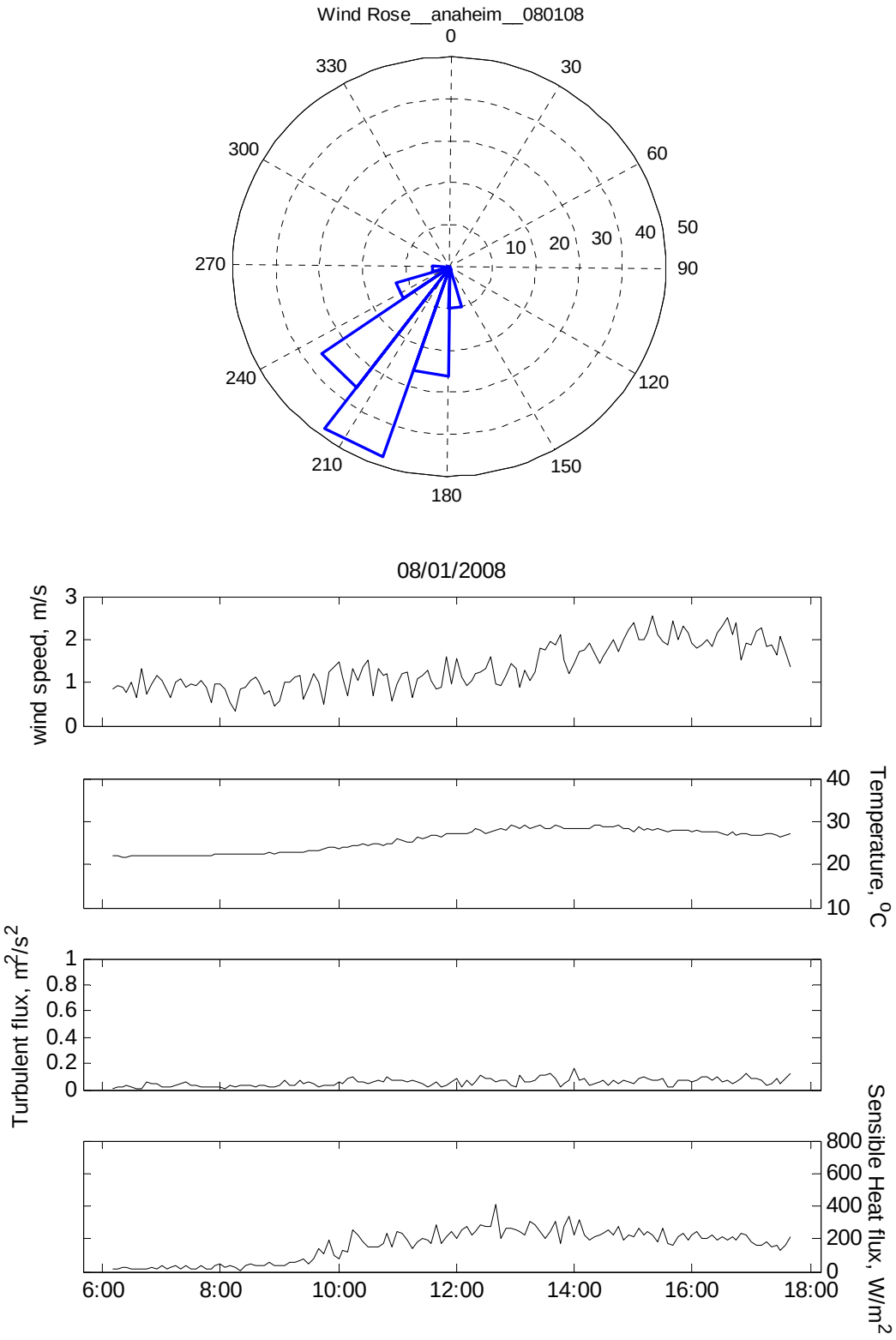

Figure E.15 Meteorological variables observed in Anaheim on 08/01/2008.

E.3. Huntington Beach

Figure E.16, E.17 and E.18 present the observations of wind direction, wind speed, air temperature, turbulent flux and sensible heat flux of Huntington Beach on 07/16/2008, 07/18/2008 and 07/21/2008. The mean wind speeds were 1.07±0.36, 1.02±0.14 and 1.19±0.37 m/s, respectively. The turbulent fluxes were 0.094±0.057, 0.062±0.017 and 0.056±0.027 m/s, respectively. The heat fluxes were 179±81, 214±56 and 243±104 m/s, respectively.

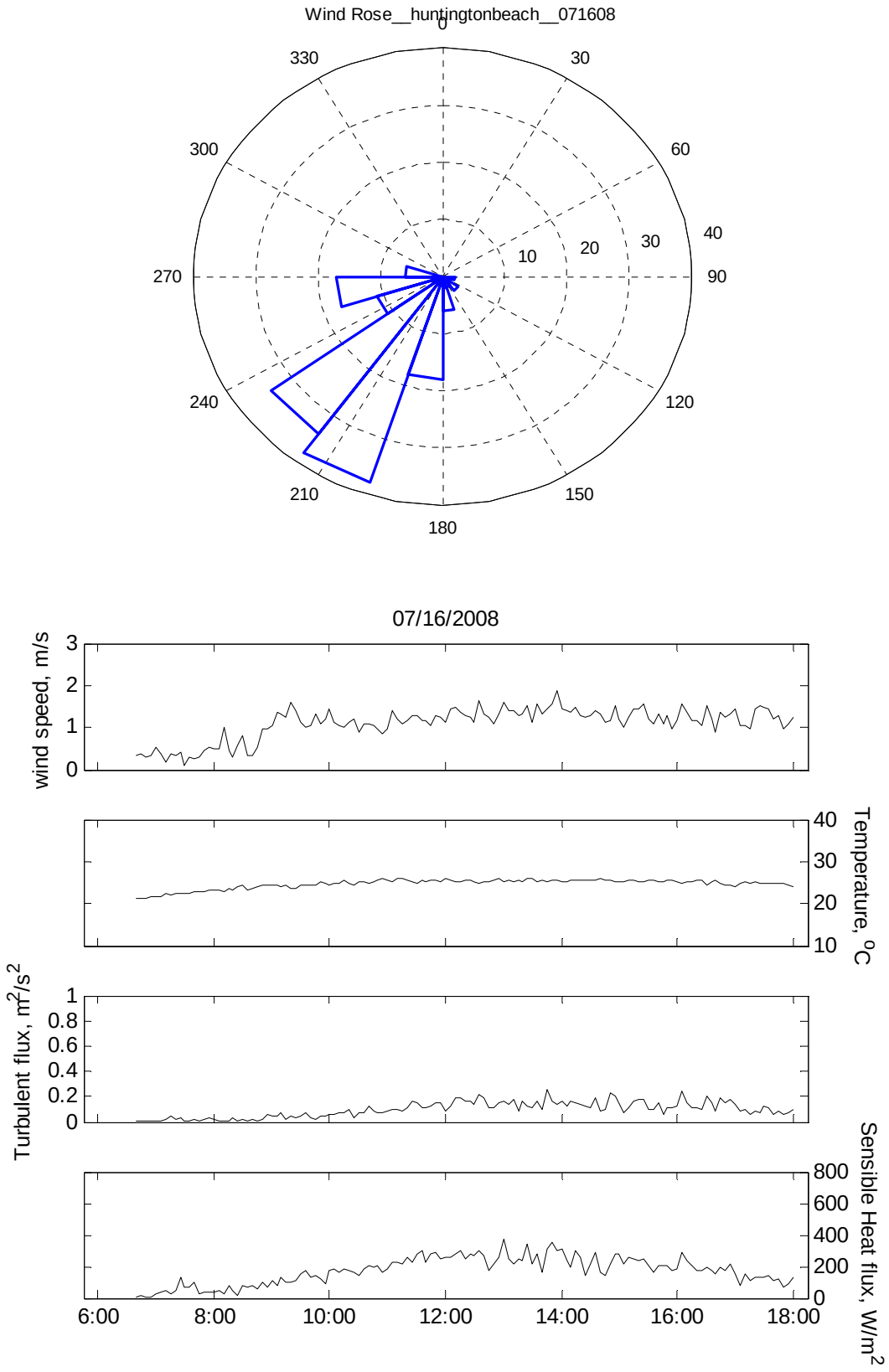

Figure E.16 Meteorological variables observed in Huntington Beach on 07/16/2008.

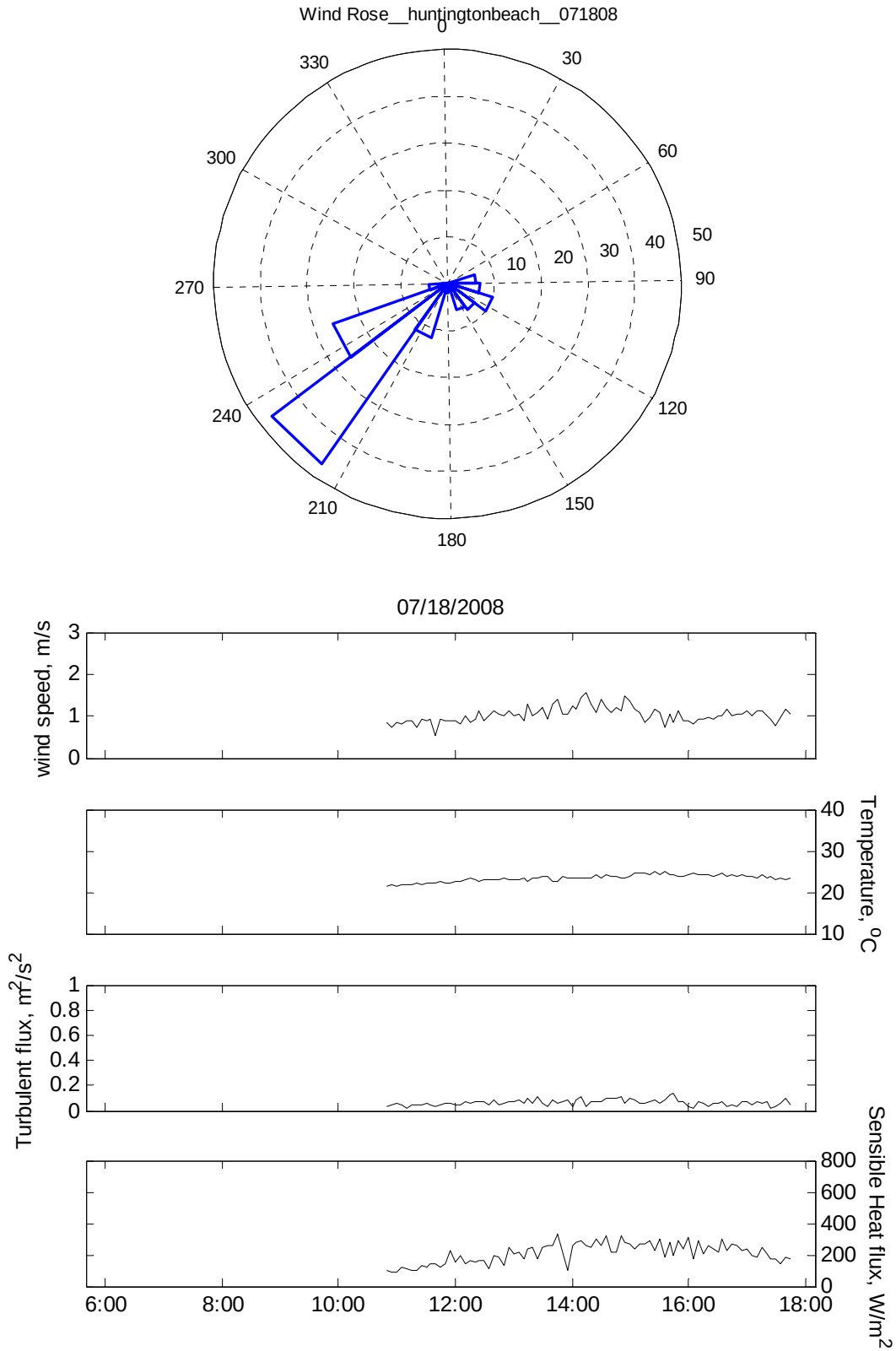

Figure E.17 Meteorological variables observed in Huntington Beach on 07/18/2008.

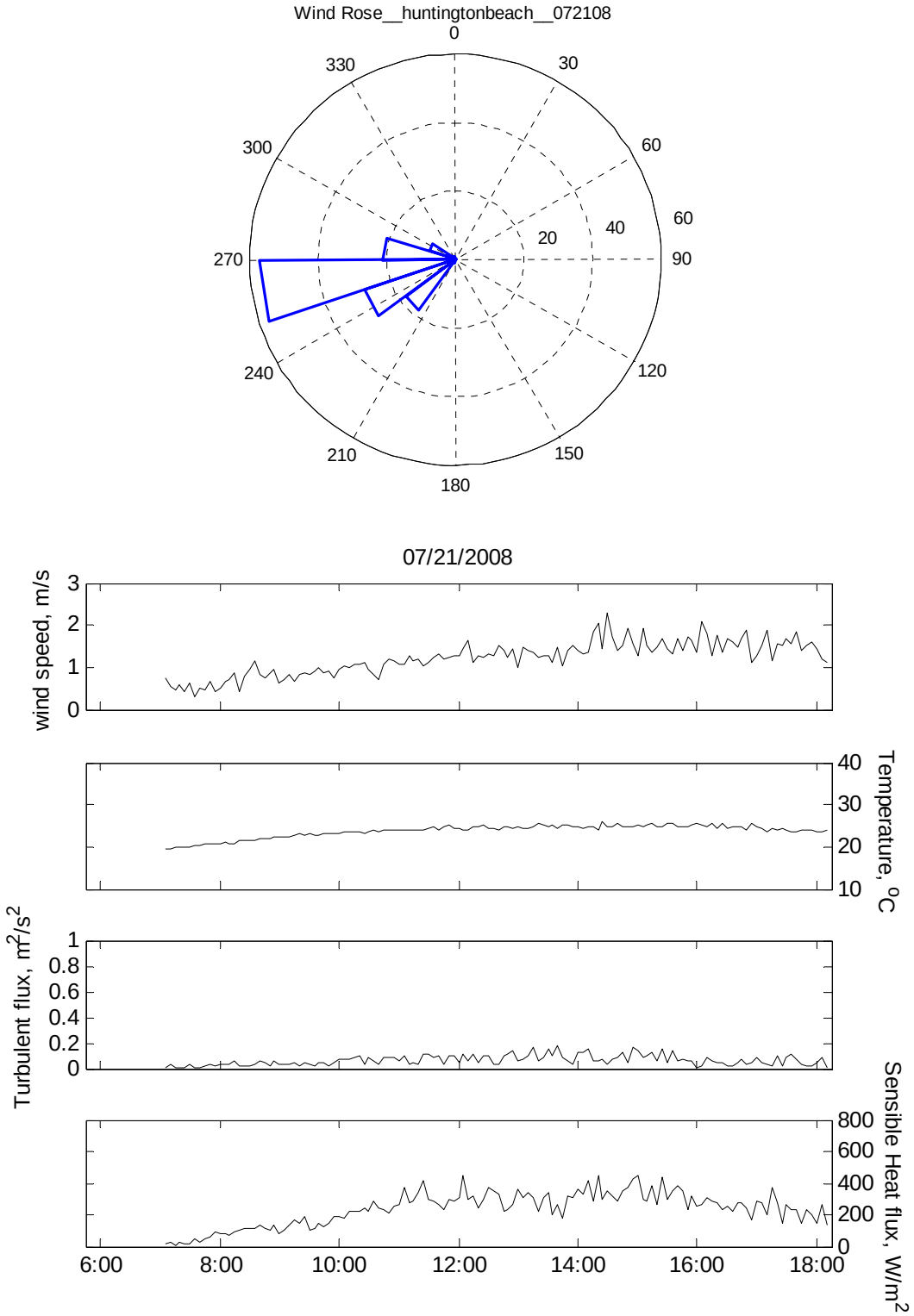

Figure E.18 Meteorological variables observed in Huntington Beach on 07/21/2008.

E.4. Long Beach

Figure E.19, E.20 and E.21 present the observations of wind direction, wind speed, air temperature, turbulent flux and sensible heat flux of Long Beach on 07/02/2008, 07/07/2008 and 07/09/2008. The mean wind speeds were 1.00±0.49, 0.67±0.34 and 0.92±0.61 m/s, respectively. The turbulent fluxes were 0.126±0.076, 0.129±0.075 and 0.149±0.085 m/s, respectively. The heat fluxes were 170±95, 220±78 and 222±101 m/s, respectively.

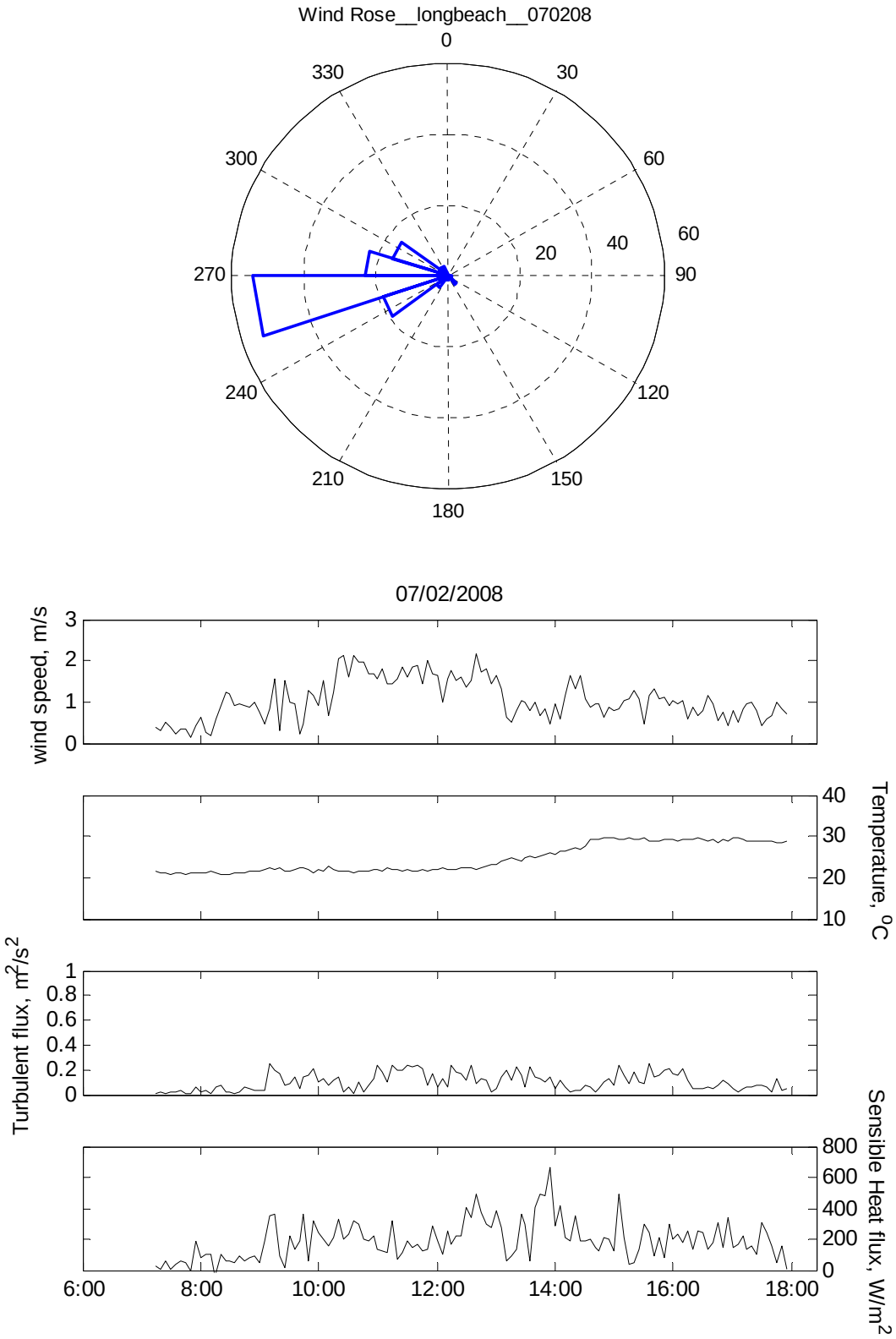

Figure E.19 Meteorological variables observed in Long Beach on 07/02/2008.

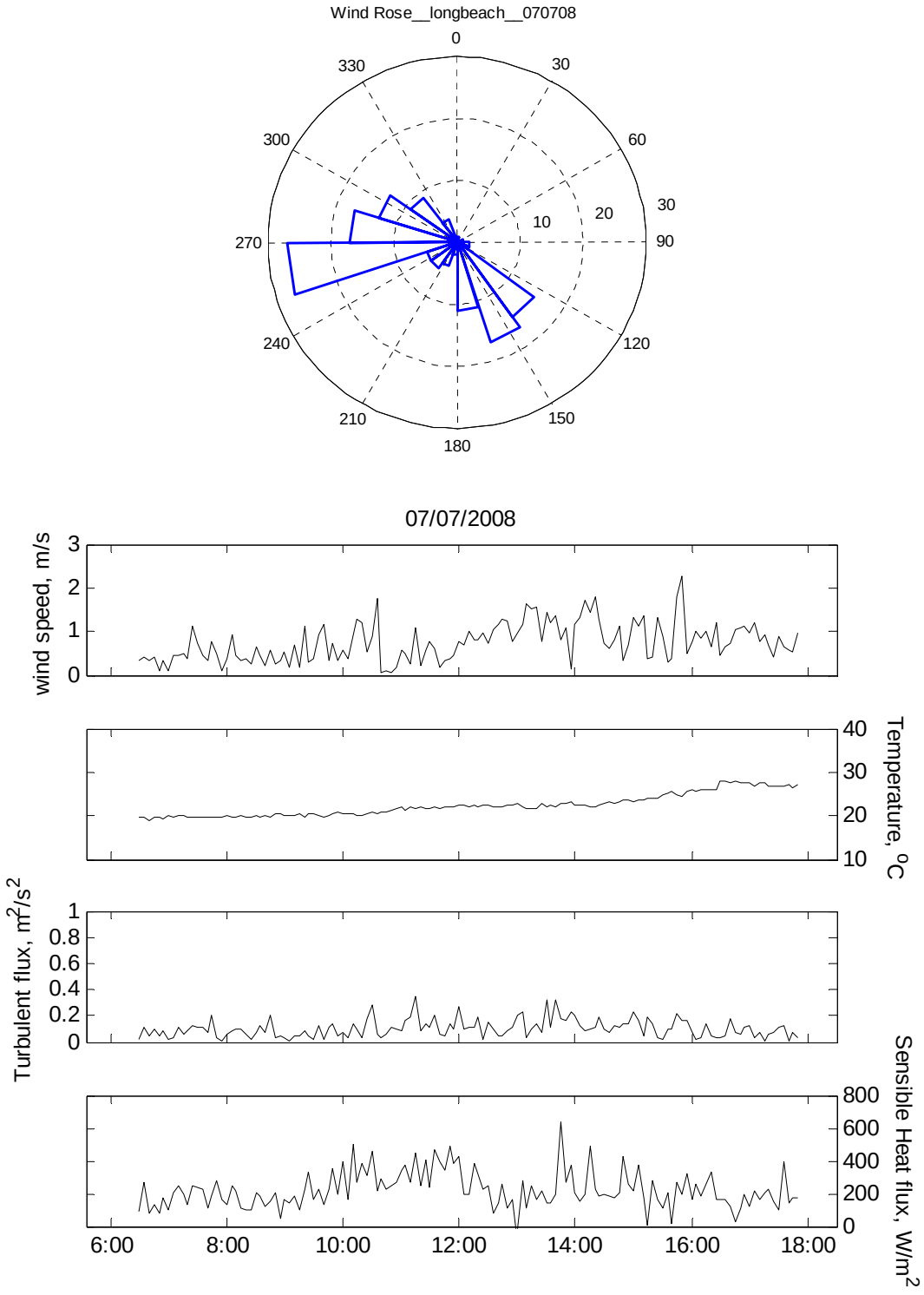

Figure E.20 Meteorological variables observed in Long Beach on 07/07/2008.

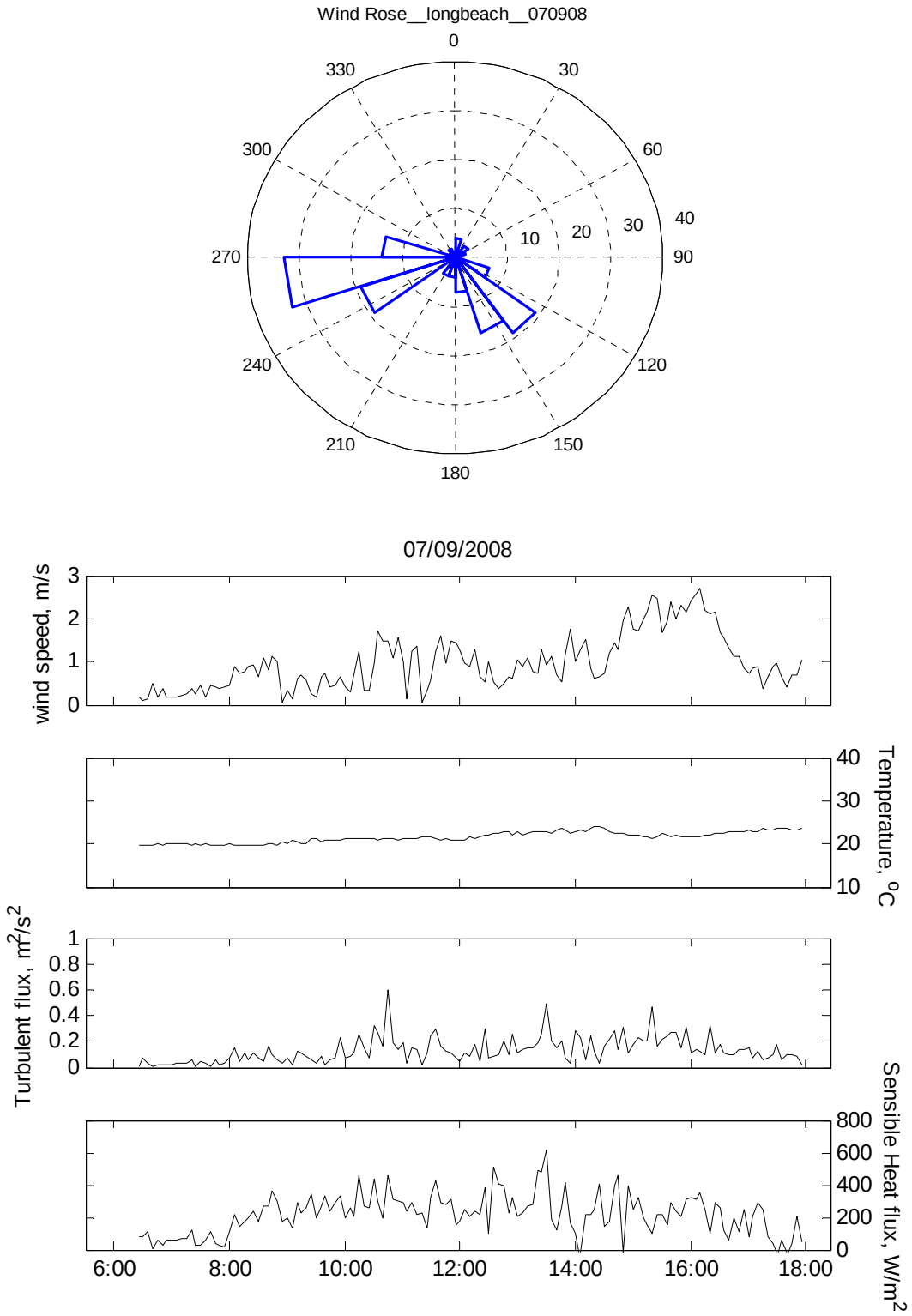

Figure E.21 Meteorological variables observed in Long Beach on 07/09/2008.

E.5 Pasadena

Figure E.22, E.23 and E.24 present the observations of wind direction, wind speed, air temperature, turbulent flux and sensible heat flux of Pasadena on 07/23/2008, 07/25/2008 and 07/29/2008. The mean wind speeds were 0.97±0.40, 0.62±0.27 and 0.74±0.42 m/s, respectively. The turbulent fluxes were 0.186±0.137, 0.125±0.069 and 0.203±0.140 m/s, respectively. The heat fluxes were 213±102, 135±61 and 204±69 m/s, respectively.

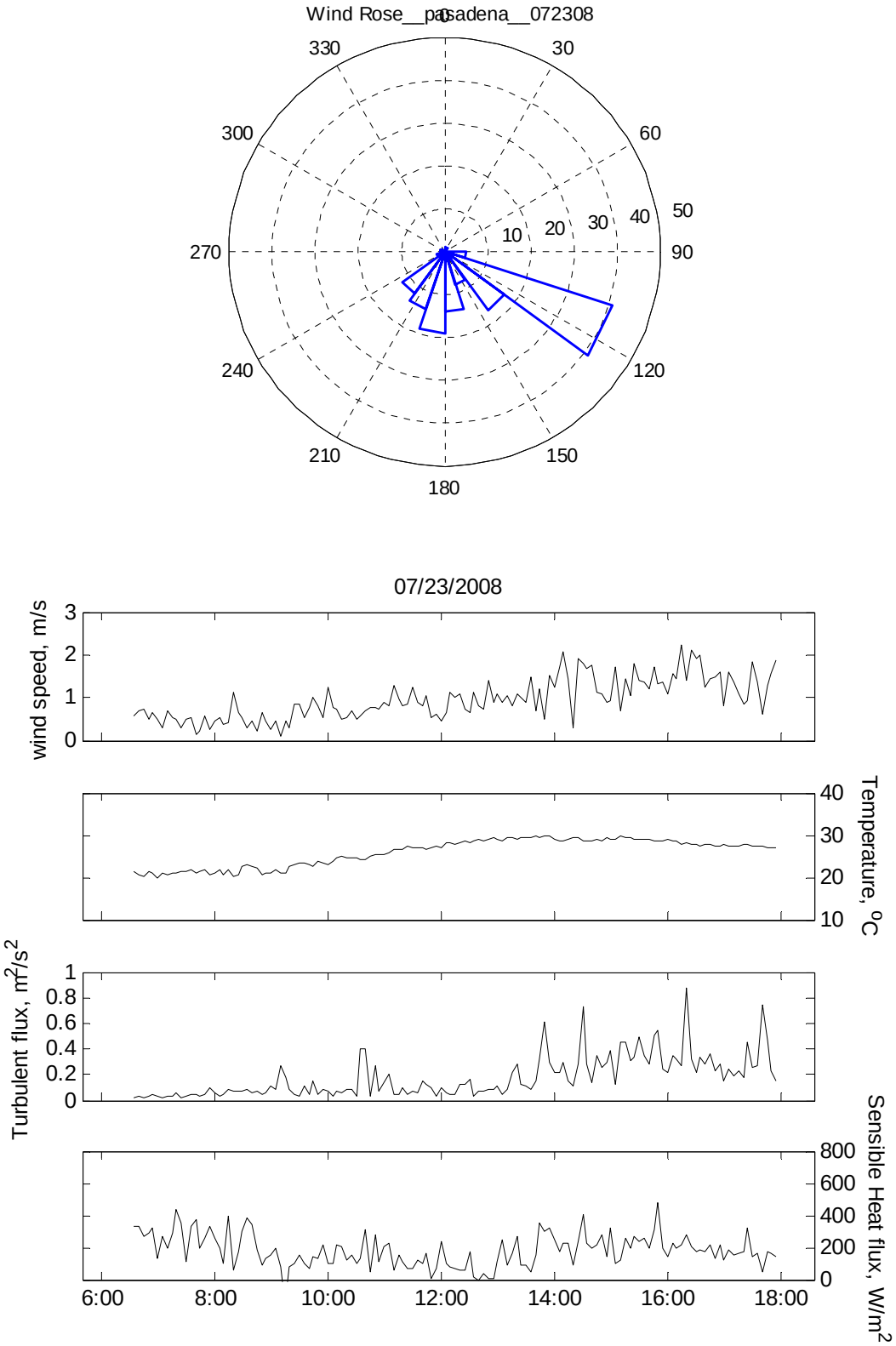

Figure E.22 Meteorological variables observed in Pasadena on 07/23/2008.

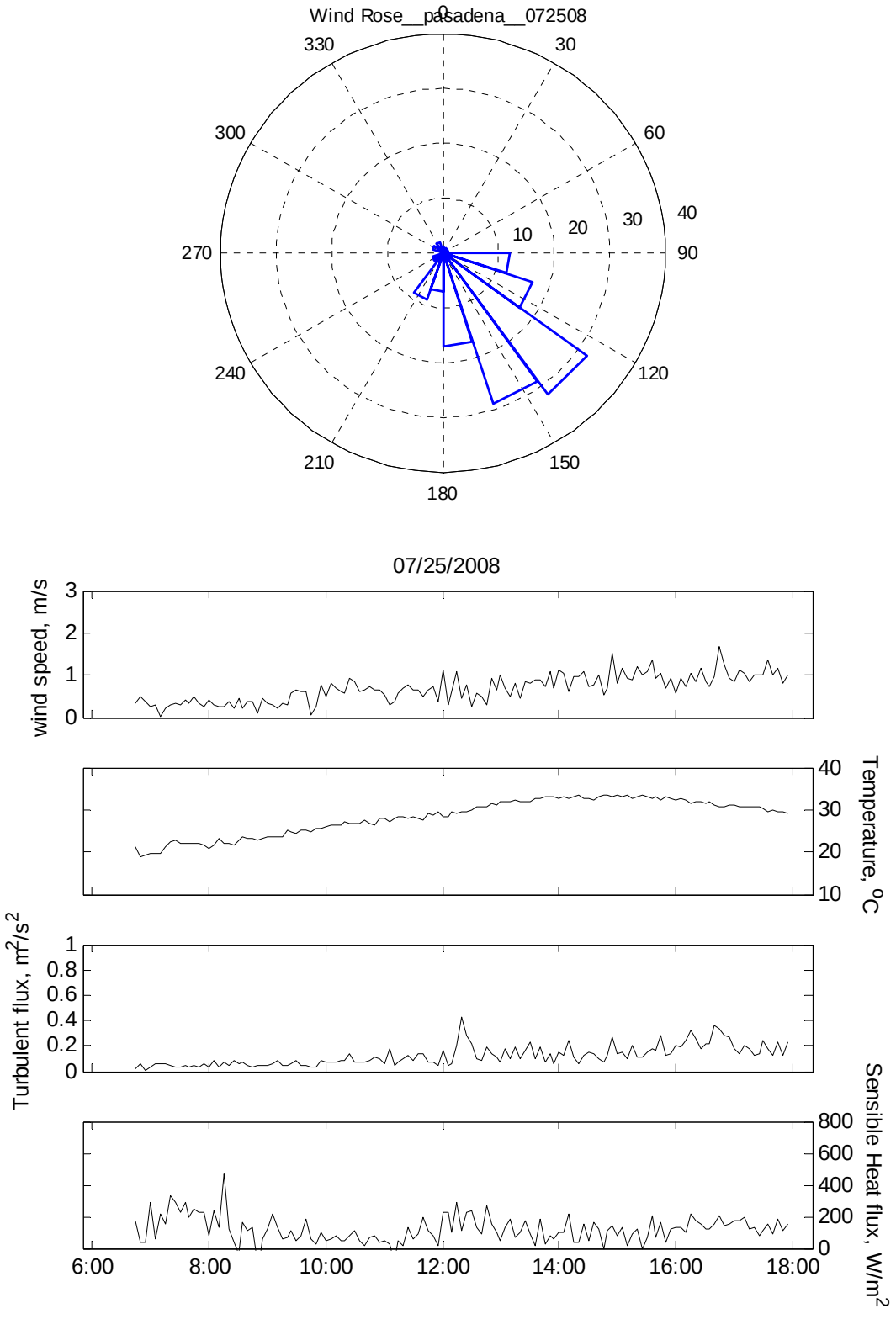

Figure E.23 Meteorological variables observed in Pasadena on 07/25/2008.

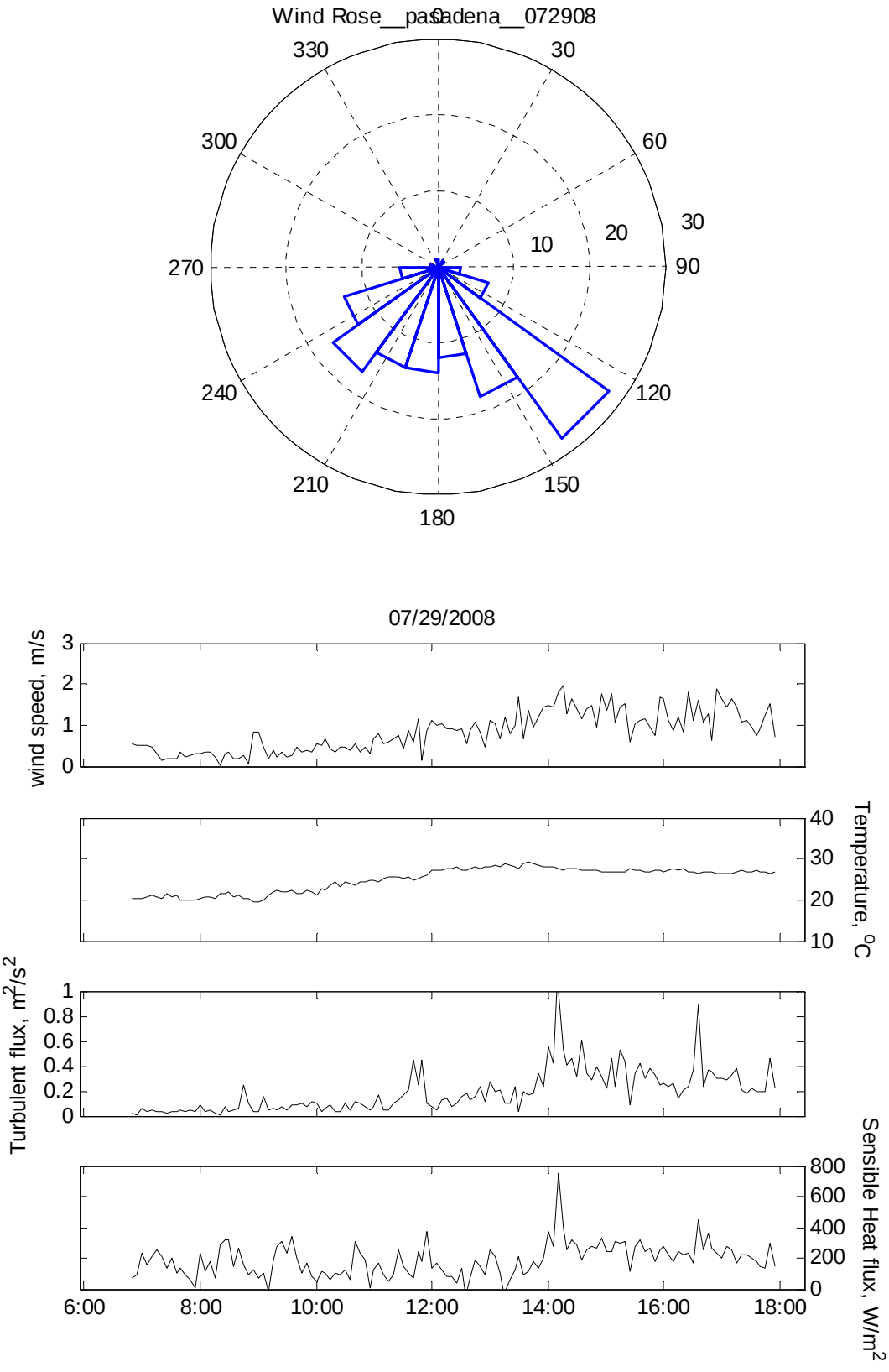

Figure E.24 Meteorological variables observed in Pasadena on 07/29/2008.